

Air Quality in Newport Beach, California:

Field Measurements of Ambient Particulates and Associated Trace Elements and Hydrocarbons

Karleen A. Boyle, Ph.D.

September 1, 2010

Prepared for: The City of Newport Beach

Submitted by: Karleen A. Boyle, Ph.D

phone: 202-270-6979 • kboylesudol@verizon.net

in association with



Environmental & Regulatory Specialists, Inc.

Wetlands Ecology & Environmental Science

David J. Tanner, President

223 62nd Street Newport Beach, California 92663

phone 949-646-8958 • fax 949-646-5496 • cell 714-299-3270

www.earsi.com • dave@earsi.com

CONTENTS

| | |
|--|---------------|
| I. Research Summary..... | 1- 5 |
| II. Technical Background..... | 6 - 10 |
| 2.1 Particulate Air Pollution..... | 6 |
| 2.2 Characteristics of PM..... | 6 |
| 2.3 Sources of PM..... | 7 |
| 2.4 Aircraft Particulate Emissions..... | 8 |
| 2.5 PM and Airport Planning and Regulatory Considerations..... | 9 |
| III. City of Newport Beach Air Quality Study..... | 11 |
| 3.1 Background..... | 11 |
| 3.2 Study Design..... | 12 |
| 3.3 Sampling locations..... | 12 |
| 3.4 Study Methods..... | 13 |
| 3.5 Results – Metals and Trace Elements..... | 16-37 |
| 3.6 Results - Particle-associated Hydrocarbons..... | 38-48 |
| 3.7 Discussion..... | 49 – 50 |
| 3.8 Conclusions and Recommendations for Future Research..... | 51 – 52 |
| 3.9 Acknowledgements..... | 53 |
| IV. Literature Cited..... | 54-56 |

| | |
|---|--------------|
| V. List of Tables..... | 57 |
| VI. List of Figures..... | 58-60 |
| VII. Appendices | |
| A.I(a) Analysis Techniques for Inorganics and Trace Elements..... | 61-67 |
| A.I(b) Calculations of precision for Inorganic Elements, OC and EC..... | 68-70 |
| A.I(c) Method Detection Limits Inorganic Elements, OC and EC..... | 71-72 |
| A.II(a) List of Hydrocarbons Analyzed..... | 73-75 |
| A.II(b) Propagation of Analytical Uncertainty | 76 |
| VIII. Maps | |
| <u>Map 1.</u> Regional view of field monitoring area. | 78 |
| <u>Map 2.</u> Zoom view of sampling stations from Lifeguard Headquarters to Main Street Parking Lot..... | 79 |
| <u>Map 3.</u> Field sampling stations upwind of John Wayne Airport (JWA)..... | 80 |
| <u>Map 4.</u> Runway sampling station and runway-adjacent sites..... | 81 |
| <u>Map 5.</u> Detail view of Runway and Parking sampling stations..... | 82 |
| <u>Map 6.</u> Freeway sampling location in relation to Runway and Parking sites..... | 83 |
| <u>Map 7.</u> Detail view of Freeway sampling location..... | 84 |

I. RESEARCH SUMMARY

Study Objective:

The purpose of this study was to measure airborne concentrations of particulate pollutants, and to characterize the chemical composition of these particles, at different locations in the city of Newport Beach, California.

Atmospheric particulate matter (PM) is associated with adverse impacts to human health, including increased risk of death from respiratory and cardiac causes. Consequently, PM is considered a criteria pollutant by the Environmental Protection Agency (EPA) and is regulated under The Clean Air Act.

Regulatory Issues:

Airports are subject to federal PM standards established under the Clean Air Act, as well as limits imposed under various state implementation plans (SIPs). Both state and federal standards for fine particulate matter (defined as particles with an aerodynamic diameter smaller than 2.5µm, termed PM_{2.5}) are established at 35 µg/m³ when averaged over 24 hours.

The chemicals associated with PM such as metals (e.g., copper), volatile organic compounds (e.g., toluene), and chlorinated volatile organic compounds (e.g., tetrachloroethylene) are considered hazardous air pollutants (HAPs) / air toxics. These compounds are regulated by the EPA based on cancer/ non-cancer risks and acute/ chronic exposure.

Study Design:

Field measurements of ambient PM_{2.5} were made at six locations in varying proximity to the two largest potential emission sources in the study area, high volume freeways (the 405 and the 5) and the John Wayne Airport. Concentrations of particle-associated metals, trace elements and hydrocarbons were measured and compared to see whether chemical profiles specific to different locations and emission sources can be distinguished, and whether the relative contributions of airport vs. automotive emissions can be assessed for different sampling sites.

Sampling Locations:

Study locations were established on a gradient beginning at the coast and continuing inland. The stable onshore flow of air in the region allowed us to establish sampling sites in areas known to be consistently upwind or downwind of potential emission sources. Data were collected at a total of six sites:

Lifeguard Headquarters (Lifeguard “HQ”): Directly adjacent to the Pacific coast. Located 10 km upwind of the Runway sampling station.

Eastbluff Boys' and Girls' Club (Boys' Club): Residential area 5 km upwind of the Runway site and adjacent to the jet departure corridor. Located 6 km from the coast, 5 km from the airport.

Santa Ana Heights Fire Station (Fire Station): Located 7 km from the coast and 3.4 km upwind of the Runway. Directly under the flight path of jets departing from JWA.

Runway: Sampling station located downwind of jet terminals, taxiway, and aircraft take-offs and landings. 37 meters upwind of and adjacent to the 405 freeway.

Main Street Parking Lot ("Parking"): 208 meters downwind of the 405 Freeway and 314 meters downwind of Runway site. Samplers were stationed on the roof of a structure in the Main Street parking lot serviced by airport shuttle buses.

Freeway: Designed to attempt to isolate freeway emissions for comparison to Runway and Parking stations. Samplers were located in an area that would receive high inputs of freeway emissions, but was distant from potential aircraft emissions. Samplers were located on an island adjacent to six lanes of merging freeway traffic and a freeway overpass at the junction of the 5 and 22 Freeways in the City of Orange, CA. The Freeway station was located 10.36 km northwest of the Runway site.

Results:

When interpreting these results, it should be noted that this study was designed as a preliminary assessment of the feasibility of using field air sampling to detect differences in the amounts and chemical composition of $PM_{2.5}$ in relation to various sources. For that reason, minimal sample sizes ($n=3$), were employed. This means that more data are needed before any of these results can be considered definitive. However, the fact that several findings proved statistically significant at such a low level of replication suggests that many of the trends observed are real.

Particle Concentrations :

$PM_{2.5}$ concentrations were highest at the Parking location, immediately adjacent to and downwind of both the runway and the 405 Freeway. In contrast, particle levels at the Freeway site in Orange, CA were approximately half that of the Runway/Freeway adjacent location. The lowest concentration of $PM_{2.5}$ was measured at the coastal Lifeguard HQ.

Particle-associated Chemicals:

Measurements of total particle mass, total carbon, and sulfate are associated with combustion particles, including vehicle and aircraft emissions. All of these elements exhibited a similar trend, reaching peak $PM_{2.5}$ concentrations at the Parking location, immediately adjacent to and downwind of both the runway and the 405 Freeway. In contrast, levels of these elements at the Freeway site in Orange, CA were between $\frac{2}{3}$ and $\frac{1}{2}$ that of the Runway/Freeway adjacent

location. When comparing the mass of PM_{2.5} and PM₁₀ fractions, the Parking and Runway locations had higher mass percentages of PM_{2.5}, indicative of higher levels of primary emissions, than the Freeway site.

Sulfate emissions were strongly associated with the airport and airport adjacent sites. PM_{2.5} sulfate was highest at the runway-adjacent Parking site, declining steadily as locations moved toward the coast, but remaining elevated above Freeway control levels at all sampling stations under the JWA flight path.

Ambient levels of metals generally considered to be potentially toxic were evaluated at all sampling stations. Nickel and vanadium were highest at the Runway and Runway-adjacent sites (Runway-adjacent sites = Parking downwind and Fire Station upwind). Lead and copper were highest at the Freeway and Parking sites.

Chemical Profiles of Sampling Sites

Chemical profiles of source sites (Runway and Freeway) were compared to see if any elements were specific to one location and whether different emission sources could be distinguished from one another. Two elements were detected only at the Runway location, uranium and yttrium. No elements were found to be unique to the Freeway or Parking sites.

Several elements were present at two or more locations, but were measured at their highest concentrations at, or adjacent to, one of the source sites. These were considered potential source-associated elements. Five elements measured at the sampling sites were elevated at both source locations: europium (Eu), tantalum (Ta), calcium (Ca), scandium (Sc) and thallium (Th). All of these except thallium and scandium showed a statistically significant effect of location, but more data are needed before it can be determined if they are associated with a runway source, freeway source, or neither.

Potential Runway-Associated Elements

A total of 10 elements were identified as potentially associated with the Runway sampling site, meaning the highest concentrations of that element were measured at the runway, or at Runway-adjacent sites (Runway-adjacent sites = Parking downwind and Fire Station upwind). For three of these elements, antimony (Sb), palladium (Pd) and potassium (K), the effect of location was strong enough to be statistically significant. The remaining seven elements measured at their highest concentrations at, or adjacent to, the runway were: nickel (Ni), vanadium (V), hafnium (Hf), indium (In), molybdenum (Mo), silver (Ag), and strontium (Sr).

Potential Freeway-Associated Elements

Eight elements were identified as potentially freeway-associated: bromine (Br), cerium (Ce), gold (Au), rubidium, (Rb), samarium (Sa), zirconium (Zr), terbium (Tb) and titanium ((Ti). Of these eight elements, terbium and titanium exhibited a statistically significant effect of location.

Emissions Profiles

The elements identified as runway or freeway-associated were used to construct emission profiles for both source locations. The chemical profiles of each of the sampling locations were compared to this source profile to determine to what extent the PM_{2.5} collected at different sampling locations might reflect the influence of runway or freeway PM.

Polycyclic Aromatic Hydrocarbons (PAHs)

A group of 7 PAHs displayed a strong association with the Runway sampling site. These compounds occurred at higher levels at the Runway or at Runway adjacent sites than at the freeway site. This same group of 7 PAHs was elevated at the sampling sites immediately upwind and downwind of the runway. As sampling sites moved away from the airport, the measured number of potential runway-associated PAHs declined from 7 at the Parking, Runway and Fire Station, to 4 at the Boys' Club location. By the time air samples were taken at the coastal station, only 3 of the original 7 runway-associated PAHs were detected: 4-methylbiphenyl (m_4bph), bibenz, 2-methyl biphenyl (m_2bph). The fact that these PAH elevations were measured even at sites upwind of the airport, suggests that samplers were detecting aircraft emissions from jets that had already completed takeoff and were gaining altitude in the JWA departure airspace.

Conclusions and Recommendations for Future Work

Our data indicate that ambient PM_{2.5} at the locations sampled in the City of Newport Beach is well within federal air quality standards. Gradients in concentrations of runway-associated elements between sampling sites suggest that aircraft particulate emissions persist a significant distance from the airport. These findings support and expand upon studies that have detected peaks in aircraft-related ultra-fine particles (UFP) much farther from airport operations than expected, over 900m downwind of LAX (Westerdahl et al., 2008) and 660m downwind of the Santa Monica Regional Airport (Hu et al., 2009).

Our sampling indicates that runway-associated emissions may be measurable at significant distances from John Wayne Airport. Total particle mass and PM-associated organic carbon, sulfate and certain trace elements were consistently elevated above freeway levels at the Runway and at sampling stations downwind of the flight path of JWA. In the case of sulfate, this elevation persisted at locations 10 km away from the airport, with the coastal Lifeguard HQ sampling site under the jet departure path exhibiting higher PM-sulfate than the Freeway

location. More data is needed to determine whether these elevated sulfate levels are aircraft-related.

This study was designed as a preliminary assessment of the feasibility of using field air sampling to detect differences in the amounts and chemical composition of $PM_{2.5}$ in relation to various sources. These objectives were met. Despite the minimal sample size ($n=3$), statistically significant differences in tested variables were detected between locations. The fact that any results proved statistically significant at this level of replication suggests that a larger-scale sampling project would yield additional useful information. Our data also indicate that chemical profiles can be useful in distinguishing between airport-associated emissions, freeway emissions and urban background PM.

II. Technical Background

This section provides background information on particulate air pollution with an emphasis on issues relevant to airports and urban planning issues. Health and regulatory issues associated with atmospheric particulate matter (PM) are described, and research findings on the characteristics of aircraft particulate emissions are summarized.

2.1 Particulate Air Pollution

The particulate component of air pollution is of concern for several reasons. Atmospheric particles contribute to the visual component of smog by absorbing and scattering light, which results in decreased visibility. Particulate matter (PM), and the chemicals associated with it, have been linked to adverse human health impacts, including increased risks of cardiac arrhythmias, heart attacks, bronchitis, and asthma attacks (Oberdorster, 2001). Epidemiological studies have found a significant association between exposure to fine and ultrafine particles and death from cardiac and respiratory disease (Pope et. al, 2002; Jerrett et. al, 2005). Children, the elderly, and people with existing heart or lung conditions are the most vulnerable to negative impacts due to fine particle exposure (Singh et. al, 2006).

Because of these adverse impacts, particulate matter (PM) is considered a criteria pollutant by the Environmental Protection Agency (EPA) and is regulated under The Clean Air Act. This federal regulation requires the EPA to establish National Ambient Air Quality Standards (NAAQS) which are intended to limit the concentration of selected pollutants in outside air at levels that protect public health. The chemicals associated with PM such as metals (e.g., copper), volatile organic compounds (e.g., toluene), and chlorinated volatile organic compounds (e.g., tetrachloroethylene) are considered hazardous air pollutants (HAPs) / air toxics. These compounds are regulated by the EPA based on cancer/ non-cancer risks and acute/ chronic exposure.

2.2 Characteristics of PM

The transport of particulate emissions in the environment and their potential to adversely impact human health depend largely on particle size. For regulatory purposes, airborne particles are divided into two size classes (Table 1). Particles smaller than 10 microns in diameter (PM_{10}) are considered “inhalable” and are monitored as air pollutants. The largest particles in the PM_{10} fraction, those between $10\mu m$ and $2.5\mu m$ in diameter are considered the “coarse” fraction. Particles of this size are usually derived from tire and brake wear and sources of windblown dust. PM_{10} tends to settle out of the atmosphere relatively quickly, and is typically not transported more than about 10 miles from its source. When inhaled, these coarse particles usually deposit in nasal passages and are not considered a significant threat to human health. The smaller particles in the PM_{10} fraction fall into the $PM_{2.5}$ category. This fraction of particles is subdivided

into two categories: “fine”, particles between 0.1µm – 2.5 µm in diameter, and “ultrafine” particles (UFP), with diameters below 0.1µm. Particles in these size classes do not readily settle out of the atmosphere and can be transported over long distances. These particles also pose a greater risk to human health because they can penetrate all the way to the alveoli of lungs. The UFP fraction especially has been linked to adverse health impacts. Because recent studies have shown that PM_{2.5} is not an accurate indicator of UFP, there is discussion of better addressing these risks by changing the regulatory standard to PM_{1.0} or PM_{0.1}. Current regulatory standards set acceptable levels for PM₁₀ at 150µg/m³ for a 24 hour average, and PM_{2.5} levels at 35µg/m³ for a 24 hour average. The standard for annual average PM_{2.5} is 15 µg/m³.

Table 1. Summary of the properties of atmospheric particles.

| | PM _{2.5} | | PM ₁₀ |
|--|---|-----------------------------------|-----------------------------|
| Particle Name | Ultrafine particles (UFP) | Fine particles | Coarse particles |
| Particle Size (aerodynamic diameter) | Below 0.1µm | Between 0.1µm – 2.5 µm | Between 2.5 µm- 10µm |
| Example | Viral cells | 1/30 the diameter of a human hair | Dust or soot (black carbon) |
| Example of source | Jet engine exhaust | Diesel engine exhaust | Windblown dust |
| Atmospheric residence time | minutes to hours (before growing to fine size class) →→ | days to weeks | minutes to days |
| Potential transport distance | 10 miles (before converting to fine size class) →→ | thousands of miles | Around 10 miles |
| Penetration of human respiratory system | Alveoli of lungs | | Nasal passages |

2.3 Sources of PM

Urban areas are subject to many sources of particulate air pollution, with mobile sources such as passenger vehicles and diesel trucks dominating at most locations. Stationary sources such as power plants and factories also contribute to PM.

Sources of Urban PM

- Passenger vehicles
- Heavy duty diesel vehicles
- Tire and brake wear
- Sand and salt piles

- Construction activities and earth moving
- Stationary power turbines
- Wood smoke
- Charbroilers
- Incinerators
- Boilers

Airports are recognized as contributing to PM emissions through the typical urban activities listed above as well as through airport-specific stationary and mobile sources:

Additional PM Sources at Airports

- Aircraft engines
- Ground support equipment (GSE) – often diesel
- Aircraft auxiliary power units (APUs)
- Training fires
- Aircraft tire and brake wear
- Emergency generators
- Airport ground transport (taxis, shuttle buses, etc.)
- Fuel storage tanks

The majority of airport PM emissions are due to mobile sources (aircraft, GSE, ground transport), with contributions from stationary sources typically estimated around 1% of the total.

2.4 Aircraft Particulate Emissions

The need for detailed information to assess the impacts of aviation emissions on air quality has spurred recent government-sponsored research in this area. During 2004 and 2005, NASA joined with the FAA's Partnership for Air Transportation Noise and Emissions Reduction (PARTNER) Center of Excellence and other researchers to collaborate on detailed studies of emissions from commercial aircraft. During a series of field studies (APEX1, JETS-APEX2, and APEX3), gas and particle emissions from modern commercial aircraft were sampled over the complete range of engine thrust settings. Emissions data were collected in the near-field plume (1-50m) from the engine exit as well as downwind (>100m) from moving aircraft during normal operations at two large commercial airports. These studies have greatly increased our understanding of the physical and chemical characteristics of aircraft emissions, and will improve the ability of air quality models to estimate airport contributions. An excellent review of these data with an emphasis on their relevance to airport operators is presented in a recent Transportation Research Board report (Whitefield, Hagen et al., 2008).

Data from the APEX studies provided a detailed profile of emissions from aircraft engines. These findings are summarized here to provide background for the interpretation of our field

data. At the point of emission from a jet engine, the exhaust contains both gases and particles. The exhaust gases consist of carbon dioxide, water vapor, sulfur dioxide, hydrocarbons and nitrogen oxides. The most abundant hydrocarbons in exhaust gases are ethylene and formaldehyde. Primary particles from jet engine combustion fall within the smallest size class of airborne particles, termed ultrafine particles (UFP). The particulate component of the exhaust is composed of organic carbon (volatile), elemental (non-volatile or “black”) carbon and sulfate from the sulfur component of jet fuel. Non-volatile PM makes up over 80% of PM emissions at all thrust conditions. At takeoff thrusts this percentage increases so that over 95% of the total PM mass is black carbon PM. Particles of organic carbon come from unburned or partially burned engine oil or jet fuel. This component of PM changes based on the engine thrust setting. At idle, organic PM is derived mainly from unburned hydrocarbons from jet fuel. At climb out and take-off settings, engine combustion efficiency increases to over 99%, so the organic component of PM is derived largely from engine oil. These organic particles and sulfate particles make up equal parts of PM at high thrust settings.

As jet exhaust moves downwind (> 10m) from the point of emission, the characteristics of its PM change. Ten to 100 times more particles are formed as exhaust gases cool and nucleate on the existing particles of black carbon and sulfate. This is termed “volatile PM”. Volatile PM has been found to nucleate preferentially on sulfate particles over black carbon particles (Onasch et al. 2008). This suggests that jet fuels with higher sulfur content will generate a higher number of organic particles. While the number of particles in the plume increases by at least an order of magnitude as the exhaust moves downwind, this increase does not significantly increase the total mass of PM measured. Particles formed by volatile PM production are so small that mass-based measurements alone do not capture them; however chemical analyses of PM will capture the chemicals associated with these particles.

2.5 PM and Airport Planning and Regulatory Considerations

Airports are subject to federal PM standards established under the Clean Air Act, as well as limits imposed under various state implementation plans (SIPs). Most major construction projects at airports require FAA funding or approval, and consequently must also comply with the National Environmental Policy Act (NEPA). Before a federal agency can approve or fund a project, NEPA requires that it be shown that emissions associated with that project will not exceed air quality standards, or worsen existing exceedances. The FAA must demonstrate conformity with these standards at any airports located in maintenance or nonattainment areas for PM₁₀ or PM_{2.5}.

In addition to regulatory concerns, airports must also address public complaints about particulate emissions in areas adjacent to the airport. Both large, high volume airports and smaller general aviation facilities receive complaints about soot and oily residue found on cars and residences near the airport and flight paths. Residents of these areas and airport workers have raised concerns about possible health impacts due to long term exposure to these particles. A primary

challenge in addressing these concerns is our ability to distinguish PM emissions from airports and aircraft from other urban sources of PM. The EPA estimates the annual average background levels for PM in the western United States range from 4 - 8 $\mu\text{g}/\text{m}^3$ for PM_{10} , and 1 - 4 $\mu\text{g}/\text{m}^3$ for $\text{PM}_{2.5}$. In the Eastern United States, estimates for PM_{10} range between 5 - 11 $\mu\text{g}/\text{m}^3$ and 2 - 5 $\mu\text{g}/\text{m}^3$ for $\text{PM}_{2.5}$. One of the primary objectives of this study is to determine whether airport-associated PM can be distinguished from other urban background sources, especially automobile traffic, in samples of ambient air.

the chemical profiles of different emission sources in the area can be distinguished from each other, and from background levels of air pollution in the region.

3.2 Study Design

Field measurements of ambient PM_{2.5} were made at six locations in varying proximity to the two largest potential emission sources in the study area, high volume freeways (the 405 and the 5) and John Wayne Airport (Maps 1 and 2). Concentrations of particle-associated metals, trace elements and hydrocarbons were measured and compared to see whether chemical profiles specific to different locations and emission sources can be distinguished, and whether the relative contributions of airport vs. automotive emissions can be assessed for different sampling sites.

3.3 Sampling locations

Lifeguard Headquarters:

This sampling location was located immediately adjacent to the Pacific Ocean, on the roof of the City of Newport Beach Lifeguard HQ. It was established 10.51 Km from the runway sampling station **GPS coordinates:** 33° 36.45' N; 117°55.73'W; elevation: 1.93 m. (Map 3).

Eastbluff Boys' and Girls' Club:

Hereafter abbreviated as “Boys' Club”. This sampling site was established in a residential area 6 Km north of the Lifeguard HQ and 5.06 Km upwind of the Runway station. **GPS coordinates:** 33° 38.44' N; 117°52.65'W; elevation: 100 ft. (Map 3).

Santa Ana Heights Fire Station:

Samplers were deployed on the roof of the training tower of the City of Newport Beach Fire Station #8, serving Santa Ana Heights. **GPS coordinates:** 33° 39.45' N; 117°52.86'; elevation 47.3 m . This location is adjacent to a lightly-trafficked business area and a driving range on the northwest side. This station was 3.44 Km southwest of the runway site and 7.1 Km from the Lifeguard HQ. (Maps 3 and 4).

Runway:

Runway samplers were deployed at the eastern edge of the runway and immediately downwind of aircraft take-offs and landings. **GPS coordinates:** 33° 41.09' N; 117° 51.80' ; elevation: 8.89 m. The runway station was located 10.51 Km from the Lifeguard HQ and 314 m from the Parking site. (Maps 4, 5 and 6).

III. City of Newport Beach Air Quality Study

3.1 Background

As a densely populated urban area with multiple sources of air pollution, the Southern California region has been the subject of numerous studies identifying the chemical components of air pollution (Geller et al., 2004), monitoring the transport and transformation of these chemicals in the atmosphere (Luria et al., 2005; Hughes et al., 2000), and attempting to identify the chemical composition and relative contributions of the various sources of air pollutants (Singh et al., 2002). The high volume of vehicle traffic in the region is well-recognized as a significant emissions source (Fine et al., 2004; Christoforou, et al., 2000; Kleeman et al., 1999; Lankey et al., 1998). As air traffic has increased, and residential developments adjacent to airports have become more common, efforts have been made to quantify the amount and types of emissions generated by airports (Westerdahl et al., 2005; Carslaw et al., 2006; Schürmann et al., 2007). These include not only emissions from the aircraft themselves, but also contributions from aircraft ground support equipment (GSE) and traffic associated with the airport, including taxis and shuttle buses. Studies in controlled environments such as jet engine test cells (Rogers et al., 2005) have generated valuable emission estimates for various aircraft, however field measurements on runways have indicated that real time variations in engine settings and idling profiles can dramatically affect the concentrations of pollutants being generated. Measurements taken at Oakland International Airport indicated that current ICAO emission inventories underestimate hydrocarbon emissions at idle by 16-45% (Herndon and Wood, 2009).

In response to complaints from airport-adjacent residents about “soot” deposition in their neighborhoods, studies have been undertaken at several airports to address this issue. Sampling of PM₁₀, VOCs, CO, and carbon soot in community air under the flight path of LAX by the South Coast Air Quality Management District (Barbosa et al., 1999) did not identify specific pollutant markers that could be correlated with aircraft operations. The report did suggest that elevated pollutant levels near the airport were influenced by high volumes of ground traffic. Field sampling of air, soil, and vegetation in sand dune habitat under the flight path of LAX documented increased concentrations of metals in ambient PM₁₀ and measured high levels of deposition of those same metals on vegetation in the dunes (Venkatesan and Boyle, 1998). Deposition studies undertaken in the city of Newport Beach under the flight path of JWA found that both PM₁₀ and particulate fallout rates were within the expected range for coastal areas of the South Coast Air Basin (Essner, et al., 1992).

The purpose of this study was to measure airborne concentrations of particulate pollutants, and to characterize the chemical composition of these particles, at different locations in Newport Beach, California. Like most urban areas, Newport Beach is subject to a variety of types of air pollution. Emissions range from recreational watercraft and residential traffic, to major interstate highways and an airport. A primary objective of this field monitoring was to determine whether

Main Street Parking Lot Station:

This station was established to determine whether characteristics of PM measured at the runway changed at a location immediately adjacent to the runway, but downwind of the 405 Freeway. This site was located in a large airport parking lot (Main Street Parking Lot) with heavy shuttle bus traffic. **GPS coordinates:** 33° 41.25' N ; 117° 51.74' ; elevation: 15.24 m. This sampling station was 314 m downwind of the runway site. (Maps 4, 5 and 6).

Freeway Station:

To attempt to isolate freeway emissions for comparison to emissions at the airport and parking stations, these samplers were located in an area that would receive high inputs of freeway emissions, but was distant from potential aircraft emissions. The freeway site was located 10.36 Km northwest of the runway site, in the city of Orange, CA. Samplers were stationed at the intersection of the 5 and 22 Freeways on a concrete island between the freeways. The sampling equipment was between 10 and 15 meters away from adjacent traffic. **GPS coordinates:** 33° 46.69' N; 117°52.30'W; elevation 51.5 m. (Maps 6 and 7).

3.4 Study Methods

Field air sampling - Measuring ambient particles and associated chemicals

All field air sampling was conducted during 5 sampling periods between August 3, 2009 and August 19, 2009 (Table 2). During this time, local weather conditions remained stable, with temperatures ranging between 63 – 83 °F (Source: NOAA, National Weather Service Data). A strong onshore flow is the typical weather pattern for this region. For this reason, study locations were established on a gradient beginning at the coast and continuing inland. The stable onshore flow allowed us to establish sampling sites in areas known to be consistently upwind or downwind of potential emission sources. At all sampling locations, air samplers were elevated 2m off the ground using portable plastic shelving. Care was taken to locate samplers at least 2m from any obstacle to air flow and to situate exhaust hoses downwind of all samplers. Field data sheets and chain-of-custody were recorded and maintained for all samples.

A total of three air samples for inorganic analysis and three samples for hydrocarbon analysis were collected at each sampling location. Sampling periods at all locations began at 0630 hours and ended at 2300 hours, for a total of 16.5 hours. This allowed us to actively sample emission sources in the area during morning and evening rush hours and throughout the time of active flight operations at John Wayne Airport. Sampling ended before the early morning hours, when air flow in the region can briefly shift from onshore to offshore flow, to avoid contaminating our samples with air from the inland valleys which has collected emissions from the entire Los Angeles Basin over the course of the day.

Table 2. Dates and locations of PM_{2.5} air sampling.

| Location | Sampling Date | | | | |
|--------------|---------------|----------|-----------|-----------|-----------|
| | 8/3/2009 | 8/5/2009 | 8/14/2009 | 8/17/2009 | 8/19/2009 |
| Lifeguard HQ | X | X | X | | |
| Boys' Club | X | X | X | | |
| Fire Station | X | | | X | X |
| Runway | | | X | X | X |
| Parking | | | X | X | X |
| Freeway | | X | | | |

Field air sampling for Particle Mass, Carbon and Inorganic Elements

Air samples were collected using Airmetrics Minivol air sampling units. These machines are portable, low-volume samplers powered by rechargeable batteries. The samplers use a pump to draw a known volume of air over a filter, which is then analyzed for the chemicals of interest. These samplers were developed by the U.S. Environmental Protection Agency, Region 10 and the Lane Regional Air Pollution Authority for use in short-term, multi-site pollution monitoring. Minivols have been used by US EPA, state and local air quality agencies for regional saturation monitoring studies (EPA 450/N-93-093). All samplers used in this study were obtained from Desert Research Institute (DRI) Reno, Nevada.

To measure concentrations of ambient atmospheric particles and the trace elements and heavy metals associated with them, two minivol samplers, with impactors restricting their intake to particles 2.5 microns and smaller, were run simultaneously during each sampling period. One sampler collected particles on a quartz filter which was later analyzed for organic and elemental carbon. The second sampler collected particles on a Teflon filter for analysis of metals and trace elements. Data collection focused on particles in the PM_{2.5} size class because smaller particles are typically associated with primary emissions and would therefore give us the best chance of detecting distinct chemical profiles for various emission sources. Particles in the PM₁₀ size range are normally associated with windblown dust, re-suspended road dust, or emissions that have undergone subsequent transformation in the atmosphere, so comparing the chemical profiles of the PM_{2.5} and PM₁₀ fractions of an air sample can provide information on the source of its particulates. To determine the partitioning of ambient particles between the PM_{2.5} and PM₁₀ size classes, two additional minivols equipped with PM₁₀ impactors were run simultaneously during one of the sampling runs at each source location. This allowed the comparison of the PM_{2.5} and PM₁₀ fractions at the Runway, Parking and Freeway locations.

All sampling filters were loaded into cartridges at the DRI laboratories, sealed in Ziploc bags, then transported to field sampling locations. Prior to each sampling run, current data on air pressure and temperature at the location were obtained from the NOAA National Weather Service website. These values were used to calibrate the sampler to a flow rate of 5 liters per minute. Flow rate was checked after each sampling period to ensure it had remained consistent. After sampling, the entire filter cartridge was sealed in a clean Ziploc bag and transported on ice to a holding refrigerator. At the conclusion of field data collection, all of the samples were shipped on ice via overnight delivery to DRI where the filters were unloaded and analyzed in the Elemental Analytical Facility. Gravimetric weights of all filters were taken. Teflon filters were analyzed for inorganic elements using X-ray Fluorescence. Quartz filters were analyzed for organic and elemental carbon using the thermal/optical reflectance and transmittance (TOR/TOT) method. See Appendix 1 of this report for details of extraction techniques and method detection limits.

Field air sampling - Measuring ambient Polycyclic Aromatic Hydrocarbons (PAHs)

To obtain data on ambient PAH levels occurring with measured particle loads, a Fine Particulate/Semi Volatile Organic Compound (FPSVOC) sampling system was run simultaneously with two minivol samplers for one sampling period at each location. The FPSVOC sampler was developed by DRI to collect particulate and semi-volatile gaseous polyaromatic hydrocarbons and other organic compounds. 113 liters per minute of air are drawn through a cyclone separator with a cut-off diameter of 2.5 μ m. Airborne particles are captured on a glass fiber filter. Compounds in the gas phase continue through the filter and are trapped in a glass sampling cartridge filled with the adsorbent XAD-2. Before and after each sampling run, a single point flow audit check was performed utilizing the Calibration Flow Rate Transfer Standard (rotameter) calibrated by DRI. At the end of a sampling period, the lower chamber of the sampling module was detached and removed to a clean location. Clean, powder-free surgical gloves were worn whenever filters and cartridges were handled. Exposed filters and canisters were wrapped in aluminum foil and stored in reflective, anti-static bags. All samples were kept on ice during transport to a holding refrigerator. At the conclusion of field data collection, all of the samples were shipped on ice via overnight delivery to DRI where the filters and cartridges were analyzed in the Organics Laboratory. See Appendix 2 of this report for details of hydrocarbon extraction and analysis methods and method detection limits.

Statistical analyses

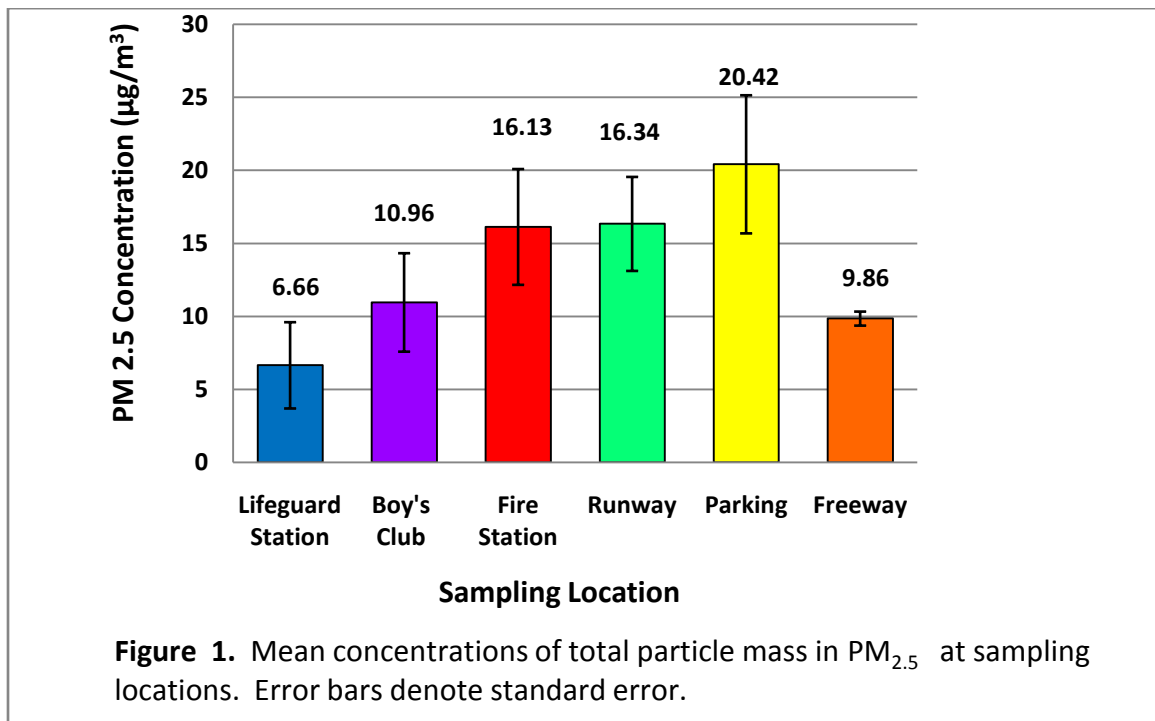
Concentrations of metals, trace elements and hydrocarbons were compared between locations to generate chemical profiles of each. 1-factor ANOVAs were used to determine whether there were statistically significant differences in trace element concentrations between sampling locations. If necessary, data were transformed before analysis to meet the assumptions of ANOVA (Table 3). If the ANOVA results were significant ($p \leq 0.05$), a posthoc Fisher's

protected least significant differences test (PLSD) was used to identify differences among means due to location.

3.5 RESULTS – Metals and Trace Elements

Mass Concentrations of ambient particles

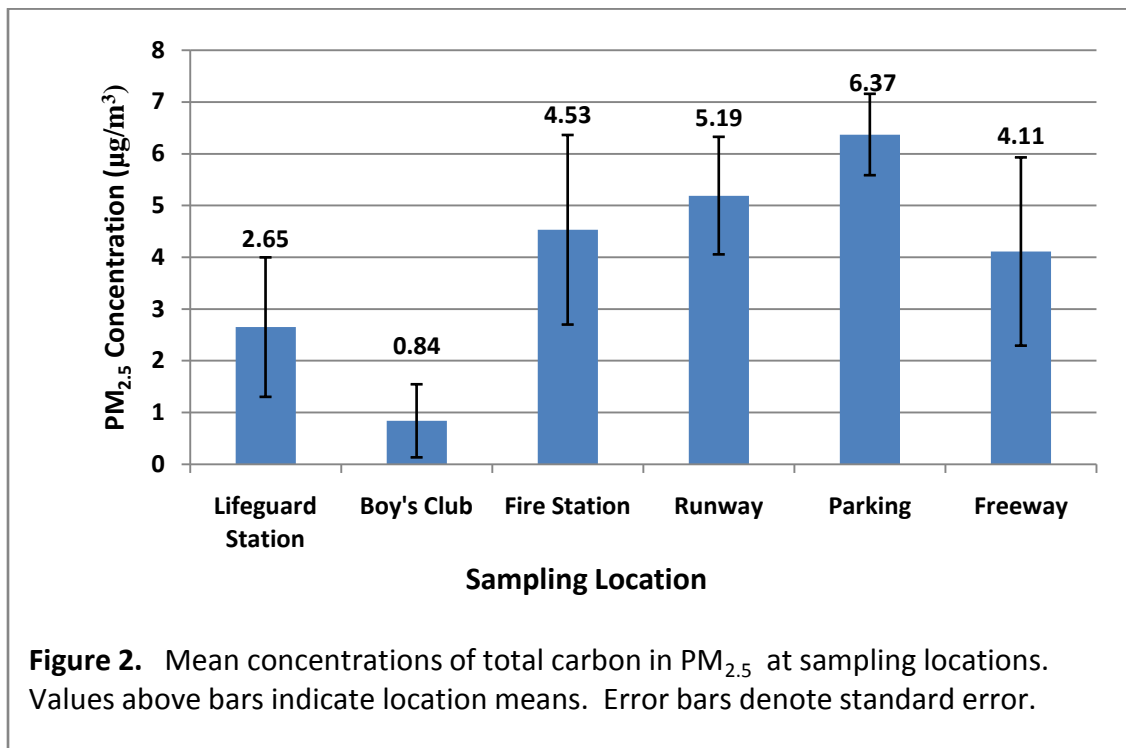
Maximum mass concentrations of ambient PM_{2.5} particles were measured at the Main St. Parking facility with mean concentrations of 20.42µg/m³ (Fig. 1). The Runway and Fire Station sampling sites exhibited the next highest particulate concentrations, exhibiting comparable levels of 16.34µg/m³ and 16.13µg/m³ respectively. Particle concentrations at the Freeway location were approximately half as high as those measured at the Parking location, averaging 9.86 µg/m³. Measurements at the Boys’ Club sampling site were similar to Freeway levels, averaging 10.96 µg/m³. The lowest levels of ambient particles occurred at the Lifeguard HQ, with a mean value of 6.66 µg/m³.



Organic and Elemental Carbon

When the graph of total carbon (TC) concentrations in PM_{2.5} (Fig. 2) is compared to Figure 1, it is evident that the trends in particle mass at the different sampling sites are similar to TC levels. Total carbon concentrations peak at 6.37µg/m³ at the Parking location, however unlike total

particle mass which declined to similar levels at both the Runway and Fire Station, TC shows a more gradual decline, remaining higher at the Runway than at the Fire Station (5.2 and 4.3 $\mu\text{g}/\text{m}^3$ respectively). TC levels at the Freeway were lower than the runway and runway-adjacent sites, but higher than the Lifeguard HQ and Boys' Club stations. Although the Boys' Club exhibited a higher total particle mass than the Lifeguard HQ, its $\text{PM}_{2.5}$ TC levels were lower than any of the other sites, measuring 0.84 $\mu\text{g}/\text{m}^3$.



Elemental carbon composed approximately 15% of the total carbon measured in $\text{PM}_{2.5}$ fractions at the runway (Fig. 3). However, at both the Parking and Freeway locations, the percentage of elemental carbon increased to around 20% in the $\text{PM}_{2.5}$ size class. A trend of increasing concentration of elemental carbon in the 2.5 fraction appears as sampling locations move inland, with EC increasing steadily from the Lifeguard HQ to a maximum at the Parking site, and dropping slightly at the Freeway. The proportion of EC to OC continues to increase on this gradient regardless of the total concentration of carbon measured (Fig. 4).

The amount of organic carbon (OC) in atmospheric particles can be used as an indicator of the proportion of particles derived from combustion sources. Higher $\text{PM}_{2.5}$ concentrations of organic carbon correlate with higher amounts of combustion particles. Comparing $\text{PM}_{2.5}$ total particle mass and organic carbon (Figs. 1 and 3) at the Boys' Club and Lifeguard HQ illustrates this well. When total particle mass is considered, the Boys' Club exhibits higher levels than the Lifeguard HQ. However, when $\text{PM}_{2.5}$ organic carbon is compared, levels at the Lifeguard HQ exceed the Boys' Club, reflecting the greater contribution of vehicle emissions to PM at that location. It is likely that the Lifeguard HQ had higher levels of OC than the residential sampling site because

of the high volume of summer beach traffic on nearby Balboa Boulevard, Newport Boulevard, and possibly West Coast Highway.

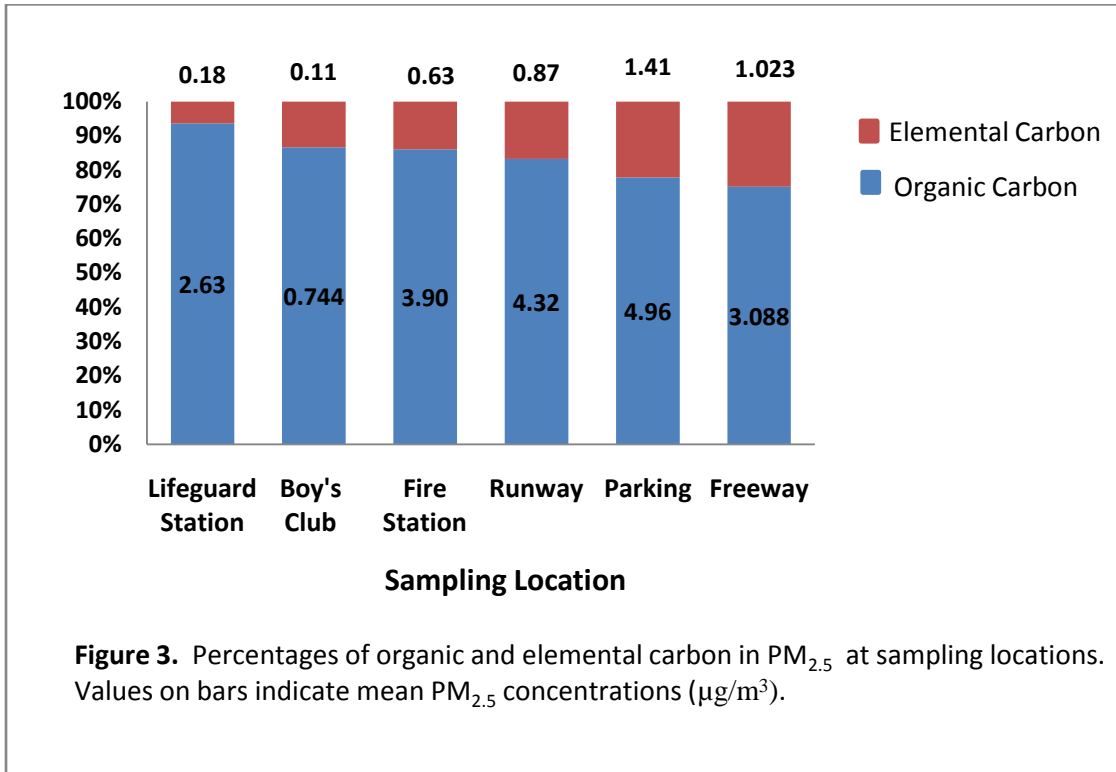


Figure 3. Percentages of organic and elemental carbon in PM_{2.5} at sampling locations. Values on bars indicate mean PM_{2.5} concentrations (µg/m³).

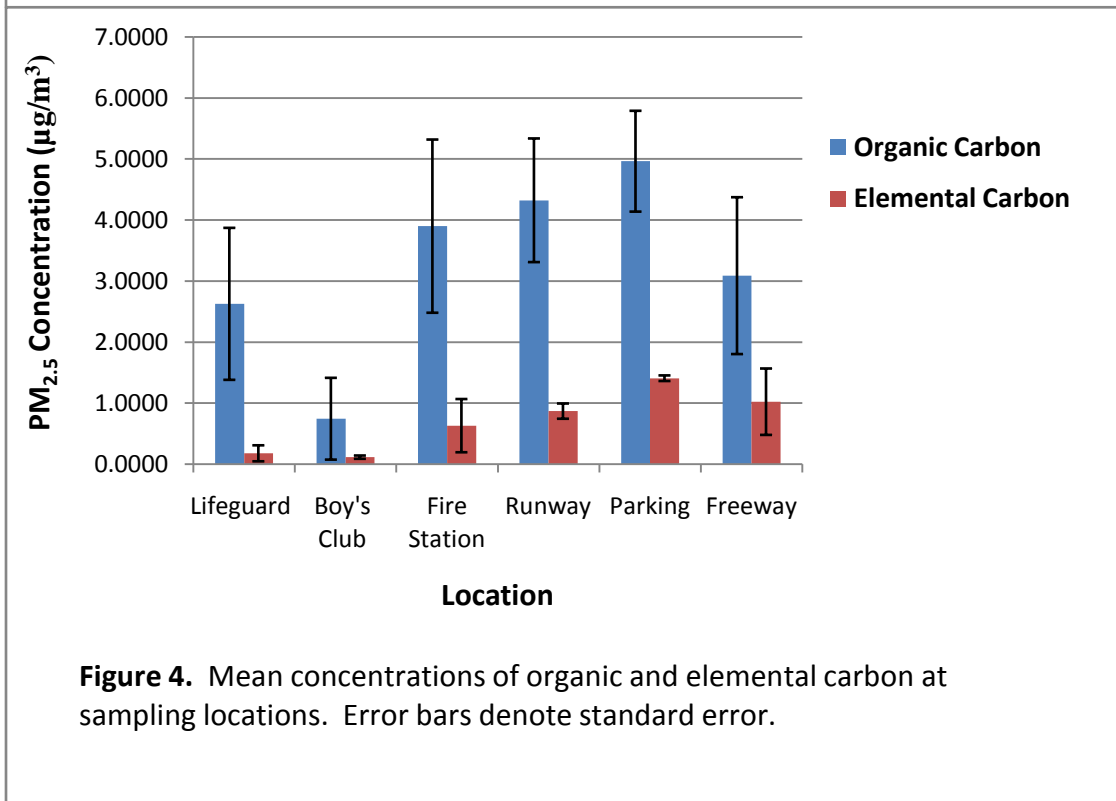
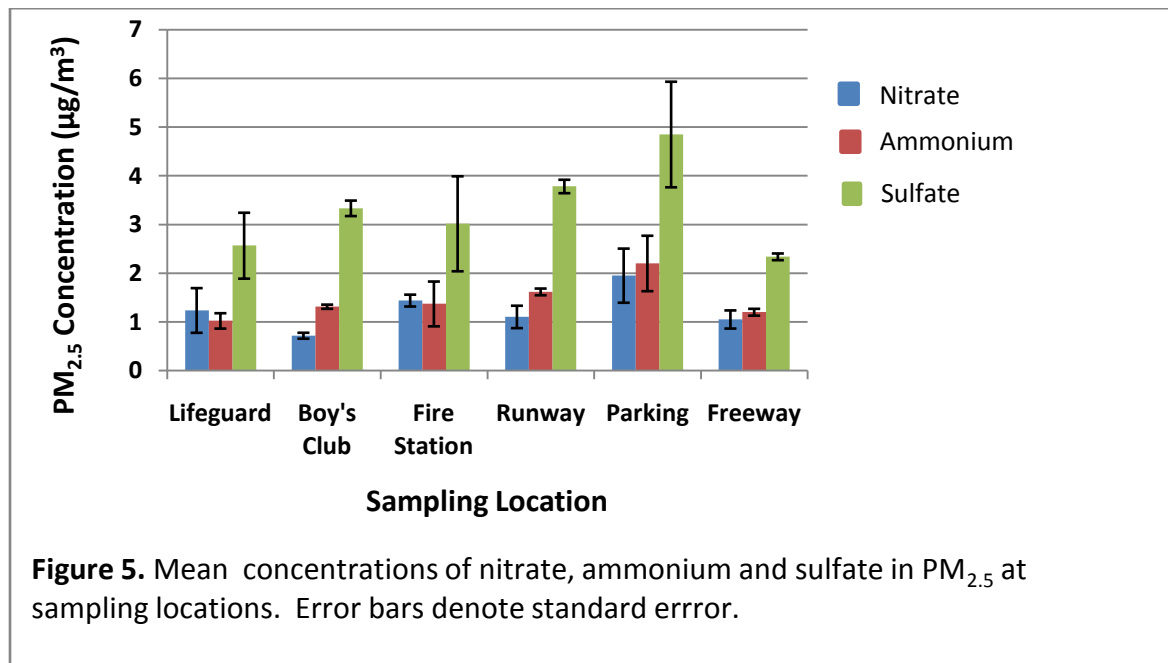


Figure 4. Mean concentrations of organic and elemental carbon at sampling locations. Error bars denote standard error.

Sulfate and Nitrogen

Trends in PM_{2.5} sulfate concentrations were similar to those exhibited by total particle mass and total carbon. Mean sulfate concentrations peaked at the parking location, measuring 4.85 µg/m³ (Fig.5). Sulfate levels declined slightly, to 3.78 µg/m³ at the Runway station, and were lower but comparable at the Fire Station and Boys' Club sites, which measured 3.02 µg/m³ and 3.33 µg/m³ respectively. Sulfate concentrations dropped further at the Lifeguard HQ, to 2.57 µg/m³, and were lowest at the Freeway sampling site, averaging 2.34 µg/m³.



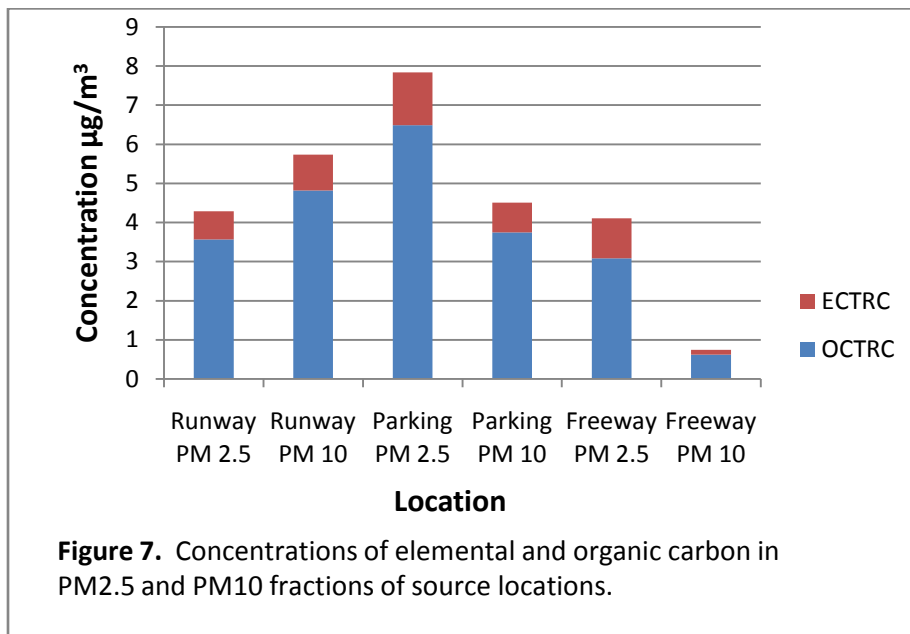
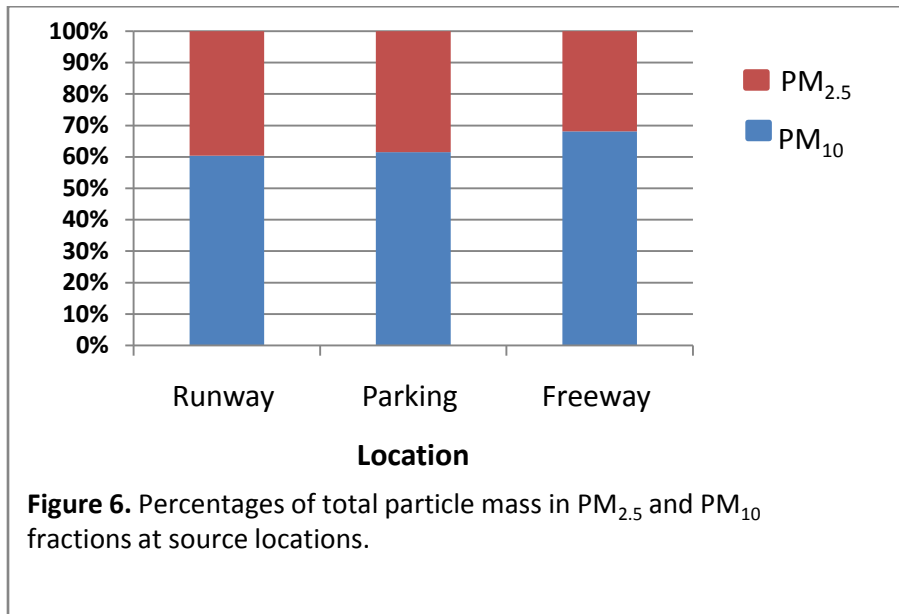
Trends in ammonium mirrored those of sulfate, peaking at the Parking location, registering the next highest levels at the Runway, then declining slightly to comparable levels at the Boys' Club and Fire Station (Fig. 5). Ammonium levels declined further to 1.20 µg/m³ at the Freeway and were lowest at the Lifeguard HQ, 1.02 µg/m³. More nitrogen was measured in the form of ammonium than nitrate at all locations except for the Fire and Lifeguard HQs, where nitrate was slightly more abundant.

PM_{2.5} nitrate exhibited a different pattern than sulfate and ammonium (Fig. 5). After peaking at 1.95 µg/m³ at the Parking location, the next highest concentrations were measured at the Fire (1.44 µg/m³) and Lifeguard (1.24 µg/m³) Stations. These locations were followed in descending order by the Runway (1.10 µg/m³), Freeway (1.05 µg/m³) and Boys' Club (0.72 µg/m³) locations.

Comparison of PM_{2.5} and PM₁₀ at potential source locations

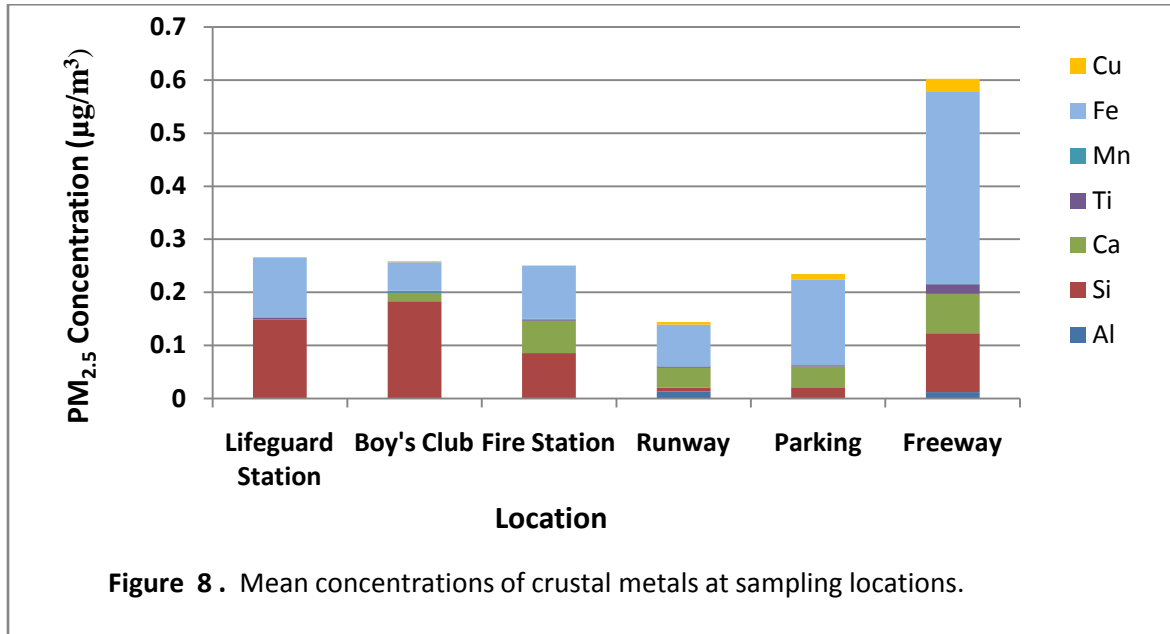
To characterize emission profiles at the three potential source locations, particle distributions between the PM_{2.5} and PM₁₀ size classes were compared. Particles in the smaller size fraction are most associated with primary emissions, while particles in the PM₁₀ fraction are typically

associated with windblown dust or older emission particles that have undergone chemical transformations in the atmosphere. Both the Parking and Runway locations had higher concentrations of particles, $31.37\mu\text{g}/\text{m}^3$ and $29.29\mu\text{g}/\text{m}^3$ respectively, and higher percentages of particles in the $\text{PM}_{2.5}$ fraction than the Freeway site (Fig. 6). Particles in the $\text{PM}_{2.5}$ size range accounted for approximately 40% of the particle mass collected at the Parking and Runway locations during a single simultaneous sampling period. In comparison to the Parking and Runway sites, the Freeway location exhibited lower particle concentrations, $21.09\mu\text{g}/\text{m}^3$, as well as a lower percentage of particles, slightly over 30%, in the $\text{PM}_{2.5}$ size range.

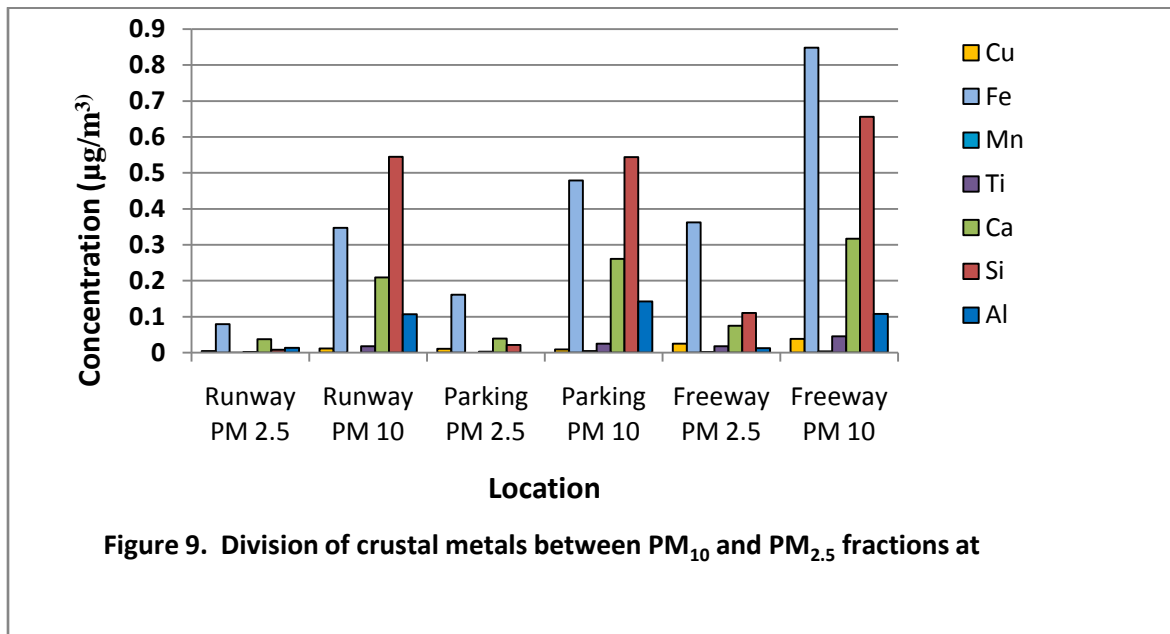


Particle-associated crustal metals

When compared across sampling locations, mean $PM_{2.5}$ concentrations of crustal metals were higher at the Freeway than at all other sites (Fig. 8). Iron dominated profiles at all locations except the Boys' Club and Lifeguard HQ which were dominated by silicon.



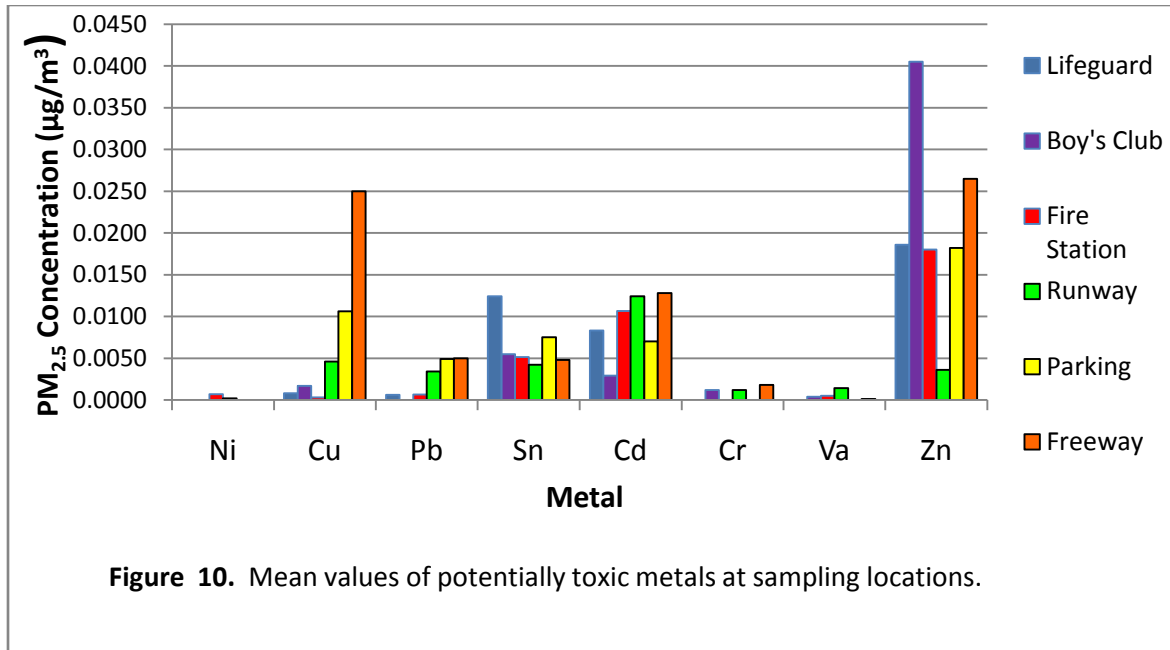
At all three locations, crustal metals normally associated with windblown dust made up the largest percentages of the PM_{10} size class (Fig. 9).



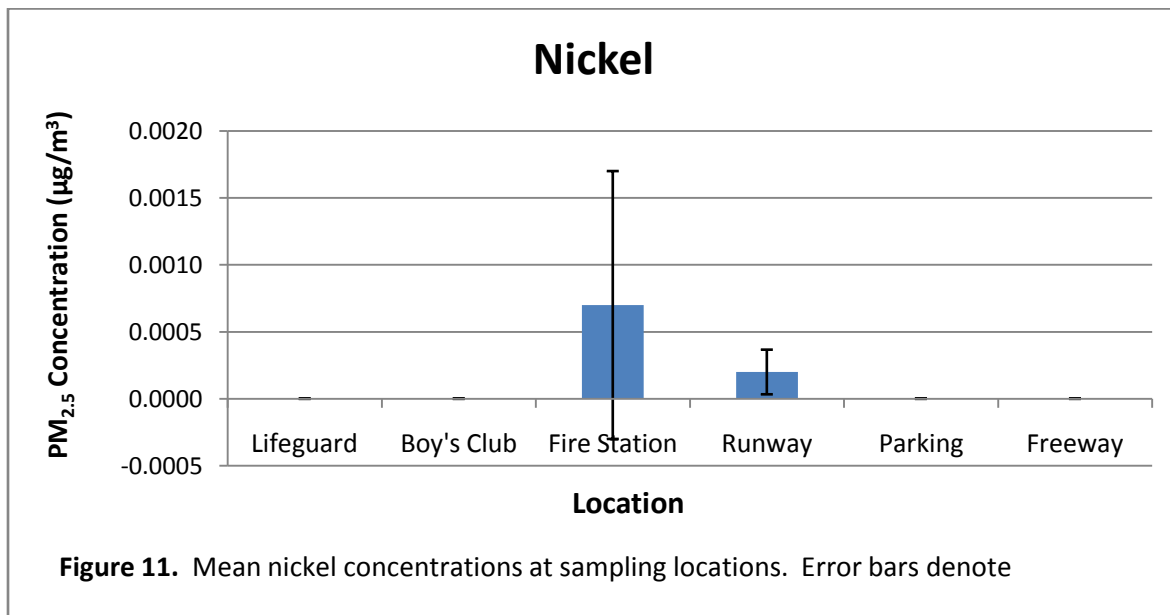
Heavy metals and trace elements associated with particles

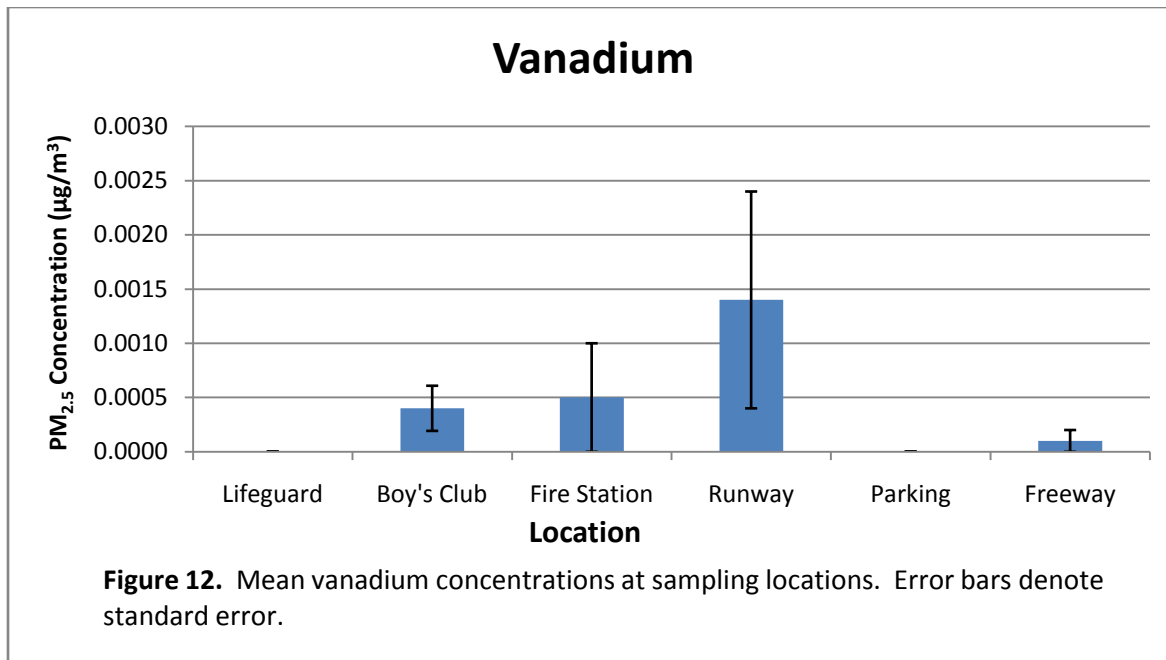
Concentrations of potentially toxic metals

Ambient levels of metals generally considered to be potentially toxic were evaluated at all sampling stations.

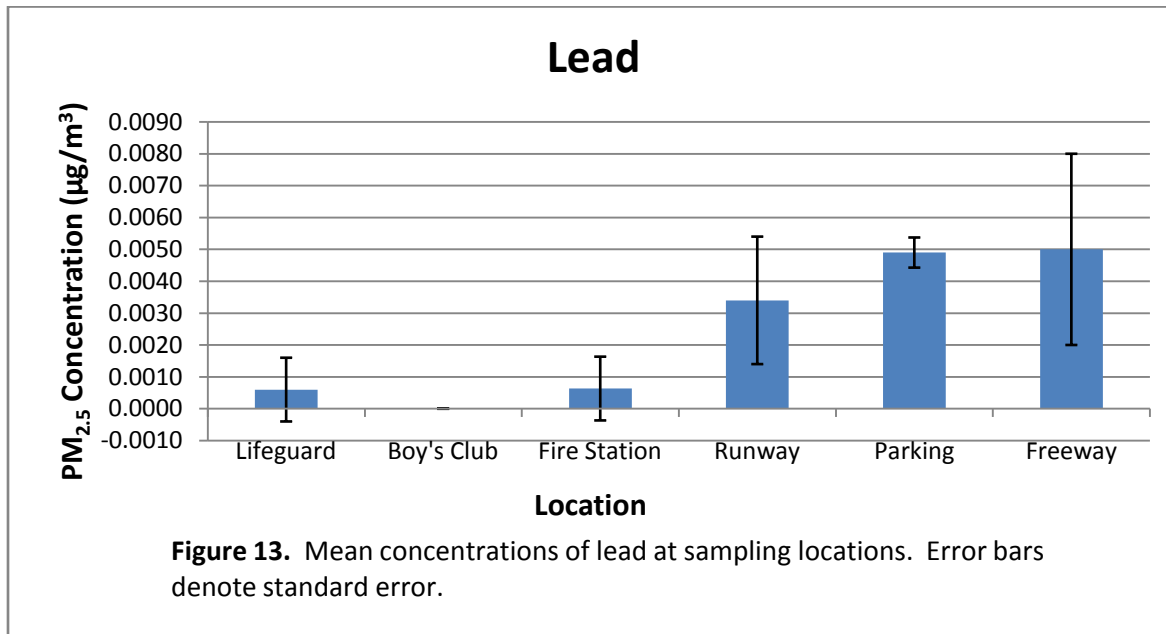


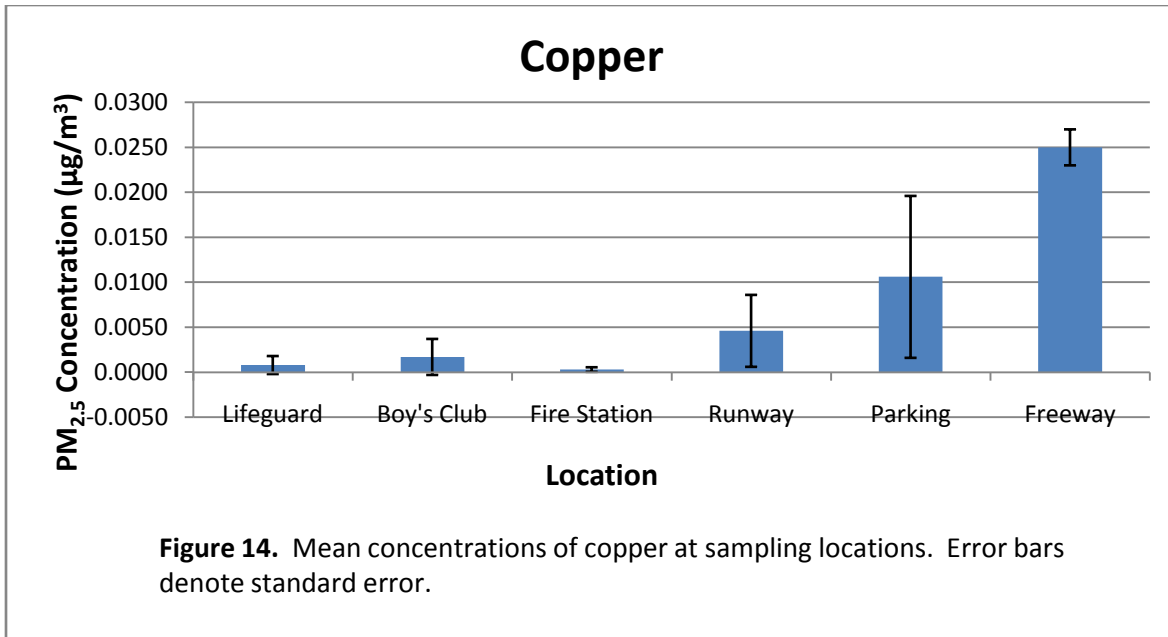
Two elements of this group of potentially toxic metals, nickel and vanadium, were measured at higher levels at the runway and runway-adjacent sites, (Figs.11 & 12).



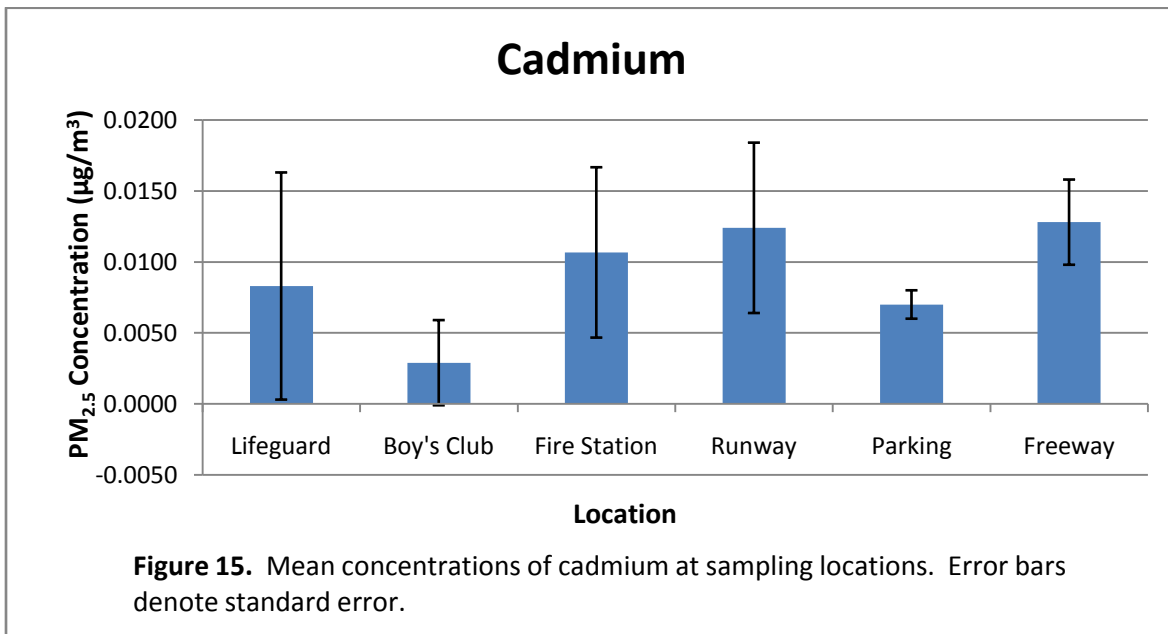


The potentially toxic metals lead and copper were measured at higher concentrations at the freeway and parking sites (Figs.13 & 14).

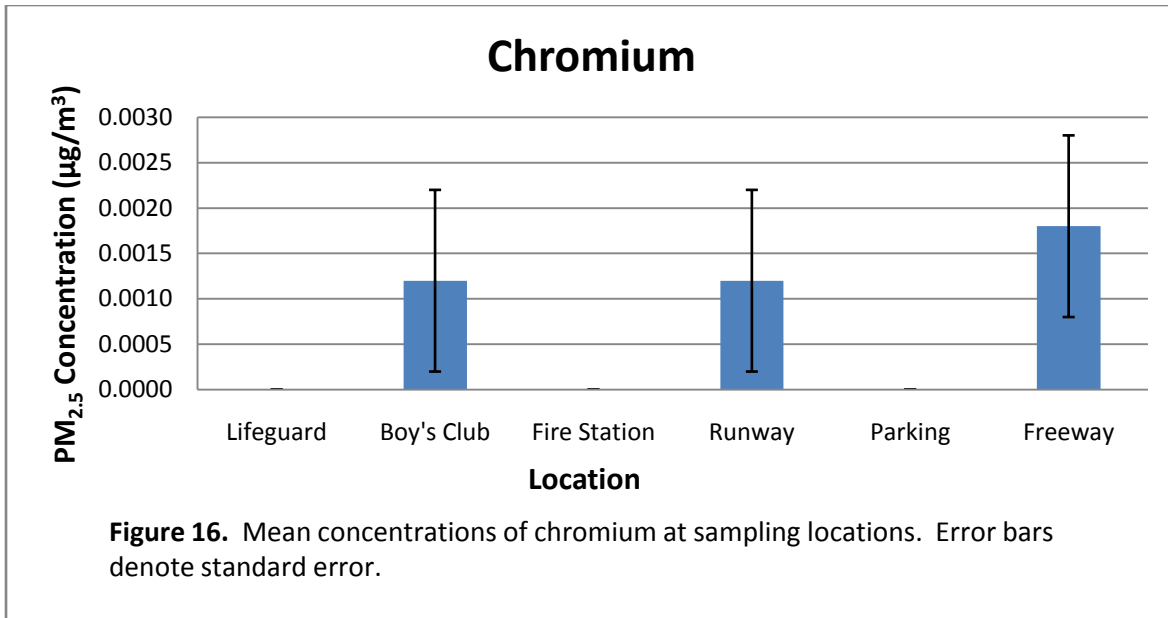




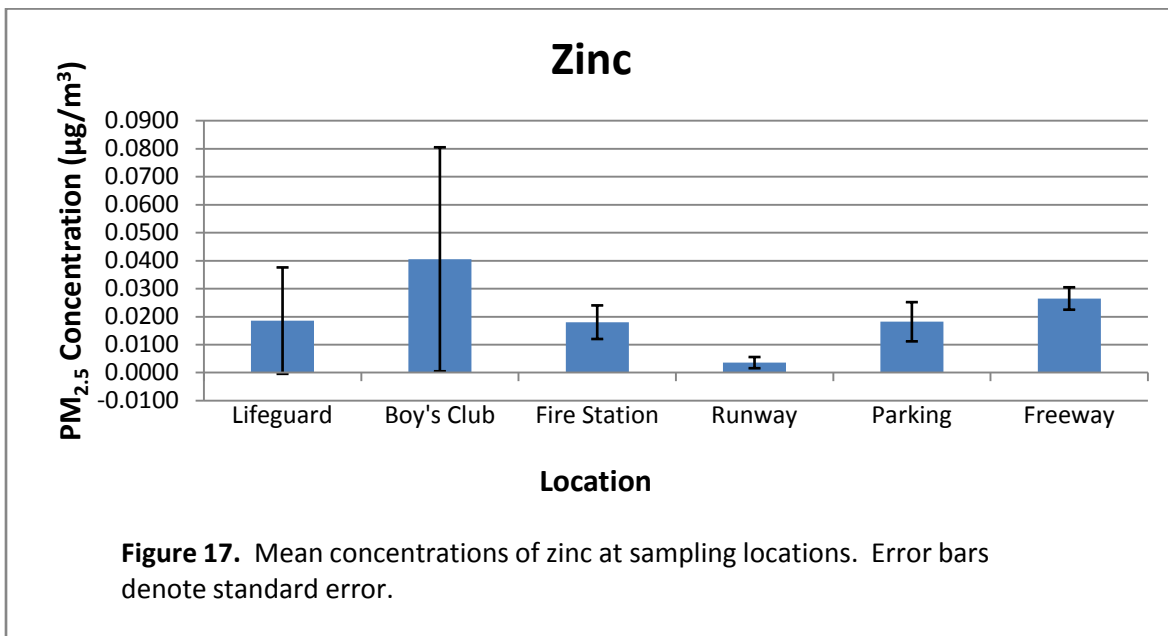
PM_{2.5} cadmium was measured in comparable amounts at all source locations (Fig. 15).

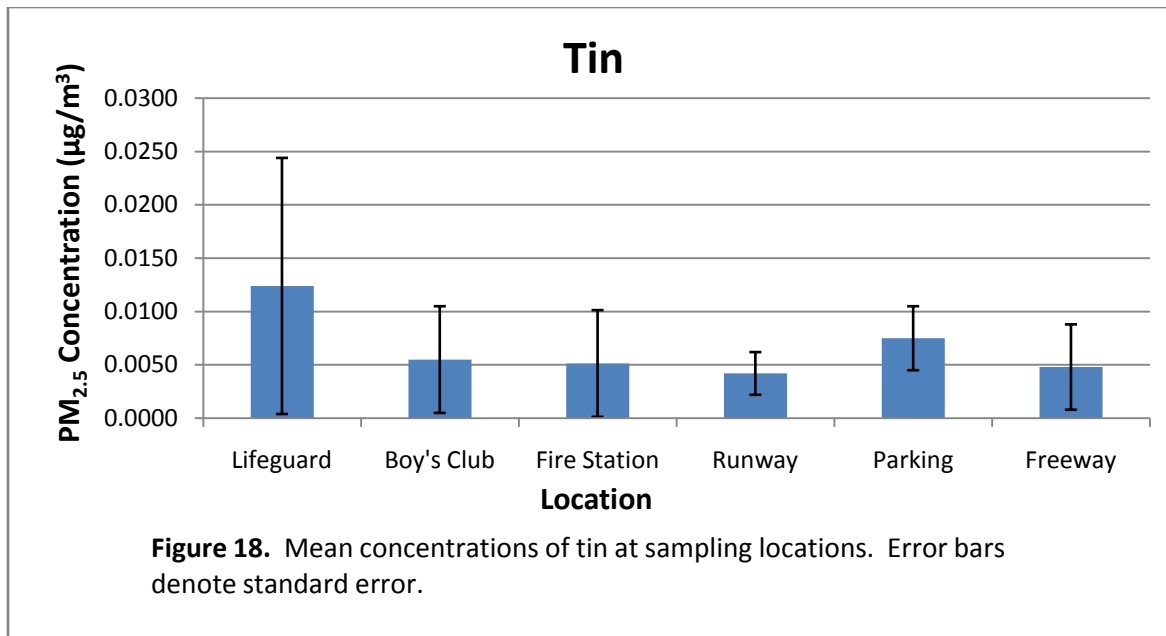


PM_{2.5} chromium was localized to three sites. Levels were comparable at the Boys' Club and Runway sites and slightly higher at the Freeway (Fig. 16).



The remaining two potentially toxic metals, zinc and tin, did not show a consistent pattern in relation to source locations (Fig. 17 & 18).

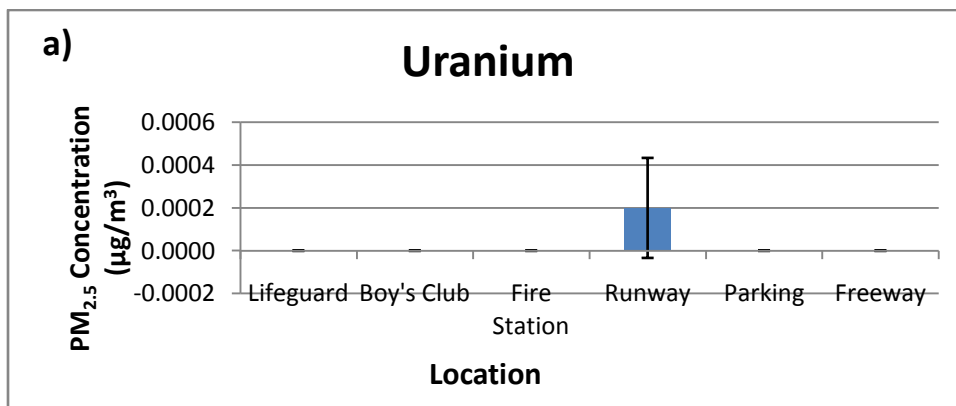




Comparing chemical profiles among locations

Location-specific Elements

Chemical profiles of source sites were compared to see if any elements were specific to one location and whether different emission sources could be distinguished from one another. Two elements were detected only at the Runway location, uranium (U) and yttrium (Yt). (Fig.19a and b). No elements were found to be unique to the Freeway location. The only other element detected at a single location was iridium (Ir) which was measured at the Boys' Club sampling station (Fig. 19c).



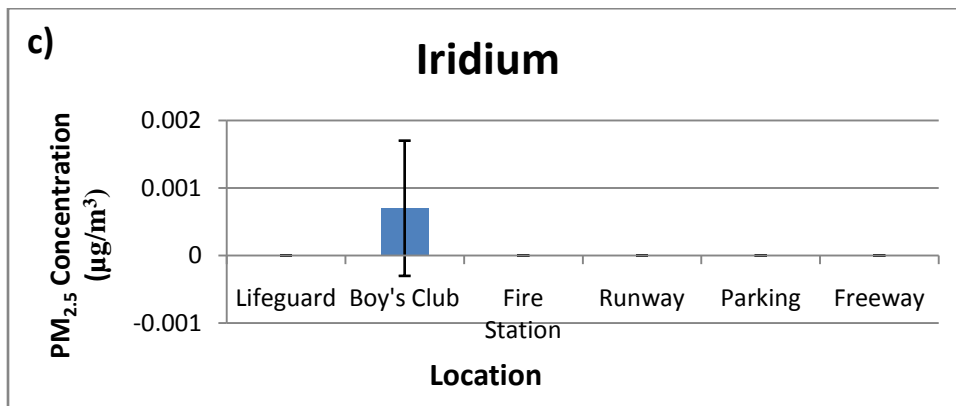
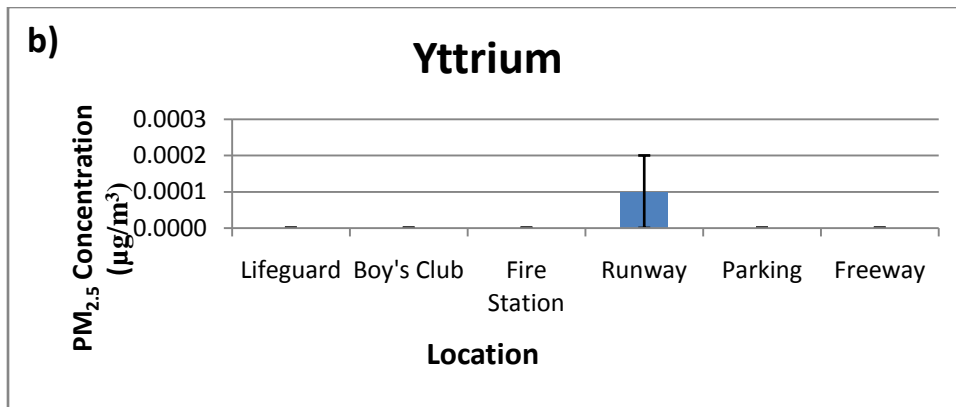


Figure 19 a- c. Elements specific to one sampling location. Error bars denote standard error.

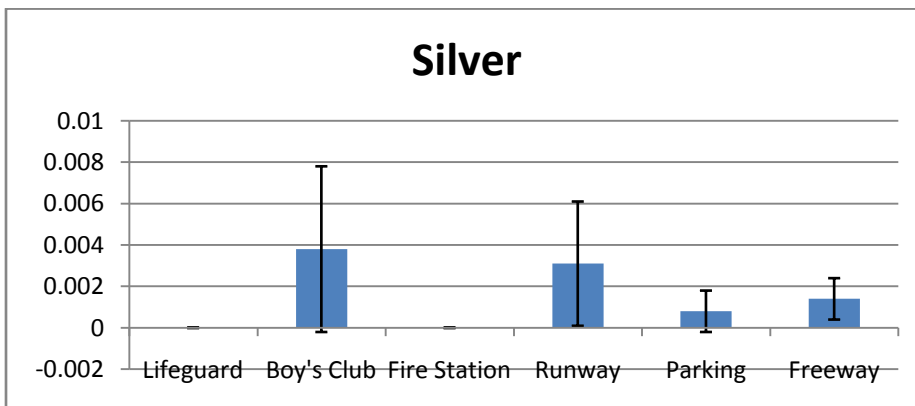
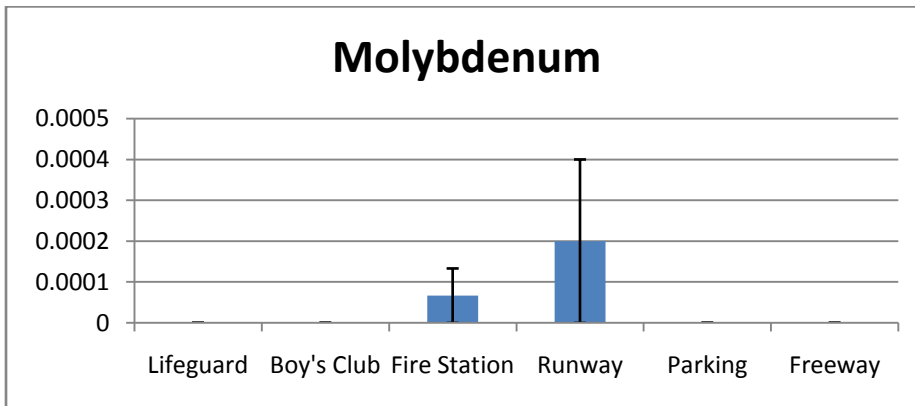
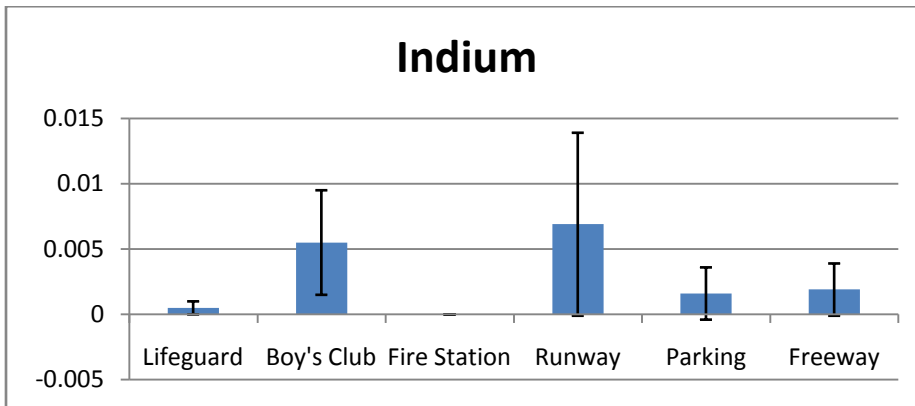
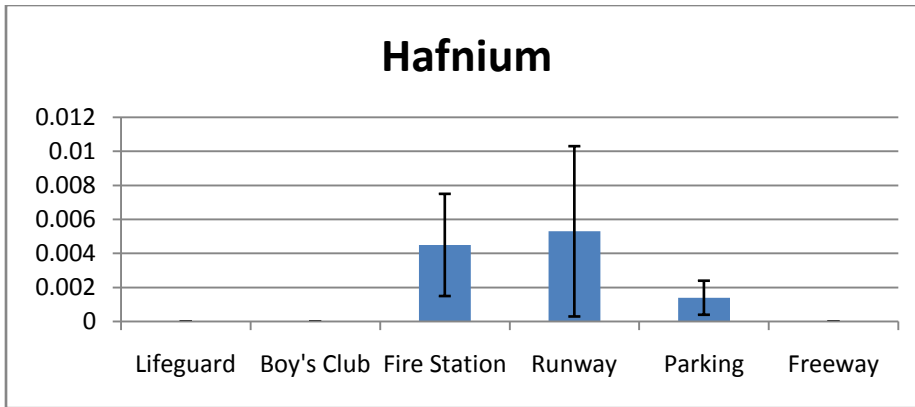
Source-associated elements

Potential Runway-associated elements

Several elements were present at two or more locations, but were measured at their highest concentrations at, or adjacent to, one of the source sites. These were considered potential source-associated elements. A total of 10 elements were identified as potentially associated with the Runway sampling site: nickel and vanadium (Fig.), hafnium (Hf), indium (In), molybdenum (Mo), silver (Ag), and strontium (Sr) (Fig.20a-e). For three of the ten elements, antimony (Sb), palladium (Pd) and potassium (K), the effect of location was strong enough to be statistically significant. Table 3 displays p-values from 1-factor ANOVAs and the results of a Fisher's Protected Least Significant Differences (PLSD) test for any elements with a p-value ≤ 0.05 .

Table 3. Results of statistically significant 1-factor ANOVAs comparing concentrations of ambient PM2.5 elements at study sites; significance level = $p \leq 0.05$. Any transformations applied to data to meet the assumptions of ANOVA are listed.

| Element | Transformation | p-value | Fisher's PLSD Results |
|----------------|----------------|------------|---|
| Antimony (Sb) | Square root | P = 0.0366 | Boys' Club significantly different from all sites except Runway. |
| Calcium (Ca) | Untransformed | P = 0.0168 | Fire Station and Freeway significantly different from Lifeguard HQ and Boys' Club. |
| Copper (Cu) | Untransformed | P = 0.0120 | Freeway significantly different from all other sites. |
| Europium (Eu) | Square root | P = 0.0501 | Runway significantly different from Boys' Club, Lifeguard HQ and Fire Station. |
| Palladium (Pd) | Untransformed | P = 0.0531 | Runway significantly different from all other locations. |
| Potassium (K) | Log | P = 0.0577 | Parking, Fire Station and Runway are all significantly different from Freeway and Boys' Club. |
| Tantalum (Ta) | Untransformed | P = 0.0457 | Freeway and Runway are significantly different from Lifeguard and Boys' Club. Runway is significantly different from Fire Station and Parking. |
| Titanium (Ti) | Untransformed | P = 0.0008 | All locations significantly different from Freeway. |
| Terbium (Tb) | Untransformed | P = 0.0001 | Freeway and Runway significantly different from Boys' Club and Lifeguard HQ. Freeway is significantly different from Fire Station, Parking and Runway |



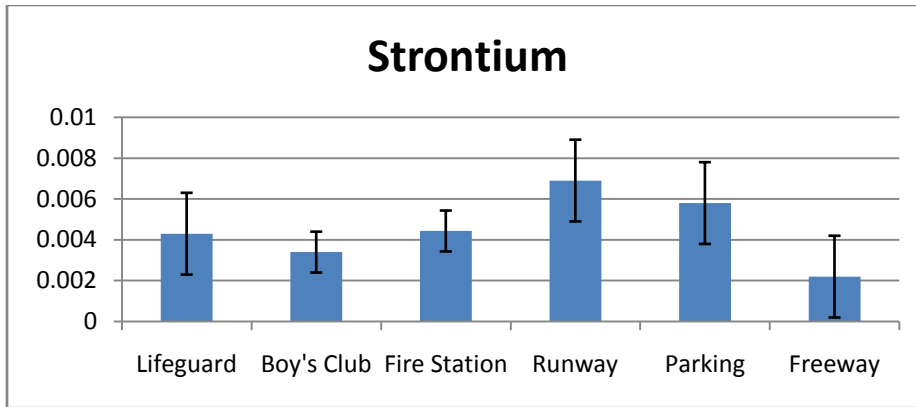
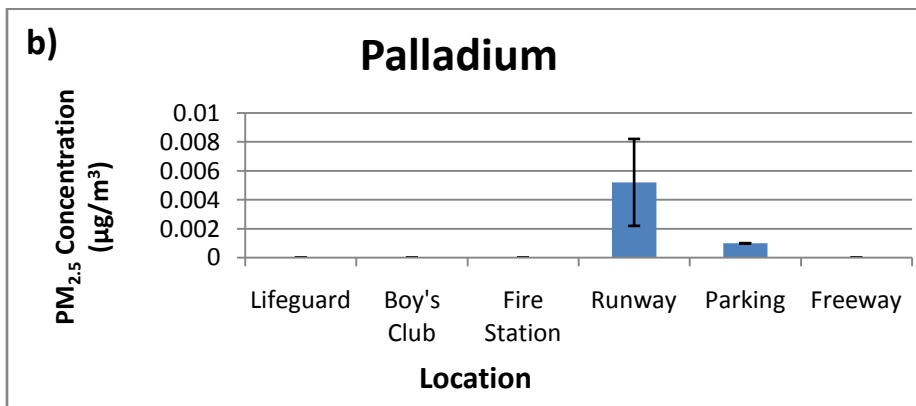
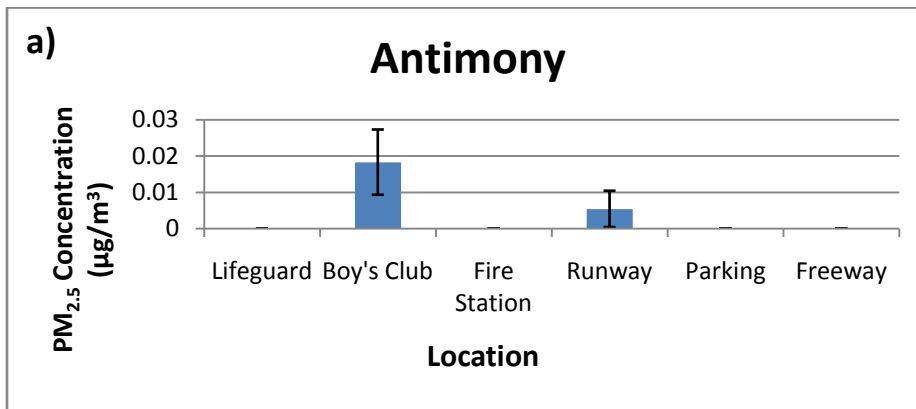


Figure 20 a- e. Elements characterized as potentially runway-associated. Error bars denote standard error.



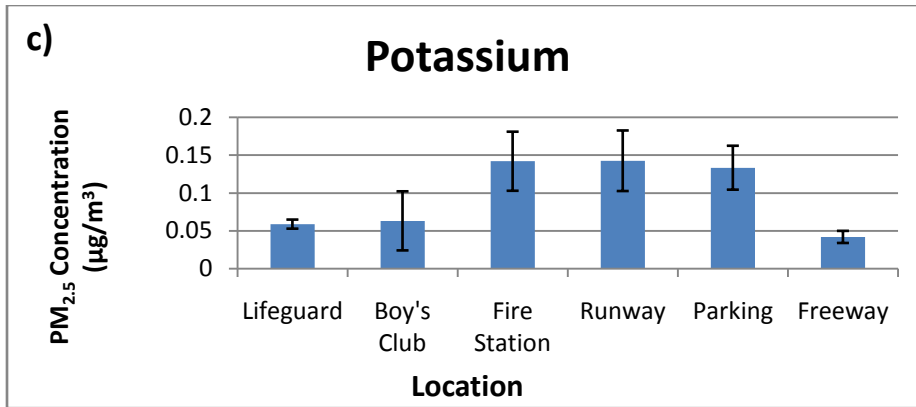
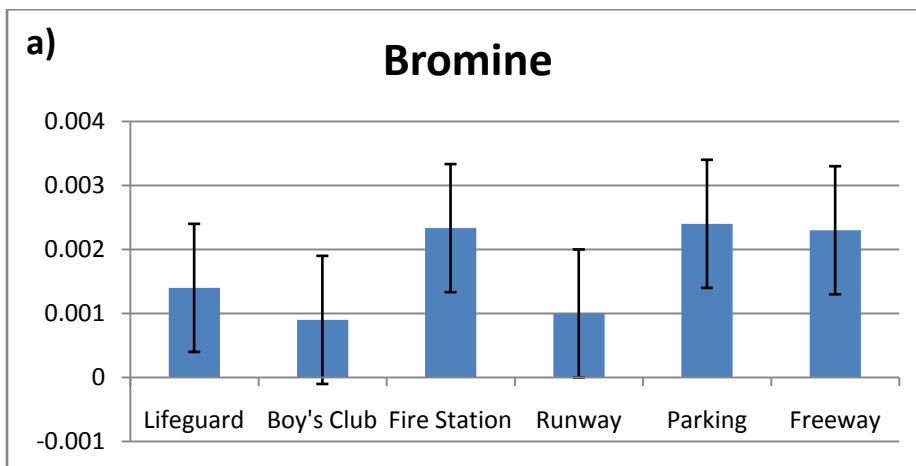
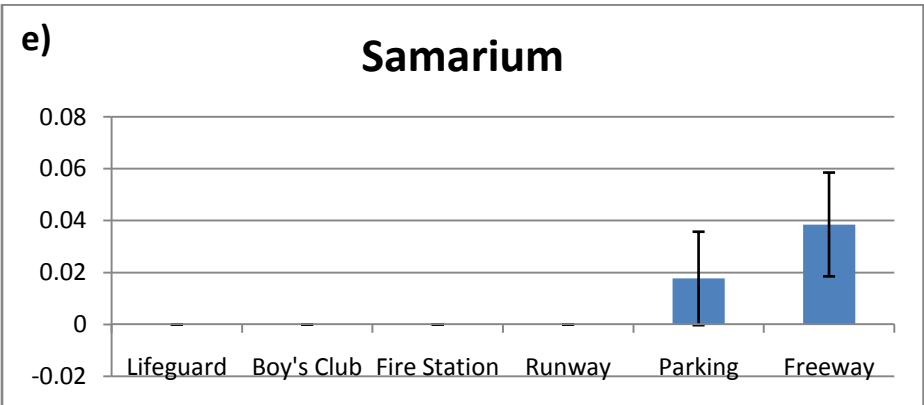
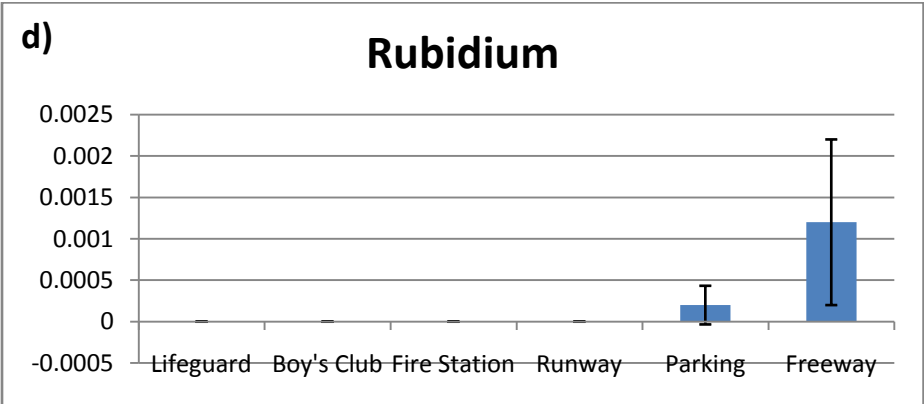
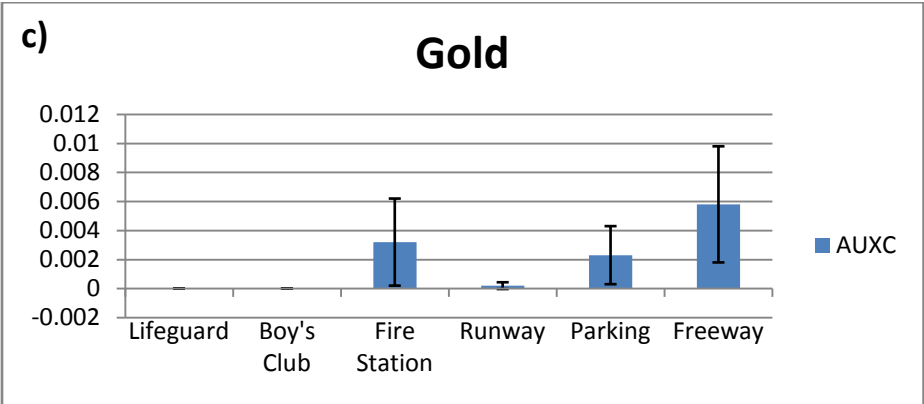
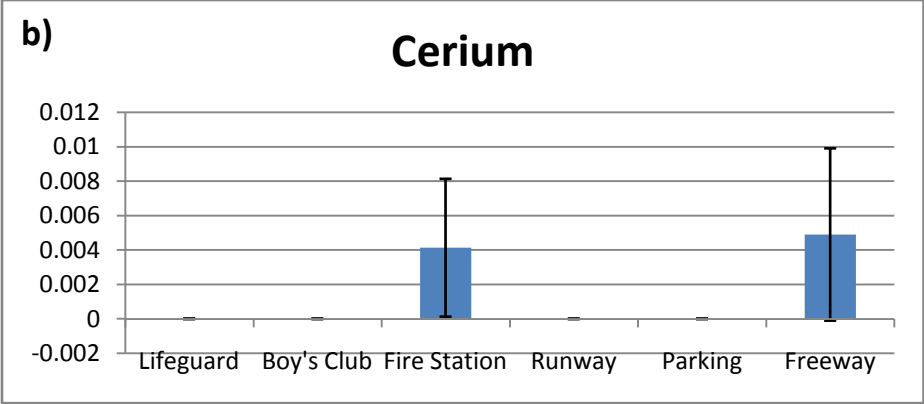


Figure 21 a – c. Elements categorized as runway-associated that exhibited a statistically significant effect of sampling location. Error bars denote standard error.

Potential Freeway-associated Elements

Eight elements were present at two or more locations, but were measured at their highest concentrations at, or adjacent to, the freeway. These were considered potentially freeway-associated elements. This category included: bromine (Br), cerium (Ce), gold (Au), rubidium, (Rb), samarium (Sa), zirconium (Zr), terbium (Tb) and titanium (Ti) (Fig. 22 a – h). Of these elements, terbium and titanium exhibited a statistically significant effect of location (Table 3).





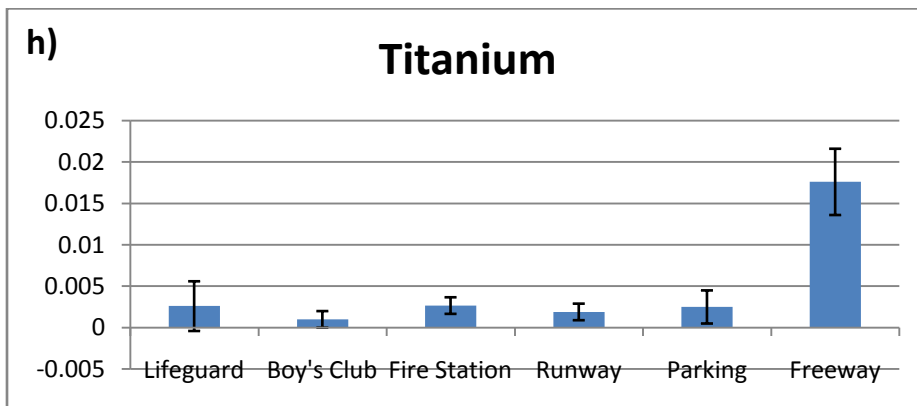
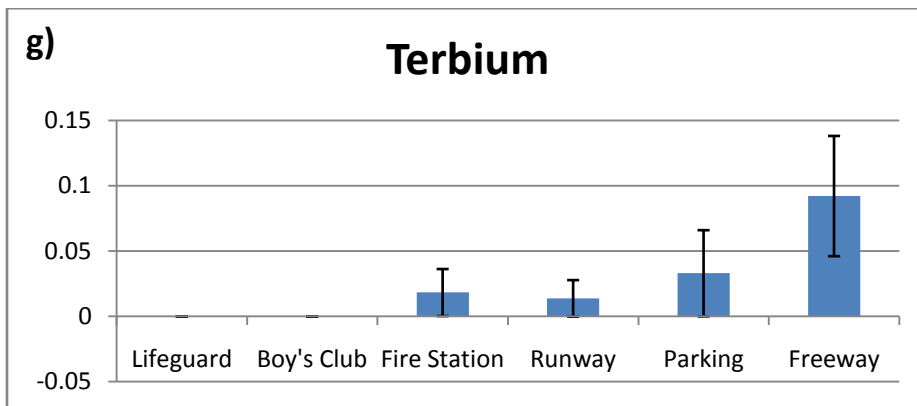
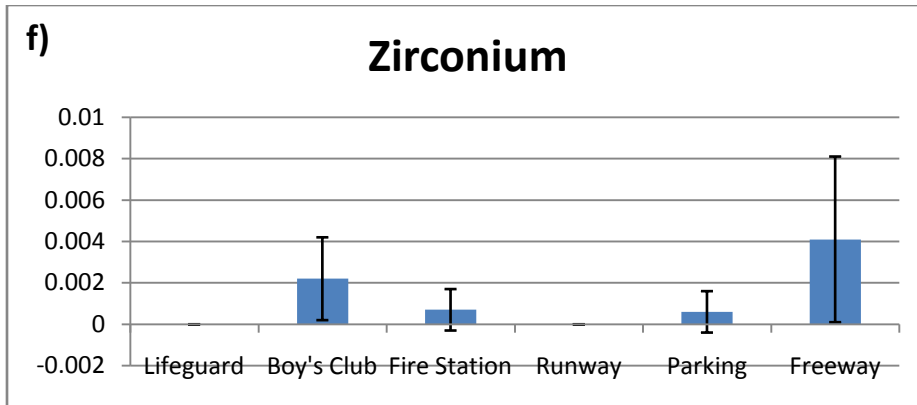
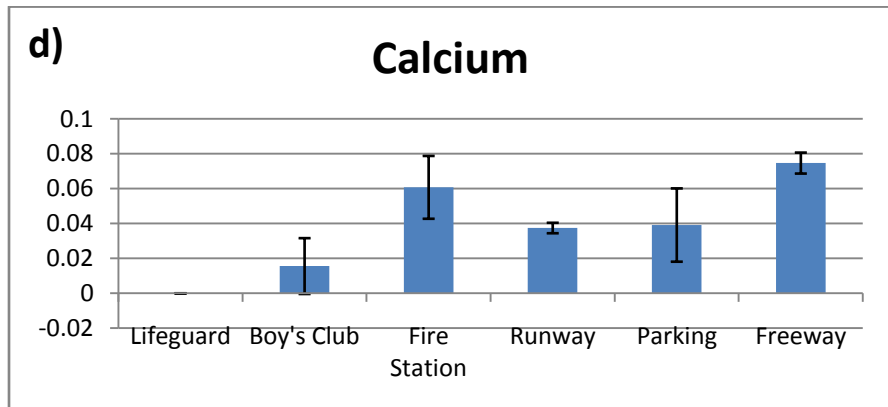
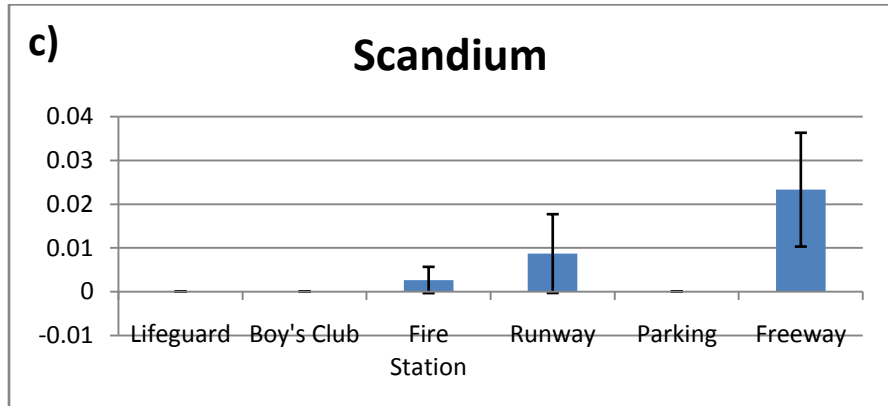
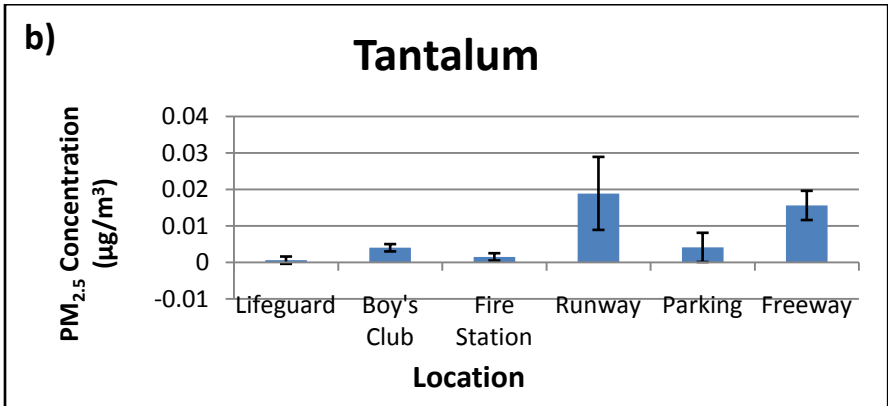
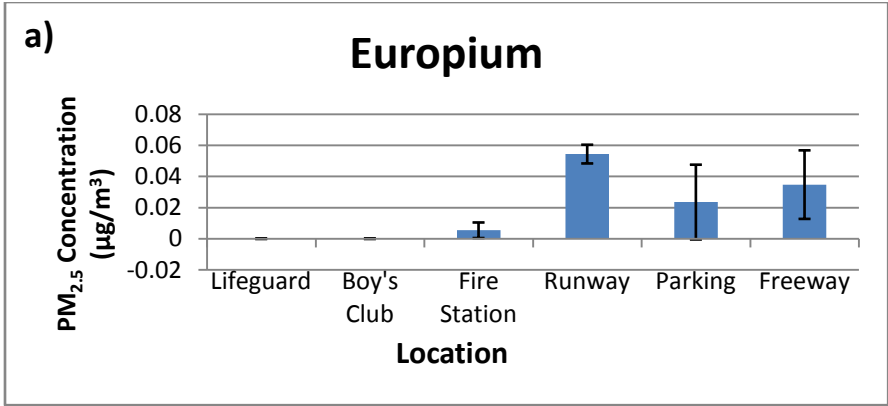


Figure 22 a – h. Elements characterized as potentially freeway-associated. Error bars denote standard error.

Uncategorized elements

Five elements measured at the sampling sites were elevated at both source locations: europium (Eu), tantalum (Ta), calcium (Ca), scandium (Sc) and thallium (Th) (Fig. 23 a - e). All of these except thallium and scandium showed a statistically significant effect of location (Table 3), but more data are needed before it can be determined if they are associated with a runway source, freeway source, or neither.



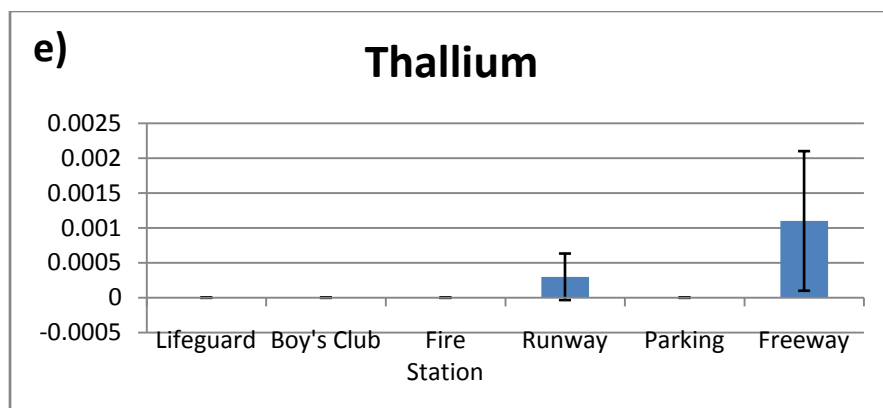


Figure 23a - e. Elements present at both runway and freeway locations. All except scandium and thallium exhibited a statistically significant effect of location.

Comparing Runway and Freeway source profiles to other locations

The elements identified as potentially runway or freeway-associated were used to construct emission profiles for both source locations. The chemical profiles of each of the sampling locations were compared to this source profile to determine to what extent the PM_{2.5} collected at different sampling locations might reflect the influence of runway or freeway PM. The number of shared elements between the sampling location and the source locations gives an indication of the influence of either runway or freeway emissions on PM at that site. When chemical profiles from other sampling locations are compared to the source profiles, varying degrees of overlap are observed.

The Lifeguard HQ profile shows elevations in two potential runway-associated elements, Sr and K. These were detected at higher levels than were measured at the Freeway. Sn is also elevated above both Runway and Freeway levels at the Lifeguard HQ (Fig. 24).

The Boys' Club residential site under the JWA flight path exhibits several elevations of potential runway-associated elements: In, Ag, Sr, K and Sb (Fig. 25). Zinc is also higher at this location than at either the Runway or Freeway sites.

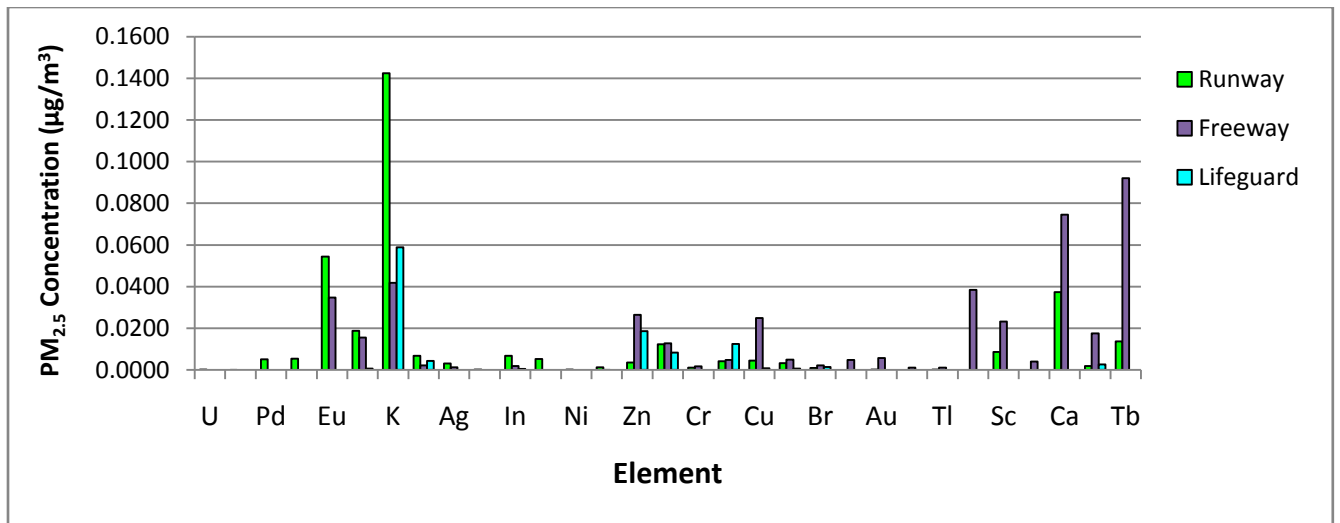


Figure 24. Comparison of the chemical profile of the Lifeguard sampling station with profiles of the Runway and Freeway locations.

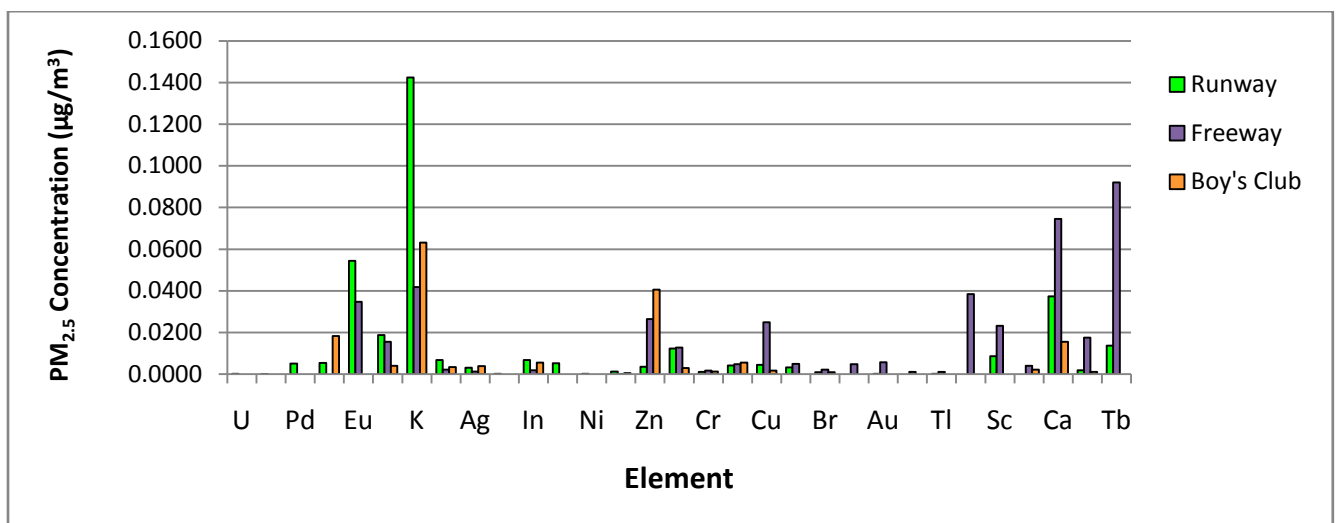


Figure 25. Comparison of the chemical profile of the Boys' Club sampling station with profiles of the Runway and Freeway locations.

When the two sampling locations adjacent to the runway and freeway are considered, elevations of both runway and freeway-associated elements are observed. The Fire Station, which is upwind of the runway but receives direct overflights of departing jets, shows clear elevations of runway-associated elements hafnium, nickel, europium and vanadium (Fig. 26). The freeway-associated elements terbium, cerium, scandium and gold are also elevated, possibly reflecting emissions from the diesel-powered fire engines operating intermittently at this location. The Parking location is downwind of, and adjacent to, both the runway and the 405 Freeway. It shows slight elevations in two runway-associated elements, palladium and hafnium (Fig. 27),

and elevations in four freeway-associated elements, rubidium, samarium, terbium and gold. It is possible that the frequent airport shuttle bus traffic observed at this site contributed to higher concentrations of freeway-associated elements at the Parking location.

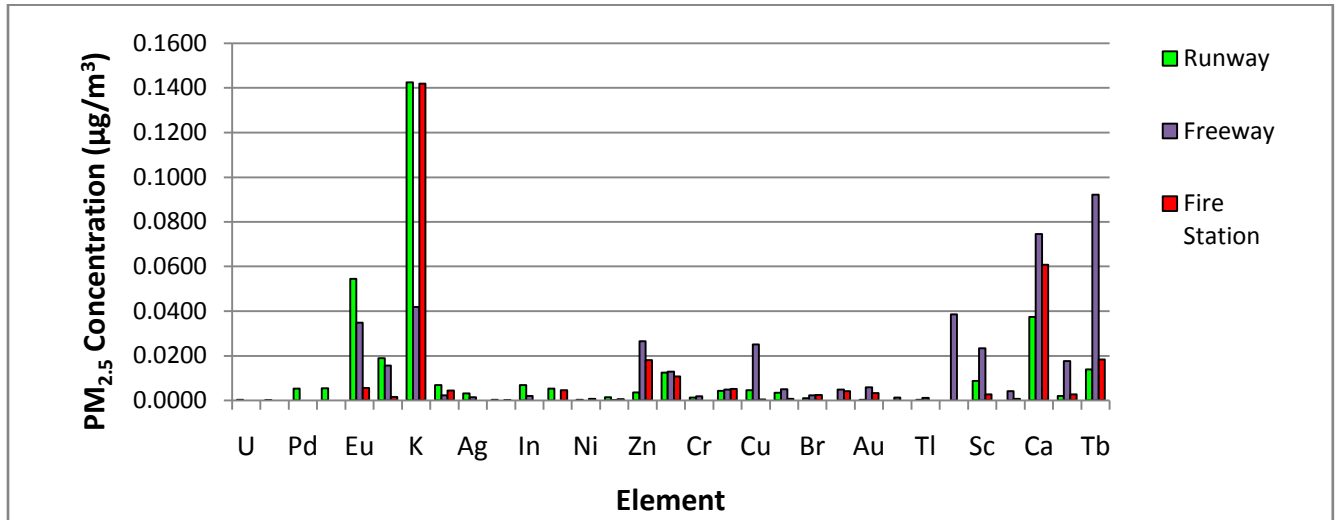


Figure 26. Comparison of the chemical profile of the Fire Station sampling site with profiles of the Runway and Freeway locations.

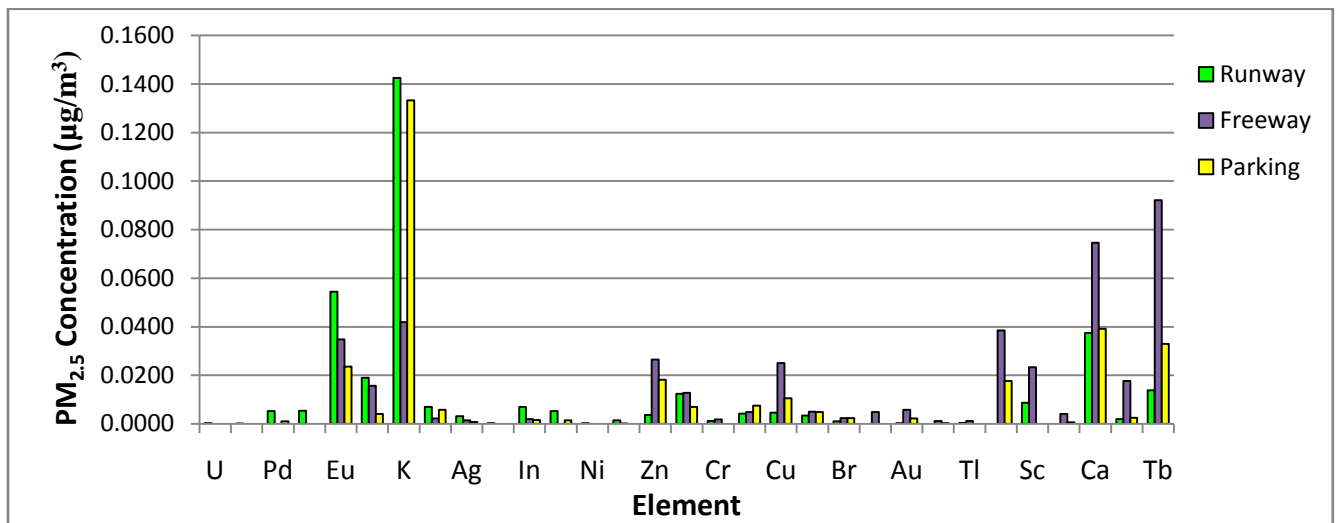


Figure 27. Comparison of the chemical profile of the Parking sampling site with profiles of the Runway and Freeway locations.

3.6 Results - Particle-associated Hydrocarbons

For discussion purposes, the suite of polycyclic aromatic hydrocarbons (PAHs) measured in the air samples will be divided into two groups: light PAH and heavy PAH. The light PAH category includes 38 compounds, from 1+2ethylnaphthalene (enap12) through xanthone (xanone). The heavier PAH category includes 70 compounds, from acenaphthenequinone (acquone) through dibenzo(b,K)fluoranthene (dbbKfl). Refer to Appendix IIa for a full listing of PAHs measured and their abbreviations. To improve the legibility of graphs in this section, heavy PAHs are divided into four groups and light PAHs are divided into three groups and displayed on separate charts.

Heavy PAHs

When chemical profiles are compared, PM_{2.5} concentrations of most heavier PAHs are higher at the Freeway than at the Runway sampling location (Fig. 28a-d). Only 7, 12-dimethylbenz(a)anthracene (dmban712) and benzo(b+j+K)fluoranthene (bbjkfl) are higher at the runway station than at any other location. The majority of PAHs measured reached their highest concentrations at the Freeway sampling location. Compounds exhibiting pronounced elevations at the freeway were: perinaphthenone (pnapone), anthraquinone (anrquone), fluoranthene (fluora), pyrene, 1-MeFl+C-MeFl/Py (c1mflpy), 1+3-methylfluoranthene (m_13fl), benzo(ghi)fluoranthene (bghifl), and chrysene-triphenylene (chr_tr).

Another group of heavy PAHs was detected at their highest concentrations at the Fire Station and Parking locations. This group included: BaP (bapyrn), perylene (peryle), 3-methylcholanthrene (mchol3), dibenz(a,h)acridine (dbahacr), dibenz(a,j)acridine (dbajacr), benzo(b)chrysene (bbchr), benzo(ghi)perylene (bghipe), anthanthrene (anthan), coronene (corone), and dibenzo(a,l)pyrene (dbalpyr).

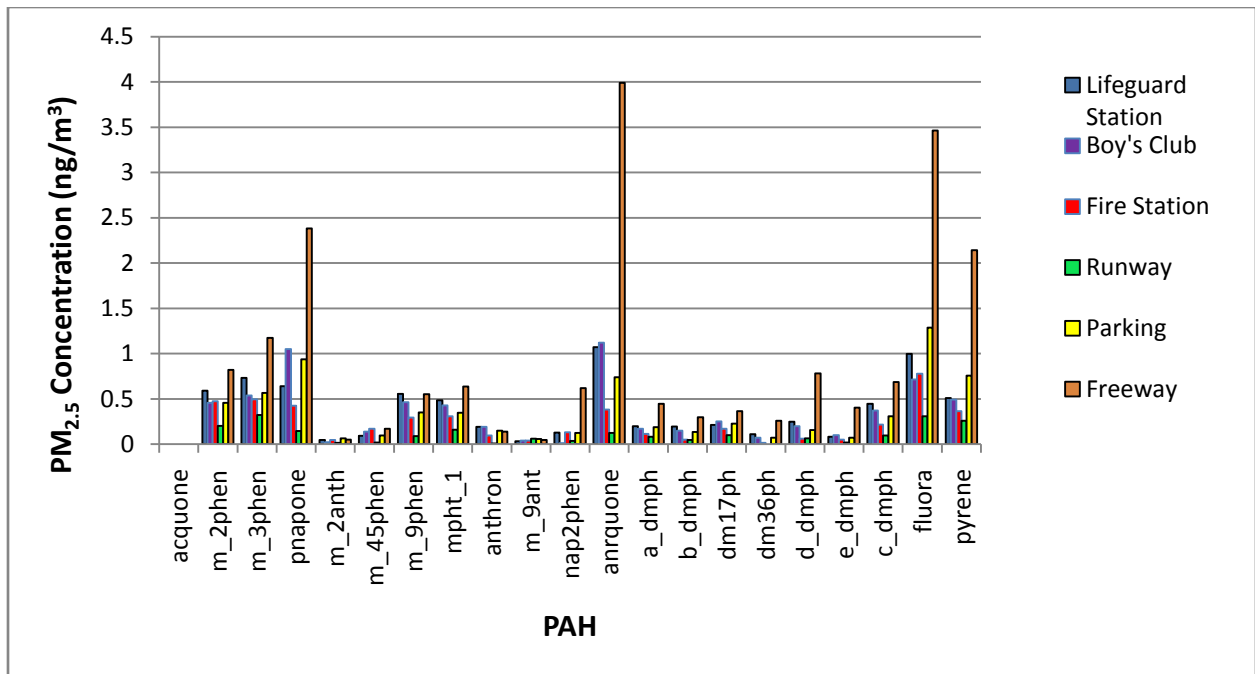


Figure 28a. Comparison of group 1 heavy PAHs in PM_{2.5} at all sampling locations.

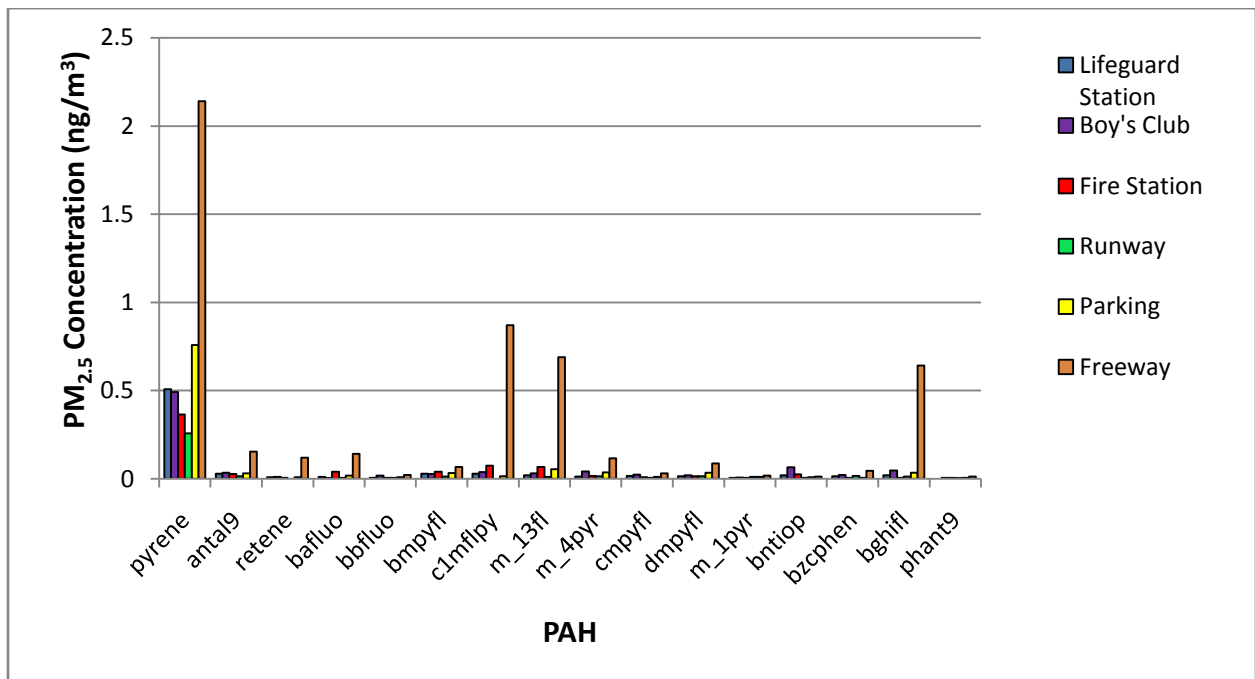


Figure 28b. Comparison of group 2 heavy PAHs in PM_{2.5} at all sampling locations.

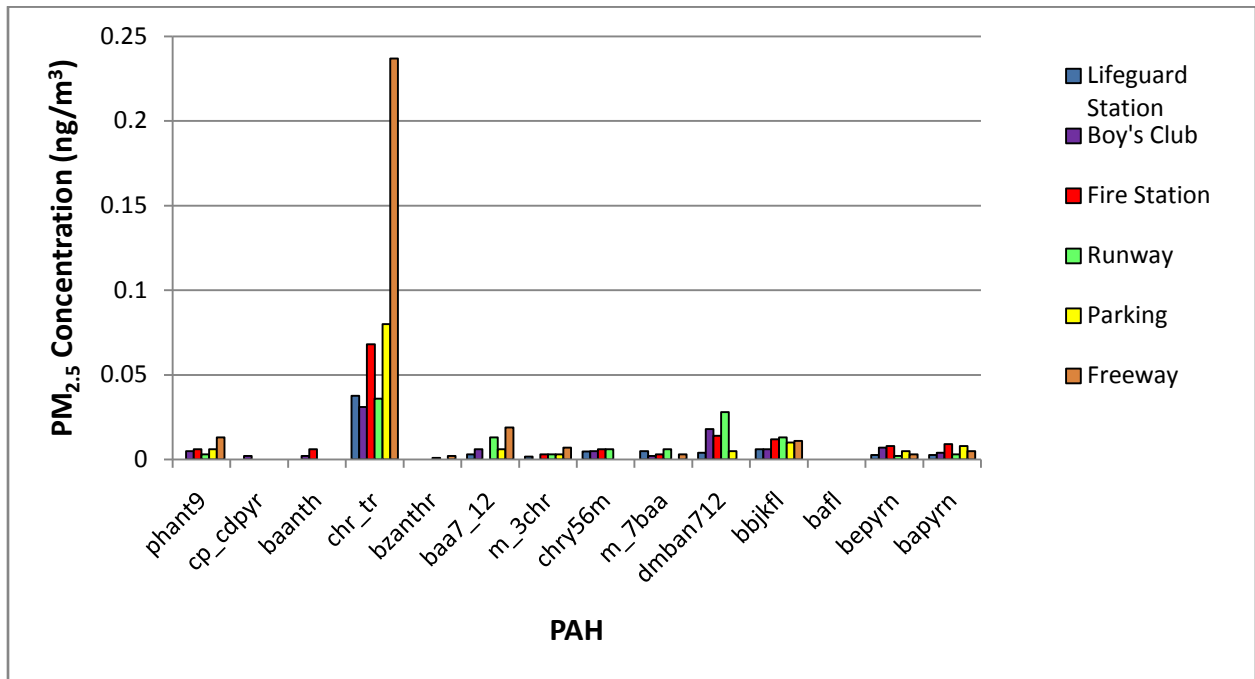


Figure 28c. Comparison of group 3 heavy PAHs in PM_{2.5} at all sampling locations.

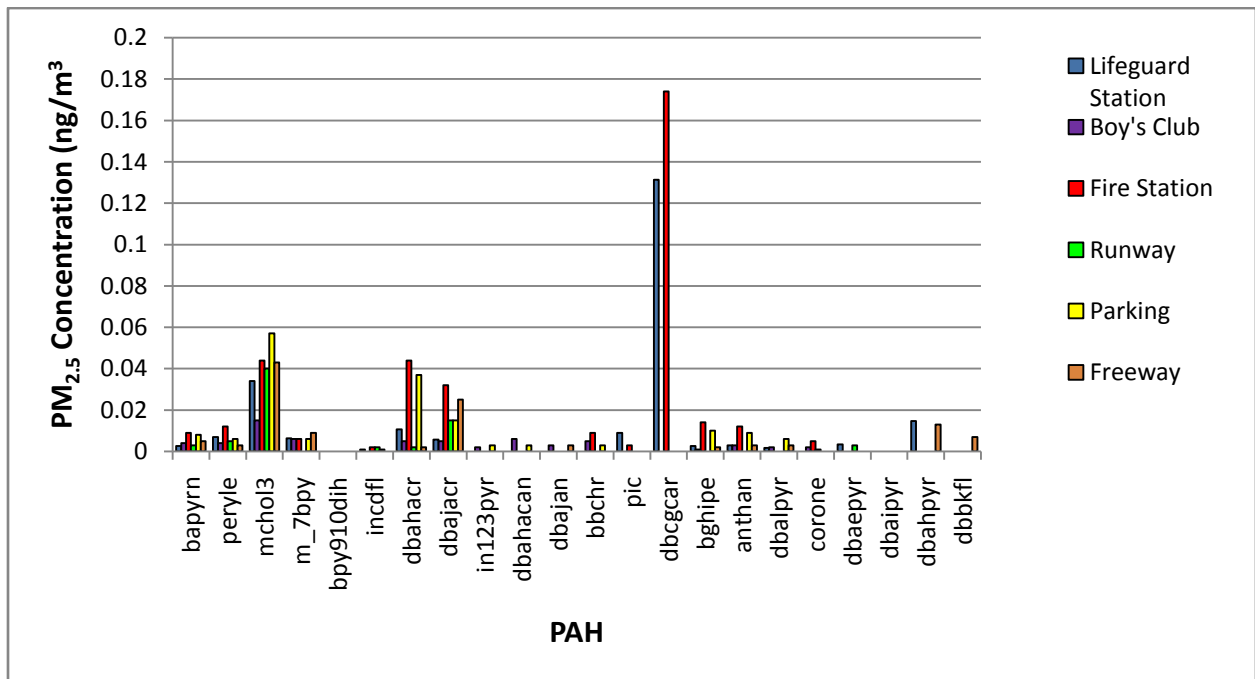


Figure 28d. Comparison of group 4 heavy PAHs in PM_{2.5} at all sampling locations.

Light PAH

In contrast to the heavy PAHs, several light PAHs were present at higher concentrations at the Runway site than at the Freeway (Fig. 29a-c). Compounds that were elevated at the Runway in comparison to the Freeway were: 2-methyl biphenyl (m_2bph), 3-methylbiphenyl (m_3bph), 4-methylbiphenyl (m_4bph), bibenz, b-trimethylnaphthalene (btmnap), c- trimethylnaphthalene (ctmnap), and ethyl-1-methylnaphthalene (em_21n).

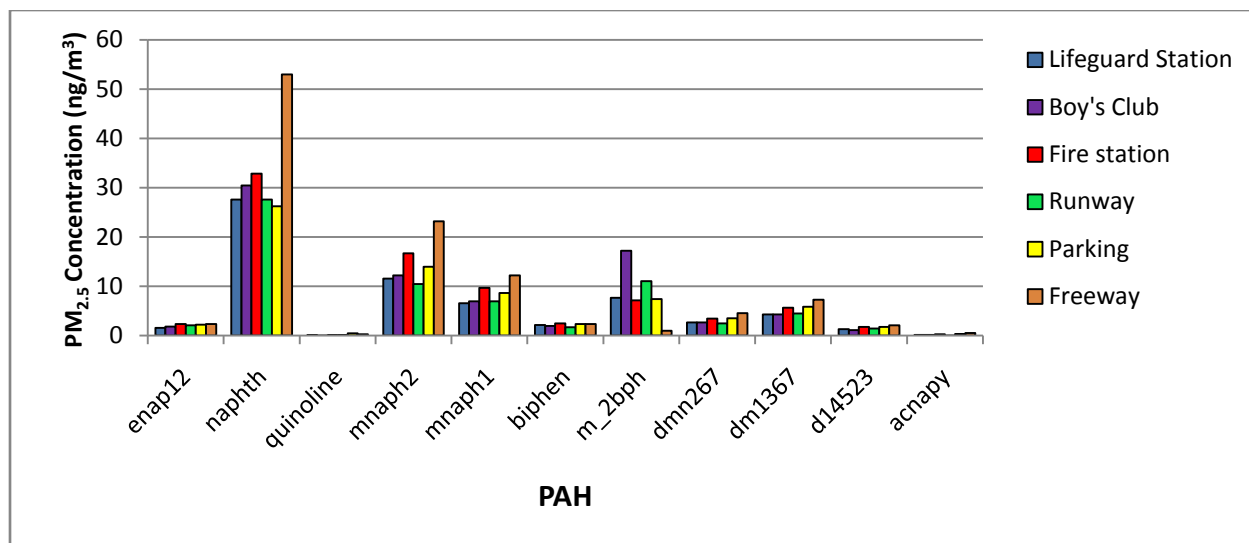


Figure 29a. Comparison of group 1 light PAHs in PM_{2.5} at all sampling locations.

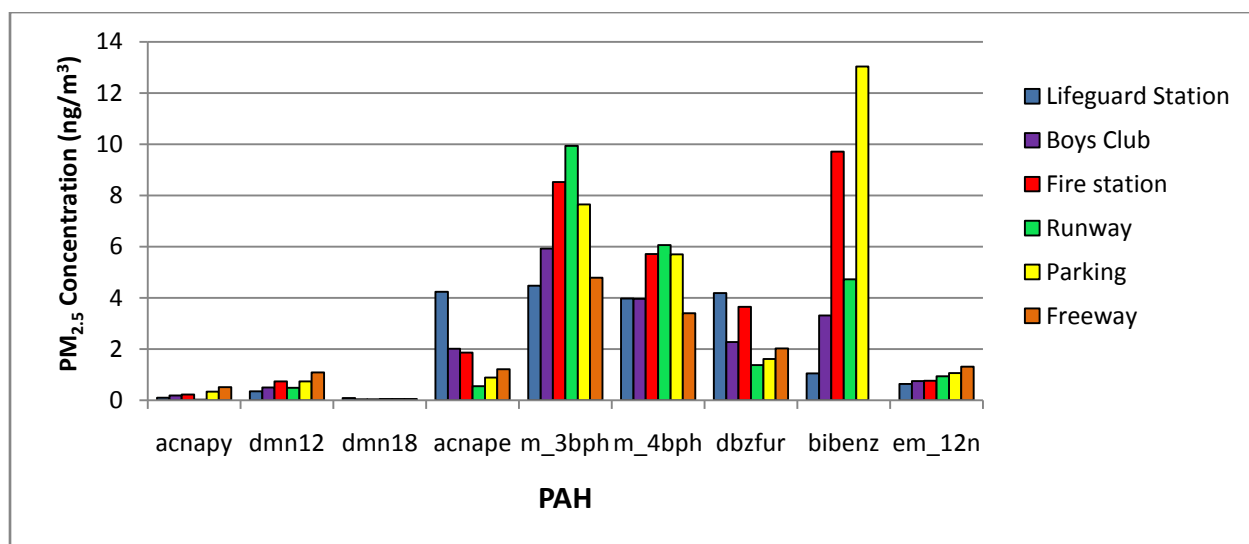


Figure 29b. Comparison of group 2 light PAHs in PM_{2.5} at all sampling locations.

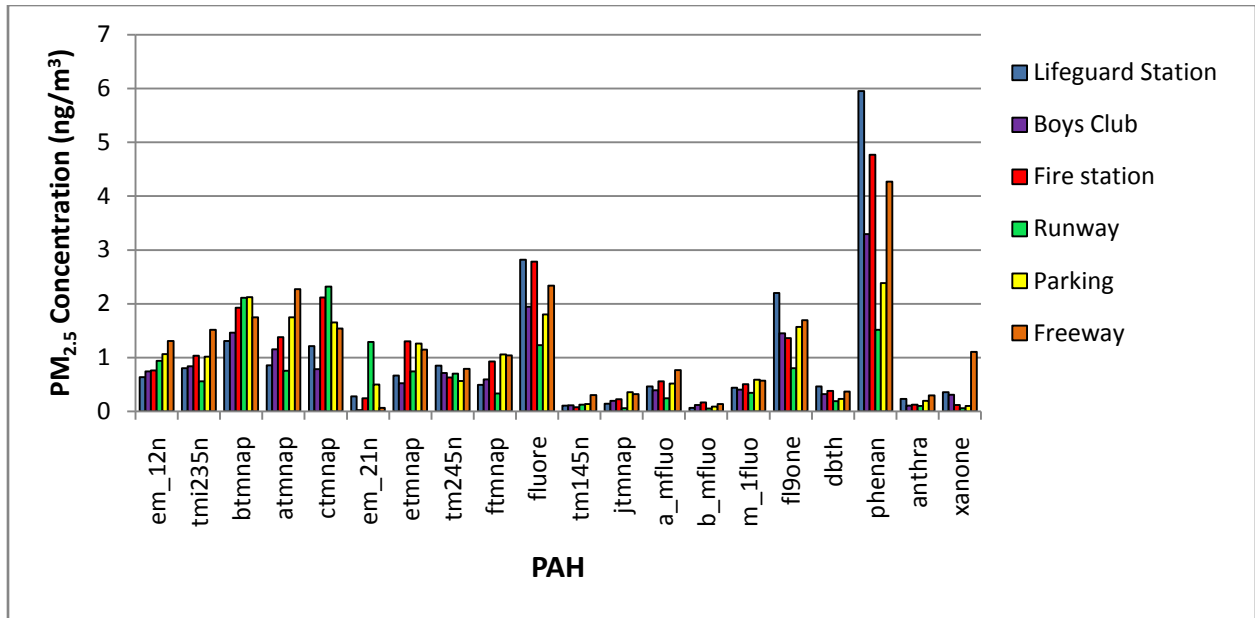


Figure 29c. Comparison of group 3 light PAHs in PM_{2.5} at all sampling locations.

Comparing sampling locations to source profiles

PAH profiles from the Runway and Freeway were compared to determine the degree of overlap of source profiles with each sampling location. The suite of 7 potential runway-associated PAHs was: 2-methyl biphenyl (m_2bph), 3-methylbiphenyl (m_3bph), 4-methylbiphenyl (m_4bph), bibenz, b-trimethylnaphthalene (btmnap), c- trimethylnaphthalene (ctmnap), and 2-ethyl-1-methylnaphthalene (em_21n). As sites moved closer to the Runway, the number of runway-associated PAHs elevated in air samples increased from 3 at Lifeguard HQ, and 4 at the Boys' Club, to 7 at the Fire Station.

The Lifeguard HQ showed elevations in three potential runway-associated PAHs, m_4bph, m_2bph, and bibenz. These three compounds were measured at concentrations below the runway measurements, but above freeway levels (Fig. 30a-c).

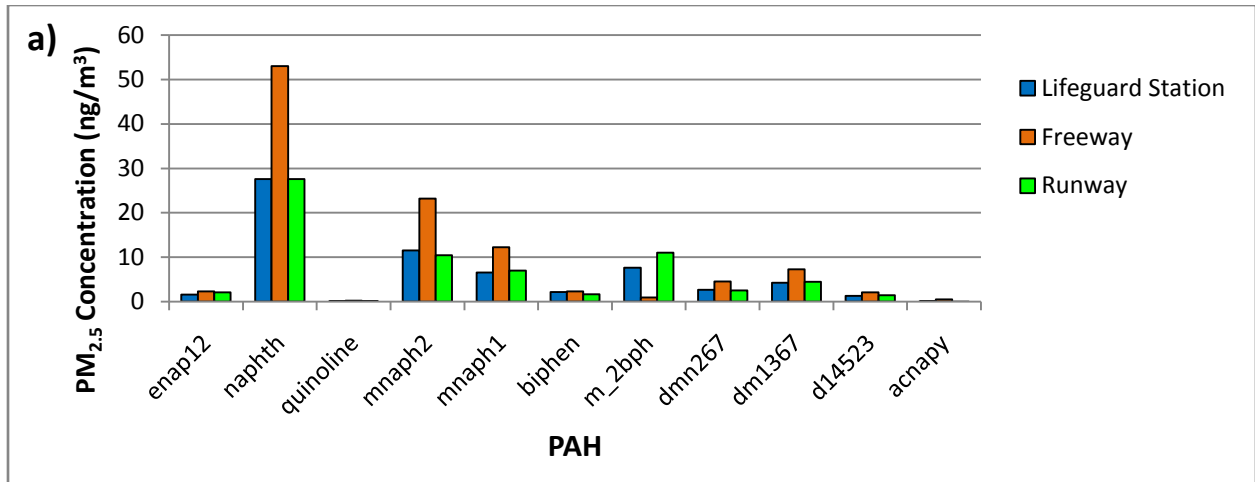


Figure 30a. Comparison of Group 1 light PAHs profile at Lifeguard HQ with profiles of the Runway and Freeway locations.

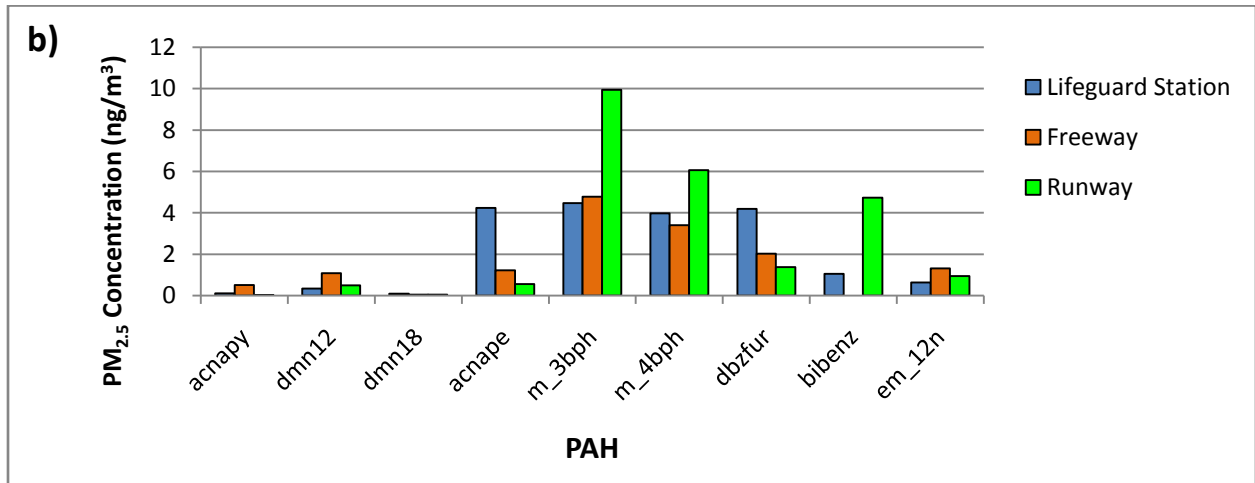


Figure 30b. Comparison of Group 2 light PAHs profile at Lifeguard HQ with profiles of the Runway and Freeway locations.

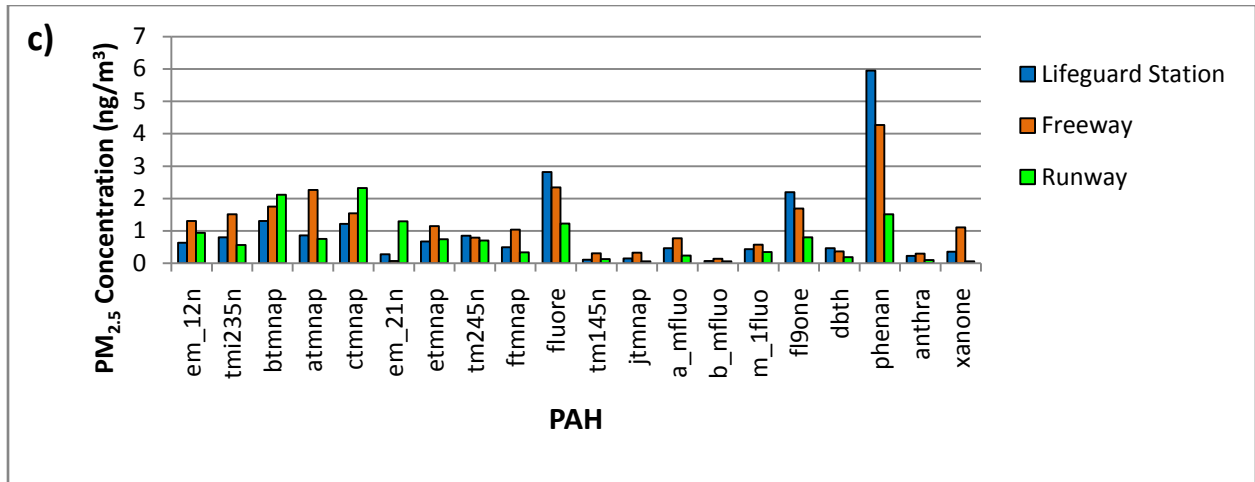


Figure 30c. Comparison of Group 3 light PAHs profile at Lifeguard HQ with profiles of the Runway and Freeway locations.

The Boys’ Club station, showed elevations in the same group of PAHs that were elevated at the Lifeguard HQ: m_4bph, m_2bph, and bibenz. In addition, elevations in m_3bph were detected at this site. The elevation in m_2bph was pronounced at the Boys’ Club. This site exhibited the highest m_2bph concentration of any of the sampling locations (Fig. 31a-c).

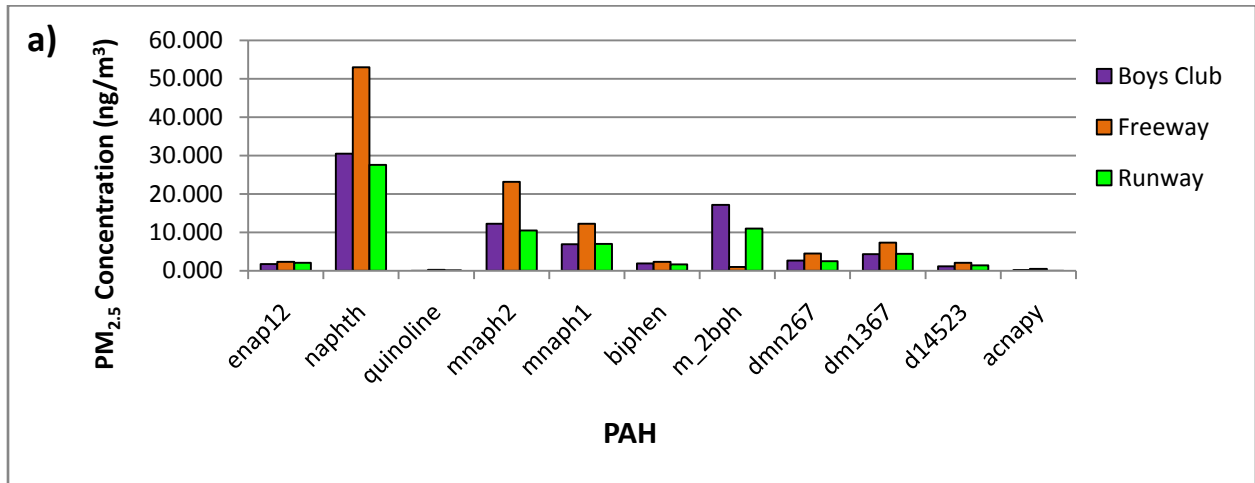


Figure 31a. Comparison of group 1 light PAHs profile at Boys’ Club with profiles of the Runway and Freeway locations.

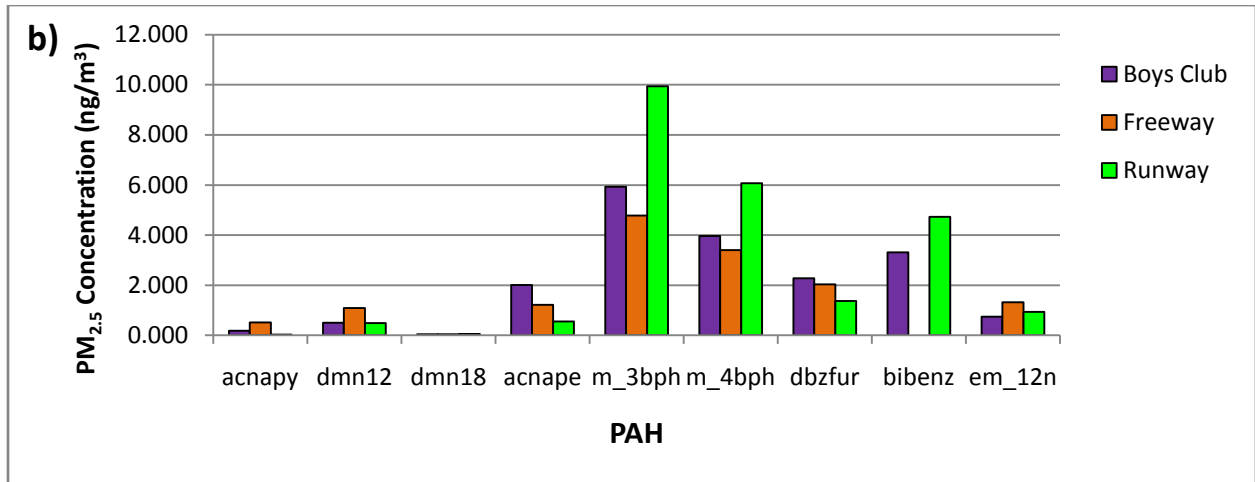


Figure 31b. Comparison of group 2 light PAHs profile at Boys’ Club with profiles of the Runway and Freeway locations.

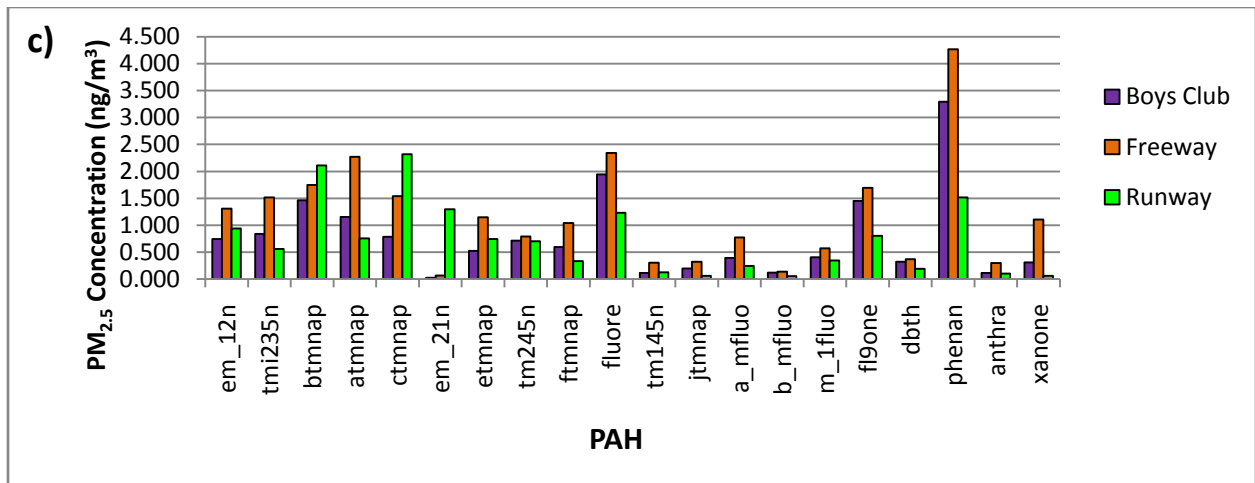


Figure 31c. Comparison of group 3 light PAHs profile at Boys’ Club with profiles of the Runway and Freeway locations.

The number of runway-associated light PAHs showing elevations increased to 7 at the Fire Station site. The same PAH elevations detected at the Boys' Club (m_2bph, m_3bph, m_4bph and bibenz) persisted at the Fire Station and additional runway-associated PAH elevations were detected: em_21n, ctmnap and btmnap (Fig. 32a-c).

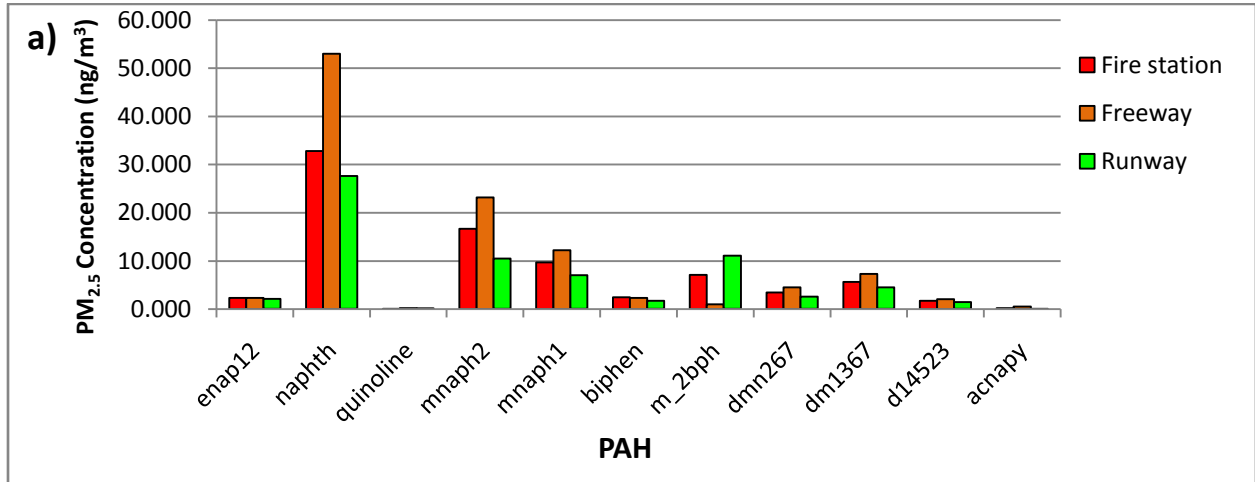


Figure 32a. Comparison of group 1 light PAHs profile at Fire Station with profiles of the Runway and Freeway locations.

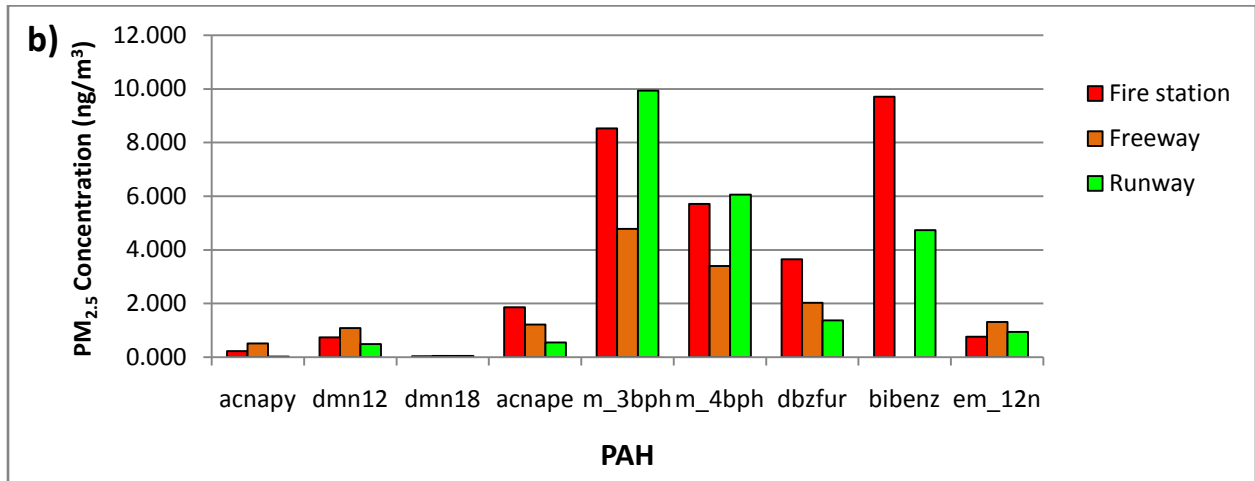


Figure 32b. Comparison of group 2 light PAHs profile at Fire Station with profiles of the Runway and Freeway locations.

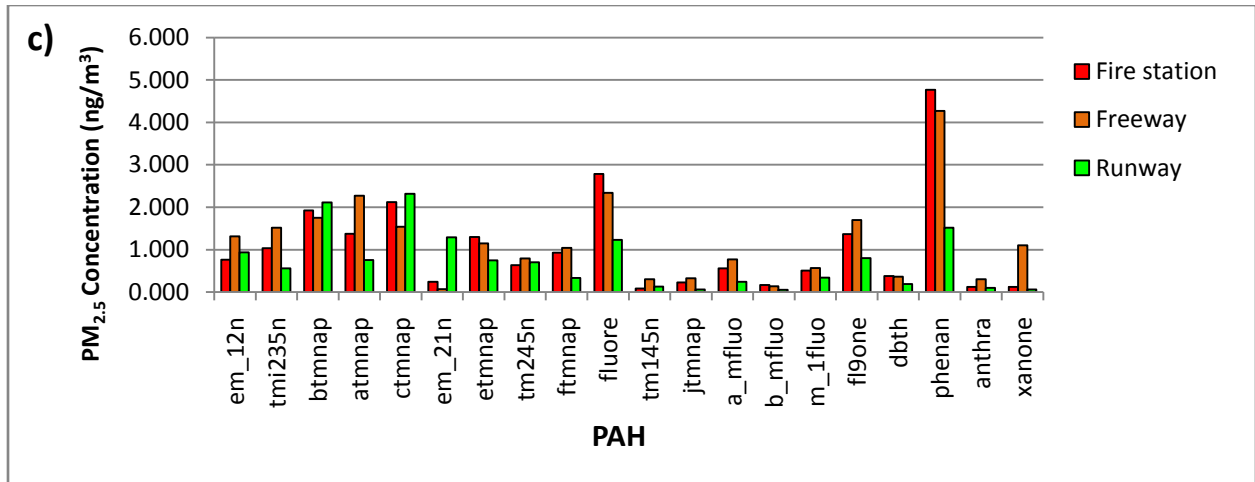


Figure 32c. Comparison of group 3 light PAHs profile at Fire Station with profiles of the Runway and Freeway locations.

The group of 7 PAHs that was elevated at the Fire Station remained elevated downwind of the airport at the Parking sampling location (Fig.33a-c).

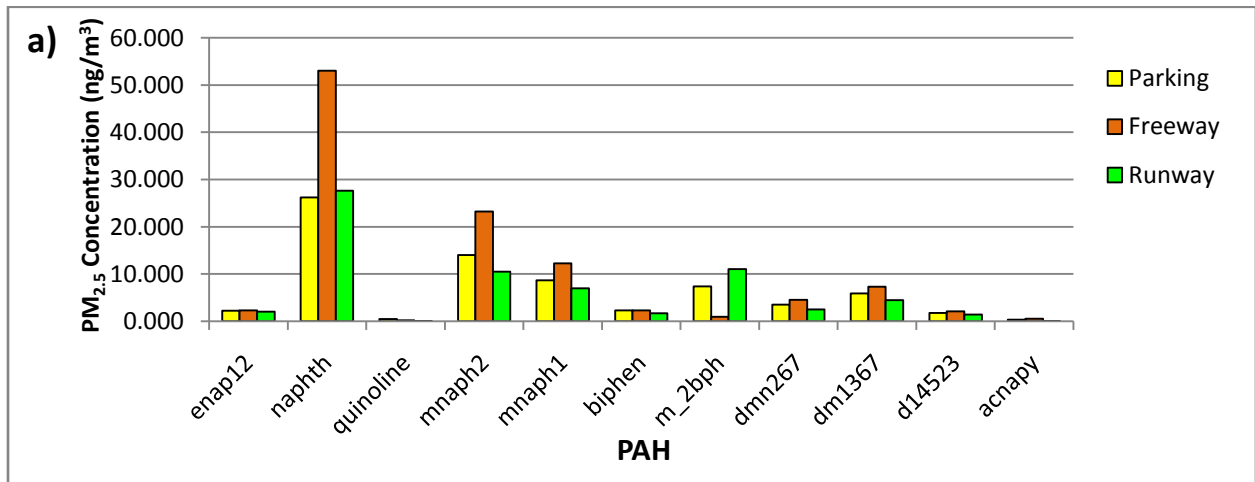


Figure 33a. Comparison of group 1 light PAHs profile at Parking site with profiles of the Runway and Freeway locations.

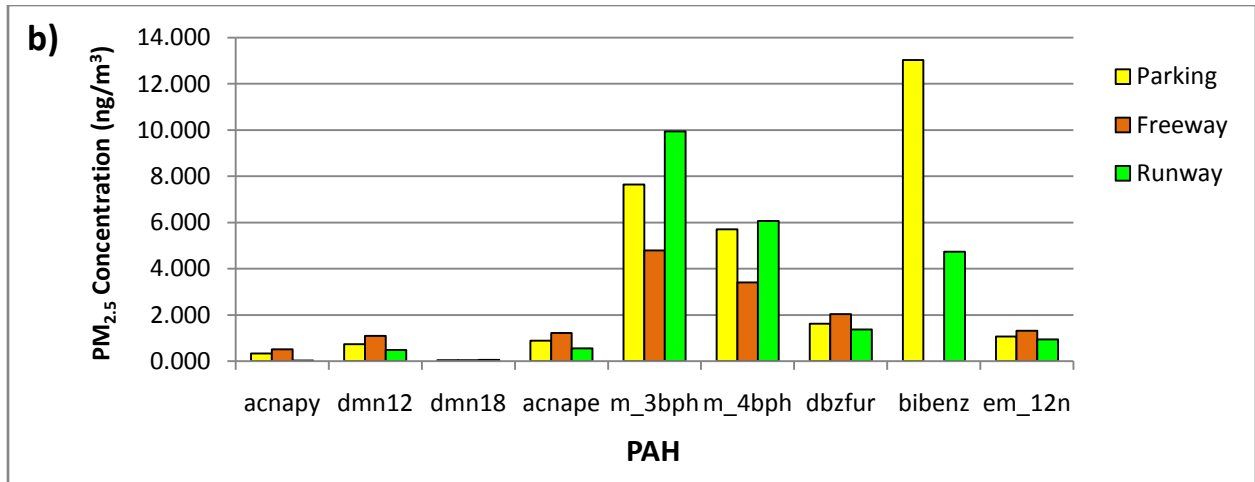


Figure 33b. Comparison of group 2 light PAHs profile at Parking site with profiles of the Runway and Freeway locations.

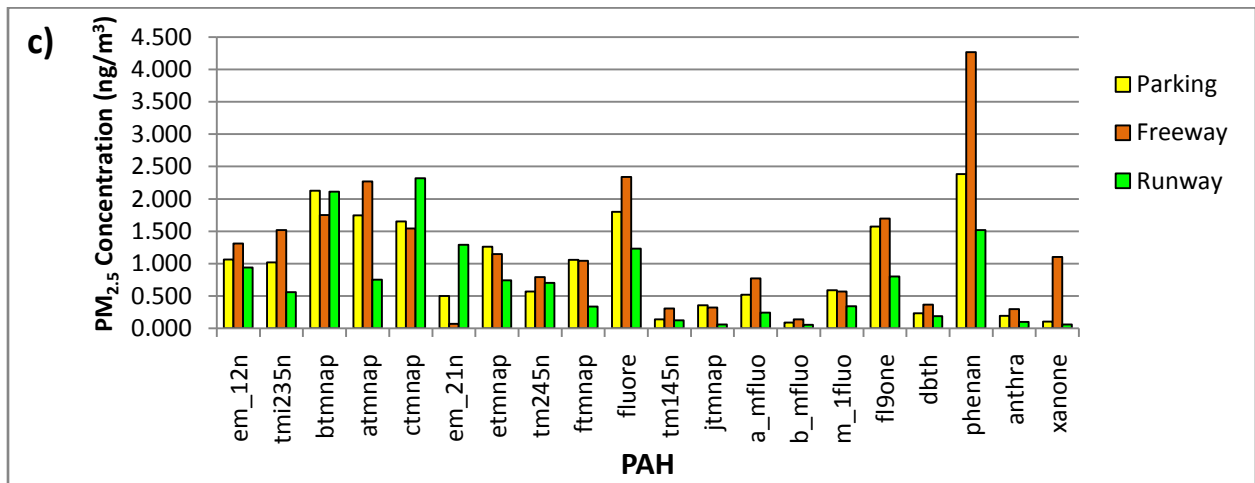


Figure 33c. Comparison of group 3 light PAHs profile at Parking site with profiles of the Runway and Freeway locations.

It is interesting to note that this consistent grouping of PAH elevations occurred even at upwind sites, suggesting that samplers were detecting aircraft emissions from jets taking off in the JWA departure corridor.

3.7 Discussion

Field Measurements of PM_{2.5}

Our data indicate that ambient PM_{2.5} at the locations sampled in Newport Beach is well within federal air quality standards. This study was designed to be a preliminary assessment of the feasibility of using field air sampling to detect differences in the amounts and chemical composition of PM_{2.5}. Our results demonstrate that this technique effectively detected measurable differences in concentrations of PM_{2.5} and the chemical composition of PM_{2.5} at different locations. Despite the minimal (n=3) sample size employed, statistically significant differences in both PM_{2.5} concentrations and chemical profiles were detected between locations. The fact that any results proved statistically significant at this level of replication suggests that a larger-scale sampling project would yield useful information. Our data also indicate that chemical profiles can be useful in distinguishing between airport-associated emissions, freeway emissions and urban background PM. This study identified differences in the chemical composition of emissions from airport and freeway sources that, with further study, may be useful as chemical “fingerprints” that would allow particulate emissions to be related to their source.

Our findings support previous work documenting elevated particle levels in areas adjacent to airports. At our Runway and runway-adjacent sampling stations, we measured levels of total particle mass and PM-associated organic carbon, sulfate and metals which were elevated above freeway levels. In the case of sulfate, this elevation persisted at locations up to 10 Kilometers from the airport, with the coastal Lifeguard HQ site under the jet departure path exhibiting higher PM_{2.5}-sulfate than the Freeway location. Westerdahl et al. (2008) documented elevations in ultrafine particles (UFP) ranging from 580-3800 counts/cm³ downwind of Los Angeles International (LAX) Airport. Other downwind locations in the study detected elevated black carbon and PM-PAH elevations ranging between 18-36ng/m³. Mean black carbon (BC) concentrations at the LAX study sites ranged between 0.3 and a high near the 710 Freeway of 22.7µg/m³. The 105 Freeway, with a lower volume of diesel truck traffic, averaged 1.5 µg/m³ of black carbon. In comparison, mean concentrations of black (elemental) carbon measured at the Freeway location in this study were comparable to measurements at the low volume freeway near LAX (1.5 µg/m³ vs 1.0µg/m³). Levels of elemental carbon (EC) measured at the JWA runway site were in the low end of EC ranges measured near LAX airport boundaries (JWA: 0.87-1.41µg/m³ vs. LAX: 1.8-3.8µg/m³). This is to be expected since the volume of air traffic handled at JWA is much lower than at LAX. The Westerdahl study documented short-term ambient PM levels and particle counts associated with individual aircraft operations. Our results suggest that these particle peaks documented for individual take-offs and landings translate into measurably increased concentrations of particle-associated metals and PAHs when averaged over hours.

Airport emissions detectable farther from source

Our measurements of potentially runway-associated elements at sites adjacent to the airport support and expand upon studies that have detected peaks in aircraft-related UFP much farther from airport operations than expected. Aircraft emission plumes have been measured up to 900m downwind of an LAX runway used for takeoffs (Westerdahl et al., 2008) and in residential areas up to 660m downwind from the Santa Monica Regional Airport (Hu et al., 2009). Aircraft-generated UFPs persist much farther from their source than UFP from roadway-traffic studies would predict. Hu et al. hypothesize that the dispersion patterns of aircraft UFPs differ from those measured in roadway studies because they are generated at a much greater magnitude. The large volumetric pulse of high concentration emissions produced by aircraft takes longer to disperse, and is therefore detectable at greater distances from the point of emission. The long persistence time of aircraft-generated UFP can contribute to highly elevated particle concentrations near airports.

Our data suggest that elevated levels of potential airport-associated elements measured at the Fire Station likely reflect emissions from aircraft overflights. During field sampling, aircraft were observed to pass directly over this station at low elevations, approximately 300-500m, during take-offs. This proximity of overflights, coupled with the fact that large amounts of fuel are being combusted on takeoff make it plausible that aircraft particulate emissions are measurable at these locations. A similar effect was documented by Westerdahl et. al. (2008) at sampling stations near LAX. They detected high levels of aircraft-related UFP at locations greater than 300m downwind of the airport. These elevations were attributed to aircraft on approach passing overhead. Additionally, field monitoring at LAX has documented elevations in ambient concentrations of airport-associated trace metals and measurable deposition of these metals on plants adjacent to the runway and in sand dune habitats overflown by aircraft (Venkatesan and Boyle, 1999). Persistent complaints of soot deposition from residents under the flight path of both LAX and JWA airports provides further anecdotal evidence that these increased particle loads persist beyond 1000m from the airport itself.

Our findings of potential runway-associated emissions in locations Kilometers away from the airport (e.g. sulfate at the Lifeguard HQ) support the results of previous airport studies. If validated with more extensive testing, these data suggest that significantly increased areas around airports should be considered potentially influenced by airport emissions. These findings suggest that the spatial scale of air sampling near airports should be increased from the scale of meters to kilometers to better understand the dynamics of aircraft emission transport.

3.8 Conclusions and Recommendations for Future Research

This study was designed as a preliminary assessment of the feasibility of using field air sampling to detect differences in the amounts and chemical composition of PM_{2.5} in relation to various sources. These objectives were met. Despite the minimal sample size (n=3), statistically significant differences in tested variables were detected between locations. The fact that any results proved statistically significant at this level of replication suggests that a larger-scale sampling project would yield additional useful information. Our data also indicate that chemical profiles can be useful in distinguishing between airport-associated emissions, freeway emissions and urban background PM.

Follow-up research to consider:

- Increase the statistical power of the current data set by adding more sampling periods at the present study locations.
- Add sampling stations in locations of concern to the airport or community, such as airport facilities or the Upper Newport Bay Ecological Reserve. This estuary has a history of eutrophication and nuisance blooms of macroalgae (Kamer et al., 2003 ; Boyle et al., 2004). It is unclear whether the amount of aircraft-derived nitrate and ammonium deposition to the bay is significant. This potential environmental impact is not addressed by our current data set.
- Add sampling stations at a set number of locations that provide a more defined spatial pattern around the airport at crosswind and downwind locations.
- Design a “before and after” field sampling study to assess the effectiveness of proposed mitigation strategies before extensive resources are expended on them.

Implications for airport planning and mitigation

Based on our findings, and those of similar studies at other airports, it seems reasonable to direct future mitigation efforts towards reducing airport particulate emissions when possible. JWA has already implemented several measures that accomplish this, including:

- Use of low-emission electric vehicles and support equipment on the commercial ramp.
- Utilization of diesel-powered preconditioned air units by commercial aircraft along with ground-based electrical power in place of jet-fueled onboard Auxiliary Power Unit (APU). The ground-based units burn about 10 times less fuel than APU's, reducing costs and lowering carbon emissions.
- Installation of electric charging stations for ground service equipment and Airport vehicles.
- Required operation of fleet vehicles, such as taxi cabs, using clean burning compressed natural gas (CNG) or other cleaner burning fuel alternatives. JWA's taxi provider, Orange County Yellow Cab, uses 100 percent CNG vehicles.

- As part of the multi-year John Wayne Airport Improvement Program, older emergency generators will be replaced with newer clean-burning generators.

Additional PM mitigation strategies that can be considered include:

- Encourage airlines to switch to lower sulfur fuels for aircraft. The EPA is working to encourage adoption of new ultra-low sulfur fuels.
- Employ “single engine taxiing” practices which are likely to decrease hydrocarbon emissions (Herndon and Wood, 2009).
- Continue research that increases our understanding of aircraft emissions.

Given the limited information currently available on airport-associated emissions, it is especially important to collect field data. Several recent studies have demonstrated that current values used for airport emissions modeling do not accurately reflect real-world conditions (Herndon and Wood, 2009; Whitefield, Hagen et al., 2008). Field studies are the most direct and effective way to improve the accuracy of airport emissions models, to measure actual emission exposure levels in the community, and to identify productive mitigation strategies.

3.9 Acknowledgements

This study would not have been possible without the assistance of many people. The author would like to thank Mr. Homer Bludau, retired City Manager of Newport Beach, Mr. Dave Kiff, current City Manager of Newport Beach and Mr. Thomas Edwards for the opportunity to carry out this study. This research was greatly assisted by Mr. Alan L. Murphy, JWA Airport Director, who allowed us to station samplers on JWA property and Mr. Jack Jennrich for his able assistance with the many logistic challenges involved. Thanks are also due to Mr. Mory Mohtashami, Branch Chief of the State of California Department of Transportation, District 12 and his staff for their assistance in obtaining permits for freeway sampling, and Mr. Rex McConnell of CalTrans for his assistance in identifying and safely establishing our sampling location on the 5 Freeway. We also thank the staff of Newport Beach Lifeguard HQ and the firefighters of Station 8 for allowing us to station samplers at their facilities, and for going above and beyond the call of duty by helping to carry 100+ pounds of air sampling equipment up four flights of stairs. Many thanks to Dr. Richard Ambrose, UCLA Dept. of Environmental Science and Engineering for helpful discussions on statistical analyses and Mr. Larry Boyle for his expert field assistance and consultations on chemistry issues. Finally, special thanks to Ms. Susan Bennion-Boyle and Dr. Mark Sudol for their invaluable logistic support.

IV. LITERATURE CITED

Barbosa, S. et al. October 1999. Air Monitoring Study at Los Angeles International Airport, South Coast Air Quality Management District, Diamond Bar, CA,

Boyle, Karleen A., K. Kamer and P. Fong. 2004. Spatial and temporal patterns in sediment and water column nutrients in a eutrophic Southern California estuary. *Estuaries and Coasts*. 27(3): 378-388.

Carslaw, D.C., S.D. Beevers, K. Ropkiins and M.C. Bell. 2006. Detecting and quantifying aircraft and other on-airport contributions to ambient nitrogen oxides in the vicinity of a large international airport. *Atmos. Environ.* 40: 5424-5434.

Christoforou, C.S., L.G. Salmon, M.P. Hannigan, P.A. Solomon and G.R. Cass. 2000. Trends in fine particle concentration and chemical composition in Southern California. *J. Air and Waste Manage. Assoc.* 50: 43-53.

Essner, S., C. Garcia and K. Kasza. December 1992. Newport Beach Fallout Study. South Coast Air Quality Management District.

Fine, P.M., S. Shen, and C. Sioutas. 2004. Inferring the sources of fine and ultrafine particulate matter at downwind receptor sites in the Los Angeles Basin using multiple continuous measurements. *Aerosol Sci. Technol.* 38: 182-195.

Geller, M.D., Fine, P.M., and Sioutas, C., 2004. The relationship between real-time and time-integrated coarse (2.5-10 μ m), intermodal (1-2.5 μ m), and fine (<2.5 μ m) particulate matter in the Los Angeles Basin. *J. Air & Waste Manage. Assoc.* 54: 1029-1039.

Herndon, Scott C., J.T. Jayne, P. Lobo, T.B. Onasch, G. Fleming, D. Hagen, P.D. Whitefield and R.C. Miake-Lye. 2008. Commercial Aircraft Engine Emissions Characterization of in-Use Aircraft at Hartsfield-Jackson Atlanta International Airport. *Environ. Sci. Technol.* 42:1877–1883.

Herndon, S.C., E.Z. Wood, M.J. Northway, R. Miake-Lye, L. Thornhill, A. Beyersdorf, B.E. Anderson, R. Dowlin, W. Dodds, and W. B. Knighton. 2009. Aircraft Hydrocarbon Emissions at Oakland International Airport. *Environ. Sci. Technol.* 43: 1730-1736.

Hu, Shishan, S. Fruin, K. Kozawa, S. Mara, A.M. Winer and S.E. Paulson. 2009. Aircraft emission impacts in a neighborhood adjacent to a general aviation airport in Southern California. *Environ. Sci. Technol.* 43: 8039-8045.

Hughes, L.S., J.O. Allen, P. Bhave, M.J. Kleeman, G.R. Cass, D.Y., D.P. Fergenson, B.D. Morrical, and K.A. Prather. 2000. Evolution of atmospheric particles along trajectories crossing the Los Angeles Basin. *Environ. Sci. Technol.* 34: 3058-3068.

Jerrett, M., R.T. Burnett, R.J. Ma, C.A. Pope, D. Krewski, K.B. Newbold, G. Thurston, Y.L. Shi, N. Finkelstein, E.E. Calle, and M.J. Thun. 2005. Spatial analysis of air pollution and mortality in Los Angeles. *Epidemiology* 16, 727-736.

Kamer, Krista, K.A. Boyle and P. Fong. 2001. Macroalgal Bloom Dynamics in a Highly Eutrophic Southern California Estuary. *Estuaries* 24(4):623-635.

Kleeman, M.J., L.S. Hughes, J.O. Allen, and G.R. Cass. 1999. Source contribution to the size and composition distribution of atmospheric particles: Southern California in September 1996. *Environ. Sci. Technol.* 33: 4331 – 4341.

Lankey, R.L., C.I. Davidson, F.C. McMichael. 1998. Mass balance for lead in the South Coast air Basin: an update. *Environmental Research* 78(2): 86-93.

Luria, M., R.L. Tanner, R.J. Valente, S.T. Bairai, D. Koracin, and A.W. Gertler. 2005. Local and transported pollution over San Diego, California. *Atmospheric Environment*. 39: 6765-6776.

Oberdorster, G. 2001. Pulmonary effects of inhaled ultrafine particles. *International Archives of Occupational and Environmental Health*. 74:1-8.

Onasch, T.B., J.T. Jayne, S.C. Herndon, P. Mortimer, D.R. Worsnop, R.C. Miake-Lye, et al. 2008. Chemical Properties of Aircraft Engine Particulate Exhaust Emissions Sampled during APEX. In prep.

Pope, C.A., R.T. Burnett, M.J. Thun, E.E Calle, D. Krewski, K. Ito and G.D. Thurston. 2002. Lung cancer, cardiopulmonary mortality, and long-term exposure to fine particulate air pollution. *Journal of the American Medical Association* 287, 1132-1141.

Rogers, F., P. Arnott, B. Zielinska, J. Sagebiel, K.E. Kelly, D. Wagner, J.S. Lighty, and A.F. Sarofim. 2005. Real-time measurements of jet aircraft engine exhaust. *J. Air & Waste Manage. Assoc.* 55: 583-593.

Schürmann, G., K. Schafer, C. Jahn, H. Hoffmann, M. Bauerfeind, E. Fleuti and B. Rappengluck. 2007. The impact of NOx, CO and VOC emissions on the air quality of Zurich airport. *Atmos. Environ.* 41: 103-118.

Singh, M., Jaques, P.A., and Sioutas, C., 2002. Size distribution and diurnal characteristics of particle-bound metals in source and receptor sites of the Los Angeles Basin. *Atmospheric Environment* 36: 1675-1689.

Singh, M. K. Bowers, and C. Sioutas. 2006. Seasonal and spatial trends in particle number concentrations and size distributions at the children's health study sites in Southern California. *Journal of Exposure Science and Environmental Epidemiology* 16: 3-18.

USEPA. 1993. EPA's Saturation Monitor Repository. *AMTIC News* 450/N-93-093.

Venkatesan, M.I. and K.A. Boyle. 1998. Analysis of Hydrocarbons and Trace Metals in Environmental Samples in support of Los Angeles International Airport 2015 Master Plan Expansion Project EIS/EIR, Institute of Geophysics and Planetary Physics, University of California at Los Angeles and Department of Organismic Biology Ecology and Evolution, University of California at Los Angeles.

Westerdahl, D. S. Fruin, T. Sax, P.M. Fine and C. Sioutas. 2005. Mobile platform measurements of ultrafine particles and associated pollutant concentrations on freeways and residential streets in Los Angeles. *Atmospheric Environment*. 39: 3597-3610.

Westerdahl, D., S.A. Fruin, P.L. Fine, C. Sioutas. 2008. The Los Angeles International Airport as a source of ultrafine particles and other pollutants to nearby communities. *Atmospheric Environment* 42: 3143-3155.

Whitefield, P.D., P. Lobo and D.E. Hagen et al. 2008. Summarizing and interpreting aircraft gaseous and particulate emissions data. Airport Cooperative Research Program (ACRP) Report 9. Transportation Research Board. www.TRB.org

V. List of Tables

| | | |
|----------------------|---|-----------|
| Table 1 | Summary of the properties of atmospheric particles..... | 7 |
| Table 2 | Dates and locations of PM _{2.5} air sampling..... | 14 |
| Table 3 | Results of statistically significant 1-factor ANOVAs comparing concentrations of ambient PM _{2.5} elements at study sites..... | 28 |

VI. List of Figures

| | |
|---|--------------|
| Figure 1. Mean concentrations of total particle mass in PM _{2.5} at sampling locations..... | 16 |
| Figure 2. Mean concentrations of PM _{2.5} total carbon..... | 17 |
| Figure 3. Percentages of organic and elemental carbon in PM _{2.5} at sampling locations..... | 18 |
| Figure 4. Mean concentrations of PM _{2.5} organic and elemental carbon at sampling locations.... | 18 |
| Figure 5. Mean concentrations of PM _{2.5} nitrate, ammonium and sulfate..... | 19 |
| Figure 6. Percentages of total particle mass in PM _{2.5} and PM ₁₀ fractions at source locations..... | 20 |
| Figure 7. Elemental and organic carbon in PM _{2.5} and PM ₁₀ fractions of source locations..... | 20 |
| Figure 8 . Mean concentrations of crustal metals at sampling locations..... | 21 |
| Figure 9. Division of crustal metals between PM ₁₀ and PM _{2.5} fractions at source locations..... | 21 |
| Figure 10. Mean values of potentially toxic metals at sampling locations..... | 22 |
| Figure 11. Mean nickel concentrations at sampling locations..... | 22 |
| Figure 12. Mean vanadium concentrations at sampling locations..... | 23 |
| Figure 13. Mean concentrations of lead at sampling locations..... | 23 |
| Figure 14. Mean concentrations of copper at sampling locations..... | 24 |
| Figure 15. Mean concentrations of cadmium at sampling locations..... | 24 |
| Figure 16. Mean concentrations of chromium at sampling locations..... | 25 |
| Figure 17. Mean concentrations of zinc at sampling locations..... | 25 |
| Figure 18. Mean concentrations of tin at sampling locations..... | 26 |
| Figure 19 a- c. Elements specific to one sampling location..... | 26-27 |
| Figure 20 a- e. Elements characterized as potentially runway-associated..... | 29-30 |
| Figure 21 a – c. Elements categorized as runway-associated that exhibited a statistically significant effect of sampling location..... | 30-31 |
| Figure 22 a – h. Elements characterized as potentially freeway-associated..... | 31-33 |

| | |
|--|--------------|
| Figure 23a - e. Elements present at both runway and freeway locations..... | 34-35 |
| Figure 24. Comparison of the chemical profile of the Lifeguard sampling station with profiles of the Runway and Freeway locations.. | 36 |
| Figure 25. Comparison of the chemical profile of the Boy’s Club sampling station with profiles of the Runway and Freeway locations..... | 36 |
| Figure 26. Comparison of the chemical profile of the Fire Station sampling site with profiles of the Runway and Freeway locations..... | 37 |
| Figure 27. Comparison of the chemical profile of the Parking sampling site with profiles of the Runway and Freeway locations..... | 37 |
| Figure 28a. Comparison of group 1 heavy PAHs in PM _{2.5} at all sampling locations..... | 39 |
| Figure 28b. Comparison of group 2 heavy PAHs in PM _{2.5} at all sampling locations..... | 39 |
| Figure 28c. Comparison of group 3 heavy PAHs in PM _{2.5} at all sampling locations..... | 40 |
| Figure 28d. Comparison of group 4 heavy PAHs in PM _{2.5} at all sampling locations..... | 40 |
| Figure 29a. Comparison of group 1 light PAHs in PM _{2.5} at all sampling locations..... | 41 |
| Figure 29b. Comparison of group 2 light PAHs in PM _{2.5} at all sampling locations..... | 41 |
| Figure 29c. Comparison of group 3 light PAHs in PM _{2.5} at all sampling locations..... | 42 |
| Figure 30a. Comparison of group 1 light PAHs profile at Lifeguard HQ with profiles of the Runway and Freeway locations. | 43 |
| Figure 30b. Comparison of group 2 light PAHs profile at Lifeguard HQ with profiles of the Runway and Freeway locations. | 43 |
| Figure 30c. Comparison of group 3 light PAHs profile at Lifeguard HQ with profiles of the Runway and Freeway locations..... | 44 |
| Figure 31a. Comparison of group 1 light PAHs profile at Boys’ Club with profiles of the Runway and Freeway locations..... | 44 |

Figure 31b. Comparison of group 2 light PAHs profile at Boys’ Club with profiles of the Runway and Freeway locations..... 45

Figure 31c. Comparison of group 3 light PAHs profile at Boys’ Club with profiles of the Runway and Freeway locations..... 45

Figure 32a. Comparison of group 1 light PAHs profile at Fire Station with profiles of the Runway and Freeway locations. 46

Figure 32b. Comparison of group 2 light PAHs profile at Fire Station with profiles of the Runway and Freeway locations..... 46

Figure 32c. Comparison of group 3 light PAHs profile at Fire Station with profiles of the Runway and Freeway locations..... 47

Figure 33a. Comparison of group 1 light PAHs profile at Parking site with profiles of the Runway and Freeway locations..... 47

Figure 33b. Comparison of group 2 light PAHs profile at Parking site with profiles of the Runway and Freeway locations..... 48

Figure 33c. Comparison of group 3 light PAHs profile at Parking site with profiles of the Runway and Freeway locations..... 48

VII. APPENDIX I(a)

Analysis of Inorganic Elements, Organic and Elemental Carbon

Source: Desert Research Institute, Reno, Nevada; Elemental Analytical Facility

Sample Collection

Filter packs containing Teflon-membrane, and quartz fiber filters were prepared for this study. All filter batches are conditioned and acceptance tested prior to use in sampling. Two percent of filters from each batch are acceptance tested by subjected them to the exact same analysis as sampled filters to ensure that they are clean before they are used for actual sampling. Teflon-membrane filters are used for the measurement of mass and elemental concentrations; quartz fiber filters are used for the determination of carbon fractions and inorganic ions in the particulate phase.

Gravimetric Analysis

Unexposed and exposed Teflon-membrane filters are equilibrated at a temperature of 21.5 ± 2 °C and a relative humidity of $35 \pm 5\%$ for a minimum of 24 hours prior to weighing. Weighing is performed on a Mettler Toledo MT5 microbalance with ± 0.001 mg sensitivity. The charge on each filter is neutralized by exposure to a ^{210}Po ionizing source for 30 seconds or more prior to the filter being placed on the balance pan. The balance is calibrated with a 200 mg Class 1.1 weight and the tare is set prior to weighing each batch of filters. After every 10 filters are weighed, the calibration and tare are re-checked. If the results of these performance tests deviate from specifications by more than ± 5 %g, the balance is re-calibrated.

Replicate weights are performed on 100% of the filters weighed before sampling (initial weights or pre-weights), and on 30% of the filters weighed after sampling (final weights or post-weights) by an independent technician. Replicate pre-sampling (initial) weights must be within ± 0.010 mg of the original weights. Replicate post-sampling (final) weights on ambient samples must be within ± 0.015 mg. Post-sampling weights on heavily loaded (i.e., greater than 1 mg) samples must be within 2% of the net weight. Pre- and post-weights, check weights, and re-weights (if required) are recorded on data sheets as well as being directly entered into a database via an internet connection.

X-ray Fluorescence

XRF analyses will be performed on Teflon-membrane filters for Na, Mg, Al, Si, P, S, Cl, K, Ca, Ti, V, Cr, Mn, Fe, Co, Ni, Cu, Zn, Ga, As, Se, Br, Rb, Sr, Y, Zr, Mo, Pd, Ag, Cd, In, Sn, Sb, Ba, La, Au, Hg, Tl, Pb, and U on a PANalytical Epsilon 5, EDXRF analyzer using a side-window, liquid-cooled, 100 KeV, 24 milliamp gadolinium anode x-ray tube and secondary fluorescors. In XRF, inner shell electrons are removed from the atoms of the aerosol deposit. An x-ray photon with a wavelength characteristic of each element is emitted when an outer shell electron occupies the vacant inner shell. The number of these photons is proportional to the number of atoms present. The characteristic x-ray peaks for each element are defined by

200 eV-wide windows in an energy spectrum ranging from 1 to 80 KeV. Eight separate XRF analyses are conducted on each sample to optimize detection limits for the specified elements.

The EDXRF system is calibrated using Micromatter (Arlington, WA) thin film standards. Multielement standards are analyzed daily to monitor for any instrument drift.

Thermal/Optical Reflectance/Transmittance Carbon Analysis

The thermal/optical reflectance and transmittance (TOR/TOT) method measures organic (OC) and elemental (EC) carbon. The TOR/TOT method is based on the principle that different types of carbon-containing particles are converted to gases under different temperature and oxidation conditions. The different carbon fractions from TOR/TOT are useful for comparison with other methods, which are specific to a single definition for organic and elemental carbon. These specific carbon fractions are analyzed following the Interagency Monitoring Protection Visual Environment (IMPROVE) thermal protocol and also help distinguish among seven carbon fractions reported by TOR/TOC:

- 1) The carbon evolved in a helium atmosphere at temperatures between ambient and 140 °C (OC1)
- 2) The carbon evolved in a helium atmosphere at temperatures between 140 and 280 °C (OC2)
- 3) The carbon evolved in a helium atmosphere at temperatures between 280 and 480 °C (OC3)
- 4) The carbon evolved in a helium atmosphere between 480 and 580 °C (OC4)
- 5) The carbon evolved in an oxidizing atmosphere at 580 °C (EC1)
- 6) The carbon evolved in an oxidizing atmosphere between 580 and 740 °C (EC2)
- 7) The carbon evolved in an oxidizing atmosphere between 740 and 840 °C (EC3)

The thermal/optical reflectance carbon analyzer consists of a thermal system and an optical system. The thermal system consists of a quartz tube placed inside a coiled heater. Current through the heater is controlled to attain and maintain pre-set temperatures for given time periods. A portion of a quartz filter is placed in the heating zone and heated to different temperatures under non-oxidizing and oxidizing atmospheres. The optical system consists of a He-Ne laser, a fiber optic transmitter and receiver and a photocell. The filter deposit faces a quartz light tube so that the intensity of the reflected laser beam can be monitored throughout the analysis.

As the temperature increases from ambient (~25 °C) to 580 °C, organic compounds are volatilized from the filter in a non-oxidizing (He) atmosphere while elemental carbon is not oxidized. When oxygen is added to the helium at temperatures greater than 580 °C, the elemental carbon burns and enters the sample stream. The evolved gases pass through an oxidizing bed of heated manganese dioxide where they are oxidized to carbon dioxide, then across a heated nickel catalyst, which reduces the carbon dioxide to methane (CH₄). The methane is then quantified with a flame ionization detector (FID).

The reflected laser light is continuously monitored throughout the analysis cycle. The negative change in reflectance is proportional to the degree of pyrolytic conversion from organic to elemental carbon, which takes place during organic carbon analysis. After oxygen is introduced, the reflectance increases rapidly as the light-absorbing carbon is burned off the filter. The carbon measured after the reflectance attains the value it had at the beginning of the analysis cycle is classified as elemental carbon. This adjustment for pyrolysis in the analysis is significant, as high as 25% of organic or elemental carbon, and it cannot be ignored.

The system is calibrated by analyzing samples of known amounts of methane, carbon dioxide, and potassium hydrogen phthalate (KHP). The FID response is ratioed to a reference level of methane injected at the end of each sample analysis. Performance tests of the instrument calibration are conducted at the beginning and end of each day's operation. Intervening samples are re-analyzed when calibration changes of more than ±10% are found.

Known amounts of American Chemical Society (ACS) certified reagent grade crystal sucrose and KHP are committed to TOR/TOT as a verification of the organic carbon fractions. Fifteen different standards are used for each calibration. Widely accepted primary standards for elemental and/or organic carbon are still lacking. Results of the TOR/TOT analysis of each filter are entered into the DRI database.

Inorganic Ions

Filter Extraction

Water-soluble chloride, nitrate, sulfate, sodium, potassium and ammonium are obtained by extracting the quartz-fiber particle filter (or any other filter used for sample collection) in 15 ml of deionized-distilled water (DDW). The filter is placed in a 16 x 150 mm

polystyrene extraction vial with a screw cap (e.g., Falcon #2045). Each vial is labeled with a bar code sticker containing the filter ID code. The extraction tubes are placed in tube racks, and the extraction solutions are added. The extraction vials are capped and sonicated for 60 minutes, shaken for 60 minutes, then aged overnight to assure complete extraction of the deposited material in the solvent. The ultrasonic bath water is monitored to prevent temperature increases from the dissipation of ultrasonic energy in the water. After extraction, these solutions are stored under refrigeration prior to analysis.

Ion Chromatographic Analysis for Inorganic Ions

Water-soluble chloride (Cl^-), nitrate (NO_3^-), and sulfate (SO_4^{2-}) are measured with the Dionex ICS-3000 (Sunnyvale, CA) ion chromatograph (IC). In IC, an ion-exchange column separates the sample ions in time for individual quantification by a conductivity detector. Prior to detection, the column effluent enters a suppressor column where the chemical composition of the component is altered, resulting in a matrix of low conductivity. The ions are identified by their elution/retention times and are quantified by the conductivity peak area.

Approximately 250 μl of the filter extract are injected into the ion chromatograph. The resulting peaks are integrated and the peak integrals are converted to concentrations using calibration curves derived from solution standards. The Dionex system for the analysis of Cl^- , NO_3^- and SO_4^{2-} contains a guard column (AG14 column, Cat. No. #37042) and an anion separator column (AS14 column, Cat. No. #37041) with a strong basic anion exchange resin, and an anion micro membrane suppressor column (250 x 6 mm ID) with a strong acid ion exchange resin, and an anion self-regenerating suppressor. The anion eluent consists of sodium carbonate (Na_2CO_3) and sodium bicarbonate (NaHCO_3) prepared in DDW. The DDW is verified to have a conductivity of less than 1.8×10^{-5} ohm/cm prior to preparation of the eluent. For quantitative determinations, the ion chromatograph is operated at a flow rate of 2.0 ml/min.

Calibration standards are prepared at least once each month by diluting the primary standard solution (Dionex Standard #57590) to concentrations covering the range of concentrations expected in the filter extracts. The calibration concentrations prepared are at 0.1, 0.2, 0.5, 1.0, and 2.0 $\mu\text{g}/\text{ml}$ for each of the analysis species. The standards are stored in a refrigerator.

Calibration curves are performed daily. Chemical compounds are identified by matching the retention time of each peak in the unknown sample with the retention times of peaks in the chromatograms of the standards. A DDW blank is analyzed after every 20 samples and a calibration standard is analyzed after every 10 samples. These quality control checks verify the baseline and calibration, respectively. Environmental Research Associates (ERA, Arvada, CO) NIST traceable standards are used daily as an independent quality assurance (QA) check. These standards (ERA Wastewater Nutrient and ERA Mineral WW) are traceable to NIST simulated rainwater standards. If the values obtained for these standards do not coincide within a pre-specified uncertainty level (typically three standard deviations of the baseline level or $\pm 10\%$), the samples between that standard and the previous calibration standards are re-analyzed.

After analysis, the chromatogram for each sample in the batch is reviewed for the following: 1) proper operational settings, 2) correct peak shapes and integration windows, 3) peak overlaps, 4) correct background subtraction, and 5) quality control sample comparisons. When values for replicates differ by more than $\pm 10\%$ or values for standards differ by more than $\pm 10\%$, samples before and after these quality control checks are designated for re-analysis in a subsequent batch. Individual samples with unusual peak shapes, background subtractions or deviations from standard operating parameters are also designated for re-analysis.

Automated Colorimetric Analysis for Ammonium and Ammonia

The Astoria Pacific (Clackamas, OR) Automated Colorimetric System (AC) is used to measure ammonium concentrations by the indolphenol method. The heart of the automated colorimetric system is a peristaltic pump, which introduces air bubbles into the sample stream. Each sample is mixed with reagents and subjected to appropriate reaction periods before submission to a colorimeter. The liquid's absorbency is related to the amount of the ion in the sample by Beer's Law. This absorbency is measured by a photomultiplier tube through an interference filter, which is specific to the species being measured.

Ammonium in the extract is reacted with phenol and alkaline sodium hypochlorite to produce indolphenol, a blue dye. The reaction is catalyzed by the addition of sodium nitroprusside. The absorbency of the solution is measured at 630 nm. Two milliliters of extract in a sample vial is placed in an autosampler, which is controlled by a computer. Five standard concentrations are prepared from ACS reagent-grade $(\text{NH}_4)_2\text{SO}_4$. Each set of samples consists of 2 distilled water blanks to establish a baseline, 8 calibration standards and a blank, then sets

of 10 samples followed by analysis of one of the standards and a replicate from a previous batch.

The system determines carry-over by analysis of a low concentration standard following a high concentration. The percent carry-over is then automatically calculated and can be applied to the samples analyzed during the run. Astoria Pacific software operating on a Dell Optiplex microcomputer controls the sample throughput, calculates concentrations, and records data on the DRI data base.

Formaldehyde has been found to interfere with the measurements when it is present in an amount, which exceeds 20% of the ammonium content. Hydrogen sulfide interferes with the measurements when it is present in concentrations, which exceed 1 mg/ml. Nitrate and sulfate are also potential interferents when present at levels, which exceed 100 times the ammonium concentration. These levels are rarely exceeded in ambient samples. The precipitation of the hydroxides of heavy metals such as calcium and magnesium is prevented by the addition of sodium citrate/sodium potassium tartrate buffer solution to the sample stream.

Soluble sodium and potassium by Atomic Absorption spectrometry

Soluble sodium, and potassium will be measured using a Varian Spectra AA-880 atomic absorption spectrophotometer. Atomic absorption spectroscopy methods rely on the principle that free, uncombined atoms will absorb light at specific wavelengths corresponding to the energy requirements of the specific atom. Atoms in the ground state absorb light and are excited into a higher energy state. Each transition between energy states is characterized by a different energy, and therefore a different wavelength of light. The atomic spectrum of each element comprises a number of discrete lines arising from both the ground and excited states. The lines which originate in the ground state atoms, called resonance lines, are the most often of interest in atomic absorption spectrometry, as ground state atoms are most prevalent in practical atomization methods.

The amount of light absorbed is proportional to the concentration of the atoms over a given absorption path length and wavelength. Standards of known concentration are prepared, matched to the sample matrix, and measured. The unknown sample absorbencies are compared to the absorbencies of the standards. Since the measured absorbance is directly

proportional to the concentration of analyte this gives a simple and accurate method of determining the unknown concentration.

The atomic absorption spectrometer is a system which allows the analyst to measure the absorbance of the analyte and relate the measured absorbance to the concentration of analyte in the sample. The instrument consists of a hollow cathode lamp containing the element of interest, a method of introducing ground state atoms into the light path, a monochromator to isolate the wavelength of interest, a photo detector to measure and amplify the absorbance signal, and a method of displaying the results. The lamp provides the spectral signature of the element to be measured. Ground state atoms are introduced into the optical path by several methods. The most common of these are: flame, either air-Acetylene or Nitrous Oxide-Acetylene, graphite furnace, metal hydride generation, or cold vapor generation. The monochromator consists of a grating that diffracts the light, and through the process of mutual interference is dispersed at different angles according to wavelength. The monochromator can be rotated to select and focus the wavelength of interest on the photodetector. The photodetector is typically a photomultiplier tube which detects and amplifies the light reaching it to useful levels. This signal is then passed on for further processing. Results can be displayed using anything from a simple analog meter reading absorbance to sophisticated computer software offering a wide variety of calculation options. The latter is standard on current instruments.

APPENDIX I(b)

Calculations of precision for Inorganic Elements, Organic and Elemental Carbon

Source: Desert Research Institute, Reno, Nevada; Elemental Analytical Facility

5.0 QUANTIFICATION

The following formulae are used in the calculation of ambient concentrations and precision estimates:

$$C_i = \frac{M_i \cdot B_i}{V}$$

$$V = F \cdot t$$

$$B_i = \frac{1}{n} \sum_{j=1}^n B_{ij}$$

for $B_i = \bar{B}_i$

$$B_i = 0$$

for $B_i = \sigma_{B_i}$

$$\sigma_{B_i} = \text{STD}_{B_i} = \sqrt{\frac{1}{n} \sum_{j=1}^n (B_{ij} - \bar{B}_i)^2}$$

for $\text{STD}_{B_i} = \text{SIG}_{B_i}$

$$\sigma_{B_i} = \text{SIG}_{B_i} = \sqrt{\frac{1}{n} \sum_{j=1}^n \sigma_{B_{ij}}^2}$$

for $\text{STD}_{B_i} = \sigma_{B_i}$

$$\sigma_{C_i} = \sqrt{\frac{\sigma_{M_i}^2 + \sigma_{B_i}^2}{V^2} + \frac{\sigma_V^2 \cdot (M_i \cdot B_i)^2}{V^4}}$$

$$D_{M_{ijp}} = M_{ijfp} \cdot M_{ijrp}$$

for mass and B_{abs}

$$D_{M_{ijt}} = M_{ijft} \cdot M_{ijrt}$$

for mass and B_{abs}

$$D_{M_{ip}} = \frac{1}{n} \sum_{j=1}^n D_{M_{ijp}}$$

for mass and B_{abs}

$$D_{M_{it}} = \frac{1}{n} \sum_{j=1}^n D_{M_{ijt}}$$

for mass and B_{abs}

$$\sigma_{M_i} = \sqrt{\frac{1}{n} \sum_{j=1}^n D_{M_{ijp}}^2 + D_{M_{ip}}^2 + \frac{1}{n} \sum_{j=1}^n D_{M_{ijt}}^2 + D_{M_{it}}^2} \quad \text{for mass and } B_{\text{abs}}$$

$$D_{M_i} = \frac{\sum_{j=1}^n |M_{ijf} - M_{ijr}|}{\sum_{j=1}^n (M_{ijf} + M_{ijr}) / 2} \quad \text{for all other species}$$

$$\sigma_{M_i} = M_i \times D_{M_i} \quad \text{for all other species}$$

$$\sigma_V = 0.05$$

where

- B_i = average amount of species i on field blanks
- B_{ij} = the amount of species i found on field blank j
- C_i = the ambient concentration of species i
- F = flow rate throughout sampling period
- F_{jf} = flow rate performance test made before sampling
- F_{jr} = flow rate performance test made after sampling
- M_i = amount of species i on the substrate
- M_{ijf} = amount of species i on sample j from analysis
- M_{ijr} = amount of species i on sample j from replicate analysis
- M_{ijfp} = pre-exposure filter weight or optical density on sample j
- M_{ijrp} = pre exposure filter weight or optical density on sample j from replicate analysis
- M_{ijft} = post-exposure filter weight or optical density on sample j
- M_{ijrt} = post exposure filter weight or optical density on sample j from replicate analysis
- t = sample duration
- V = volume of air sampled
- σ_{B_i} = blank precision for species I
- $\sigma_{B_{ij}}$ = blank precision for species I on field blank j
- σ_{C_i} = propagated precision for the concentration of species i
- σ_{M_i} = precision of amount of species i on substrate
- σ_V = precision of sample volume

Gaseous species concentrations are converted from the analyte ion to the gaseous species form by multiplying C_i by the ratio of analyte species formula weight to gaseous species formula weight. Nitrate in nitric acid is determined by subtracting the total particulate nitrate determined by the denuded Nylon filter from the total nitrate determined on the non-denuded Teflon/Nylon sample. The precision of this measurement is determined by adding in quadrature the precisions of these two observables as specified in Bevington (1969). Calculations for other denuder difference measurements such as ammonia are done in an analogous manner.

7.0 REFERENCES

Bevington, P.R. (1969). *Data Reduction and Error Analysis for the Physical Sciences*. McGraw Hill, New York, NY

APPENDIX I(c)

Method Detection Limits Inorganic Elements, Organic and Elemental Carbon

Source: Desert Research Institute, Reno, Nevada; Elemental Analytical Facility

| Species | Analysis Method ^a | MDL (µg/filter) | Acronym |
|--|------------------------------|-----------------|---------|
| Mass | GRAV | 1.0000 | MSGC |
| Chloride (Cl ⁻) | IC | 1.5005 | CLIC |
| Nitrate (NO ₃ ⁻) | IC | 1.5005 | N3IC |
| Sulfate (SO ₄ ⁼) | IC | 1.5005 | S4IC |
| Ammonium (NH ₄ ⁺) | AC | 1.5005 | N4CC |
| Soluble Sodium (Na ⁺) | AAS | 0.2362 | NAAC |
| Soluble Potassium (K ⁺) | AAS | 0.1498 | KPAC |
| Organic Carbon (OC) Fraction 1 | TOR | 0.0516 | O1TC |
| Organic Carbon (OC) Fraction 2 | TOR | 1.2900 | O2TC |
| Organic Carbon (OC) Fraction 3 | TOR | 3.8700 | O3TC |
| Organic Carbon (OC) Fraction 4 | TOR | 0.1290 | O4TC |
| Pyrolyzed organic carbon via transmittance | TOR | 0.1290 | OPTTC |
| Pyrolyzed organic carbon via reflectance | TOR | 0.1290 | OPTRC |
| Organic Carbon (OC) | TOR | 5.0310 | OCTRC |
| Elemental Carbon (EC) Fraction 1 | TOR | 0.0387 | E1TC |
| Elemental Carbon (EC) Fraction 2 | TOR | 0.0387 | E2TC |
| Elemental Carbon (EC) Fraction 3 | TOR | 0.0387 | E3TC |
| Elemental Carbon (EC) | TOR | 0.1290 | ECTRC |
| Total Carbon (TC) | TOR | 5.4180 | TCTC |
| Sodium (Na) | XRF | 3.7541 | NAXC |
| Magnesium (Mg) | XRF | 1.1341 | MGXC |
| Aluminum (Al) | XRF | 0.4483 | ALXC |
| Silicon (Si) | XRF | 0.3613 | SIXC |
| Phosphorus (P) | XRF | 0.1177 | PHXC |
| Sulfur (S) | XRF | 0.0506 | SUXC |
| Chlorine (Cl) | XRF | 0.0487 | CLXC |
| Potassium (K) | XRF | 0.0459 | KPXC |
| Calcium (Ca) | XRF | 0.0727 | CAXC |
| Scandium (Sc) | XRF | 0.1938 | SCXC |
| Titanium (Ti) | XRF | 0.0346 | TIXC |
| Vanadium (V) | XRF | 0.0082 | VAXC |
| Chromium (Cr) | XRF | 0.0382 | CRXC |
| Manganese (Mn) | XRF | 0.0834 | MNXC |
| Iron (Fe) | XRF | 0.0760 | FEXC |
| Cobalt (Co) | XRF | 0.0041 | COXC |
| Nickel (Ni) | XRF | 0.0131 | NIXC |
| Copper (Cu) | XRF | 0.0442 | CUXC |
| Zinc (Zn) | XRF | 0.0391 | ZNXC |
| Gallium (Ga) | XRF | 0.1281 | GAXC |
| Arsenic (As) | XRF | 0.0147 | ASXC |
| Selenium (Se) | XRF | 0.0290 | SEXC |

| | | | |
|-----------------|-----|--------|------|
| Bromine (Br) | XRF | 0.0412 | BRXC |
| Rubidium (Rb) | XRF | 0.0271 | RBXC |
| Strontium (Sr) | XRF | 0.0633 | SRXC |
| Yttrium (Y) | XRF | 0.0376 | YTXC |
| Zirconium (Zr) | XRF | 0.1012 | ZRXC |
| Niobium (Nb) | XRF | 0.0667 | NBXC |
| Molybdenum (Mo) | XRF | 0.0640 | MOXC |
| Palladium (Pd) | XRF | 0.1549 | PDXC |
| Silver (Ag) | XRF | 0.1473 | AGXC |
| Cadmium (Cd) | XRF | 0.1152 | CDXC |
| Indium (In) | XRF | 0.1271 | INXC |
| Tin (Sn) | XRF | 0.1372 | SNXC |
| Antimony (Sb) | XRF | 0.2063 | SBXC |
| Cesium (Cs) | XRF | 0.0585 | CSXC |
| Barium (Ba) | XRF | 0.0632 | BAXC |
| Lanthanum (La) | XRF | 0.0433 | LAXC |
| Cerium (Ce) | XRF | 0.0417 | CEXC |
| Samarium (Sm) | XRF | 0.0862 | SMXC |
| Europium (Eu) | XRF | 0.1325 | EUXC |
| Terbium (Tb) | XRF | 0.0976 | TBXC |
| Hafnium (Hf) | XRF | 0.3950 | HFXC |
| Tantalum (Ta) | XRF | 0.2579 | TAXC |
| Wolfram (W) | XRF | 0.3610 | WOXC |
| Iridium (Ir) | XRF | 0.1192 | IRXC |
| Gold (Au) | XRF | 0.1960 | AUXC |
| Mercury (Hg) | XRF | 0.0971 | HGXC |
| Thallium (Tl) | XRF | 0.0654 | TLXC |
| Lead (Pb) | XRF | 0.0945 | PBXC |
| Uranium (U) | XRF | 0.1648 | URXC |

^a GRAV = gravimetry. OP = optical density. C = ion chromatography. AC=automated colorimetry.
AAS=atomic absorption spectrophotometry.

TOR=thermal/optical reflectance. XRF=x-ray fluorescence.

Minimum detectable limit (MDL) is the concentration at which instrument response equals three times the standard deviation of the response to a known concentration of zero.

Filter assumed to be a 47 mm filter

Appendix II(a)

List of Hydrocarbons Analyzed

Source: Desert Research Institute, Reno, Nevada; Organic Analytical Facility

| Field_name | compound | |
|------------|------------------------------|---------|
| ENAP12 | 1+2ethylnaphthalene | ENAP12U |
| NAPHTH | naphthalene | NAPHTHU |
| QUINOLINE | Quinoline | |
| MNAPH1 | 1-methylnaphthalene | |
| MNAPH2 | 2-methylnaphthalene | |
| BIPHEN | Biphenyl | |
| DM1367 | 1,3+1,6+1,7dimethylnaphth | |
| DMN267 | 2,6+2,7-dimethylnaphthalene | |
| M_2BPH | 2-methylbiphenyl | |
| DMN18 | 1,8-dimethylnaphthalene | |
| ACNAPY | Acenaphthylene | |
| ACNAPE | Acenaphthene | |
| D14523 | 1,4+1,5+2,3-dimethylnaphth | |
| DMN12 | 1,2-dimethylnaphthalene | |
| DBZFUR | Dibenzofuran | |
| M_3BPH | 3-methylbiphenyl | |
| M_4BPH | 4-methylbiphenyl | |
| FLUORE | Fluorene | |
| BTMNAP | B-trimethylnaphthalene | |
| EM_12N | 1-ethyl-2-methylnaphthalene | |
| EM_21N | 2-ethyl-1-methylnaphthalene | |
| ETMNAP | E-trimethylnaphthalene | |
| FTMNAP | F-trimethylnaphthalene | |
| JTMNAP | J-trimethylnaphthalene | |
| TM145N | 1,4,5-trimethylnaphthalene | |
| TM245N | 2,4,5-trimethylnaphthalene | |
| TMI235N | 2,3,5+I-trimethylnaphthalene | |
| ATMNAP | A-trimethylnaphthalene | |
| CTMNAP | C-trimethylnaphthalene | |
| ANTHRA | Anthracene | |
| PHENAN | Phenanthrene | |
| | 9- | |
| FL9ONE | fluorenone | |
| A_MFLUO | A-Methylfluorene | |
| B_MFLUO | B-Methylfluorene | |

| | |
|----------|---------------------------|
| M_1FLUO | 1-Methylfluorene |
| DBTH | Dibenzothiophene |
| M_45PHEN | 4,5-methylenephenanthrene |
| PNAPONE | Perinaphthenone |
| ACQUONE | Acenaphthenequinone |
| MPHT_1 | 1-methylphenanthrene |
| M_2ANTH | 2-methylantracene |
| M_2PHEN | 3-methylphenanthrene |
| M_3PHEN | 2-methylphenanthrene |
| M_9PHEN | 9-methylphenanthrene |
| XANONE | Xanthone |
| NAP2PHEN | 2-phenylnaphthalene |
| M_9ANT | 9-methylantracene |
| ANTHRON | Anthrone |
| FLUORA | Fluoranthene |
| A_DMPH | A-dimethylphenanthrene |
| B_DMPH | B-dimethylphenanthrene |
| C_DMPH | C-dimethylphenanthrene |
| DM17PH | 1,7-dimethylphenanthrene |
| DM36PH | 3,6-dimethylphenanthrene |
| D_DMPH | D-dimethylphenanthrene |
| E_DMPH | E-dimethylphenanthrene |
| ANRQUONE | Anthraquinone |
| BAFLUO | benzo(a)fluorene |
| BBFLUO | benzo(b)fluorene |
| PYRENE | Pyrene |
| ANTAL9 | 9-Anthraaldehyde |
| RETENE | Retene |
| BMPYFL | B-MePy/MeFl |
| C1MFLPY | 1-MeFl+C-MeFl/Py |
| CMFYFL | C-MePy/MeFl |
| DMPYFL | D-MePy/MeFl |
| M_13FL | 1+3-methylfluoranthene |
| M_1PYR | 1-methylpyrene |
| M_4PYR | 4-methylpyrene |
| BGHIFL | Benzo(ghi)fluoranthene |
| BZCPHEN | benzo(c)phenanthrene |
| BNTIOP | Benzonaphthothiophene |
| CHR_TR | Chrysene-Triphenylene |
| PHANT9 | 9-phenylantracene |
| CP_CDPYR | Cyclopenta(c,d)pyrene |
| BAANTH | Benz(a)anthracene |
| BZANTHR | Benzanthrone |

| | |
|-----------|--------------------------------------|
| DMBAN712 | 7,12-dimethylbenz(a)anthracene |
| CHRY56M | 5+6-methylchrysene |
| M_3CHR | 3-methylchrysene |
| M_7BAA | 7-methylbenz(a)anthracene |
| BAFL | Benzo(a)fluoranthene |
| BBJKFL | Benzo(b+j+k)fluoranthene |
| BAA7_12 | Benz(a)anthracene-7,12-dione |
| MCHOL3 | 3-methylcholanthrene |
| BAPYRN | BaP |
| BEPYRN | BeP |
| PERYLE | Perylene |
| DBAHACR | dibenz(a,h)acridine |
| DBAJACR | dibenz(a,j)acridine |
| INCDFL | Indeno[123-cd]fluoranthene |
| M_7BPY | 7-methylbenzo(a)pyrene |
| BPY910DIH | 9,10-dihydrobenzo(a)pyrene-7(8H)-one |
| IN123PYR | Indeno[123-cd]pyrene |
| DBAHACAN | Dibenzo(ah+ac)anthracene |
| DBAJAN | Dibenzo(a,j)anthracene |
| DBCRCAR | 7H-dibenzo[c,g]carbazole |
| ANTHAN | Anthanthrene |
| BGHIPE | Benzo(ghi)perylene |
| BBCHR | Benzo(b)chrysene |
| PIC | Picene |
| DBALPYR | Dibenzo(a,l)pyrene |
| DBAIPYR | Dibenzo(a,i)pyrene |
| CORONE | Coronene |
| DBAEPYR | Dibenzo(a,e)pyrene |
| DBAHPYR | Dibenzo(a,h)pyrene |
| DBBKFL | Dibenzo(b,k)fluoranthene |

Appendix IIb

Analysis of Polycyclic Aromatic Hydrocarbons

Source: Desert Research Institute, Reno, Nevada; Organics Analytical Facility

Propagation of Analytical Uncertainty

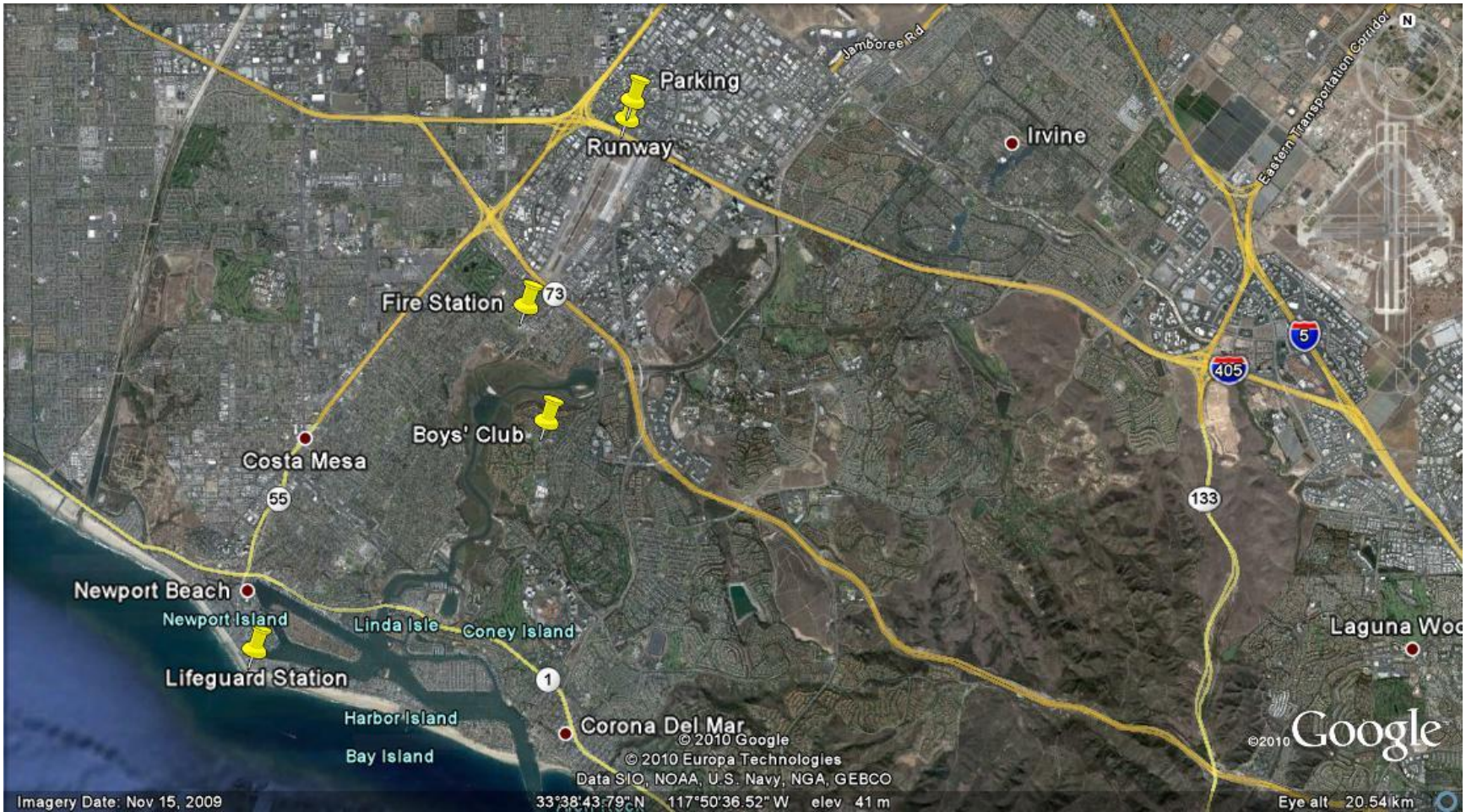
All analytical results were evaluated in terms of their associated measurement errors according to the following equation:

$$\text{Uncertainty} = \text{Square Root } ((\text{analyte concentration} * \text{replicate precision})^2 + (\text{analyte detection limit})^2)$$

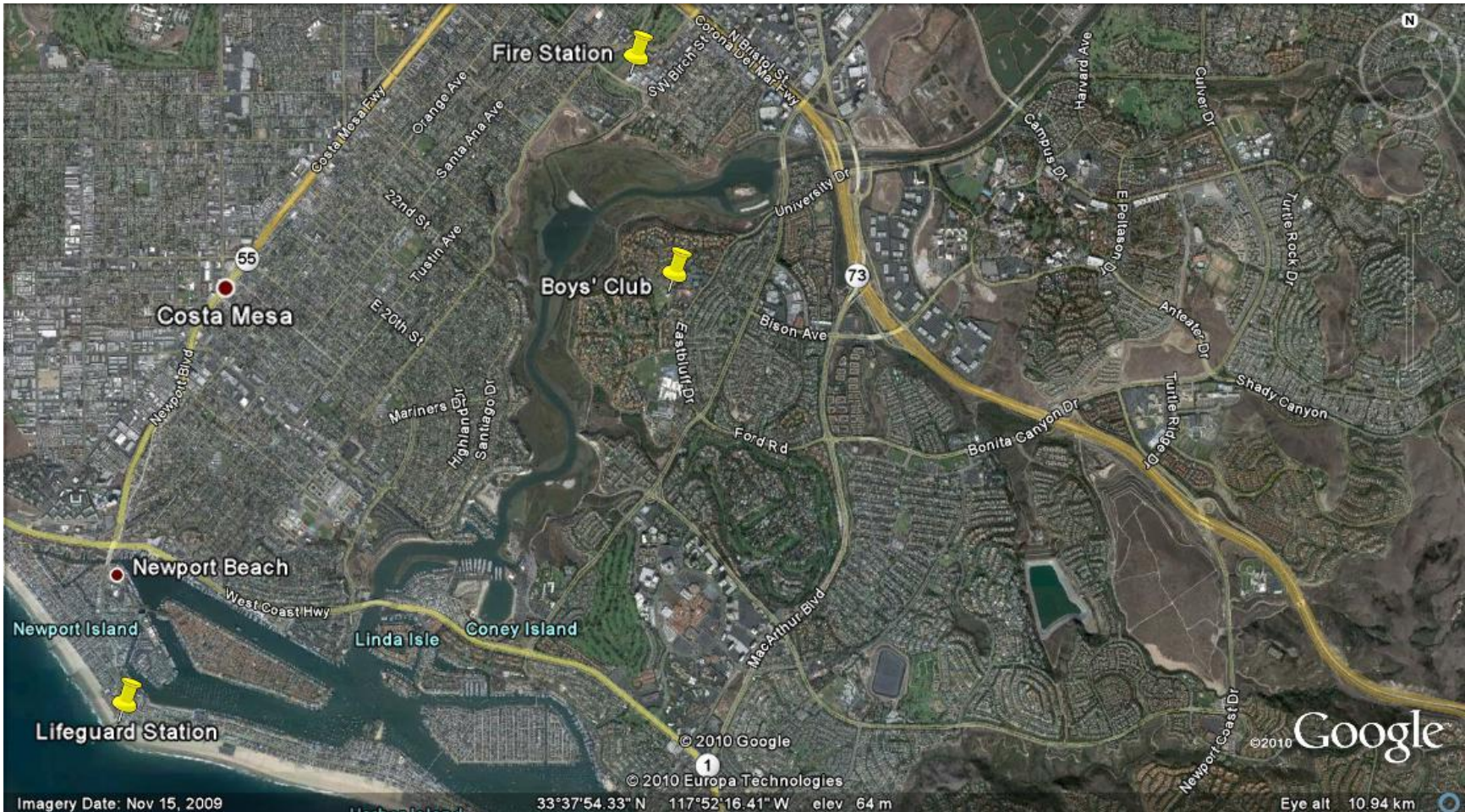
Replicate precision for each analyte is determined by multiple injections (replicates) of at least ten per cent of all of the analyzed samples. Precision is then determined by:

$$(C1-C2)/((C1+C2)/2) * 100$$

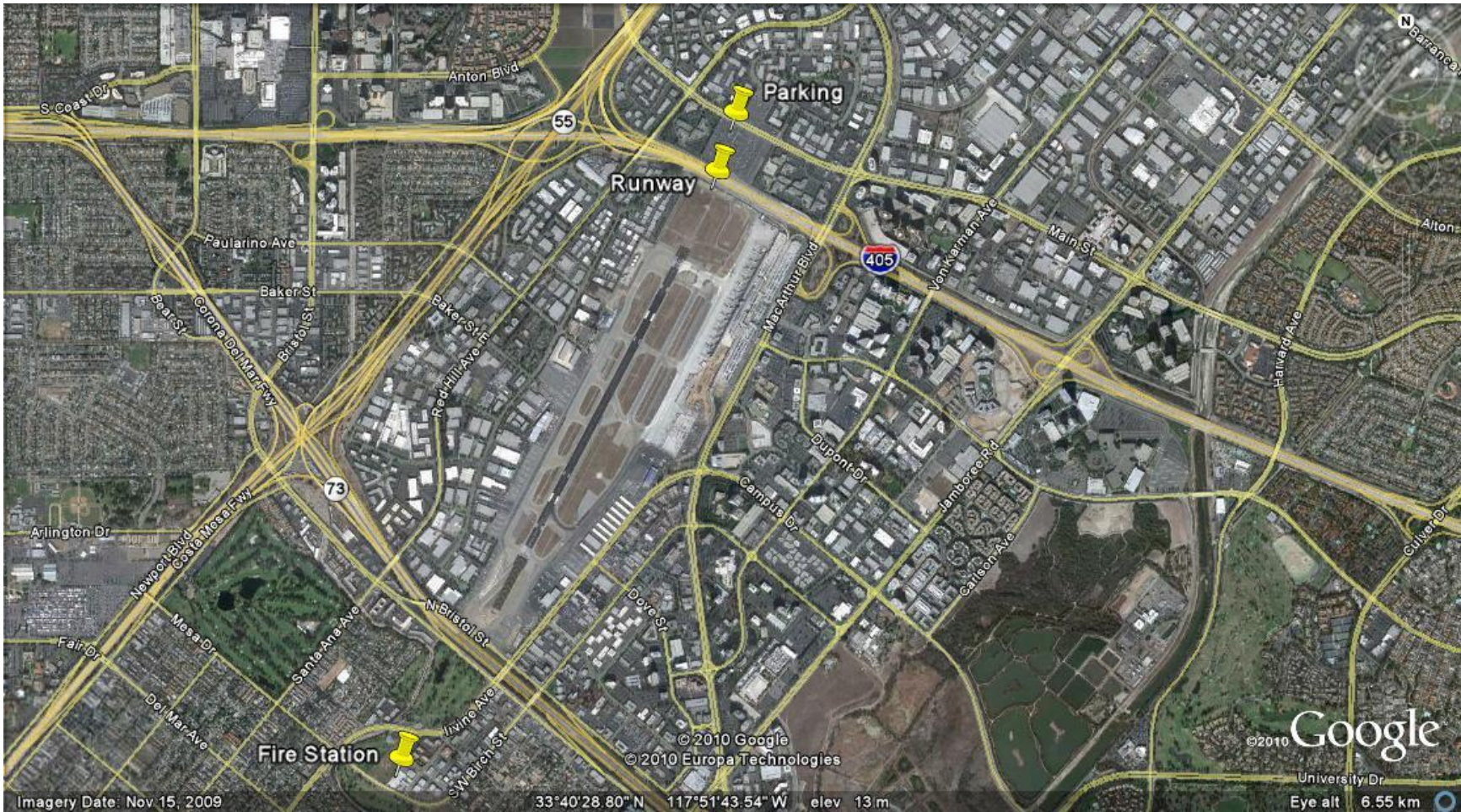
By this equation the analytical minimum detection limit (MDL) will determine the analyte uncertainty when sample concentrations approach zero. Similarly, the MDL will have little impact on the uncertainty of a higher concentration sample, where the concentration is many times the detection limit. In addition to this, the uncertainty in the volume flow is incorporated into the final uncertainty by a similar root-mean-square method. In this way the uncertainty most accurately represents the true uncertainty of the sample. Also, all samples are corrected for lot-specific sampling media blank values prior to the final concentration calculations. Software programs have been developed by DRI to automate the data processing and reporting functions.



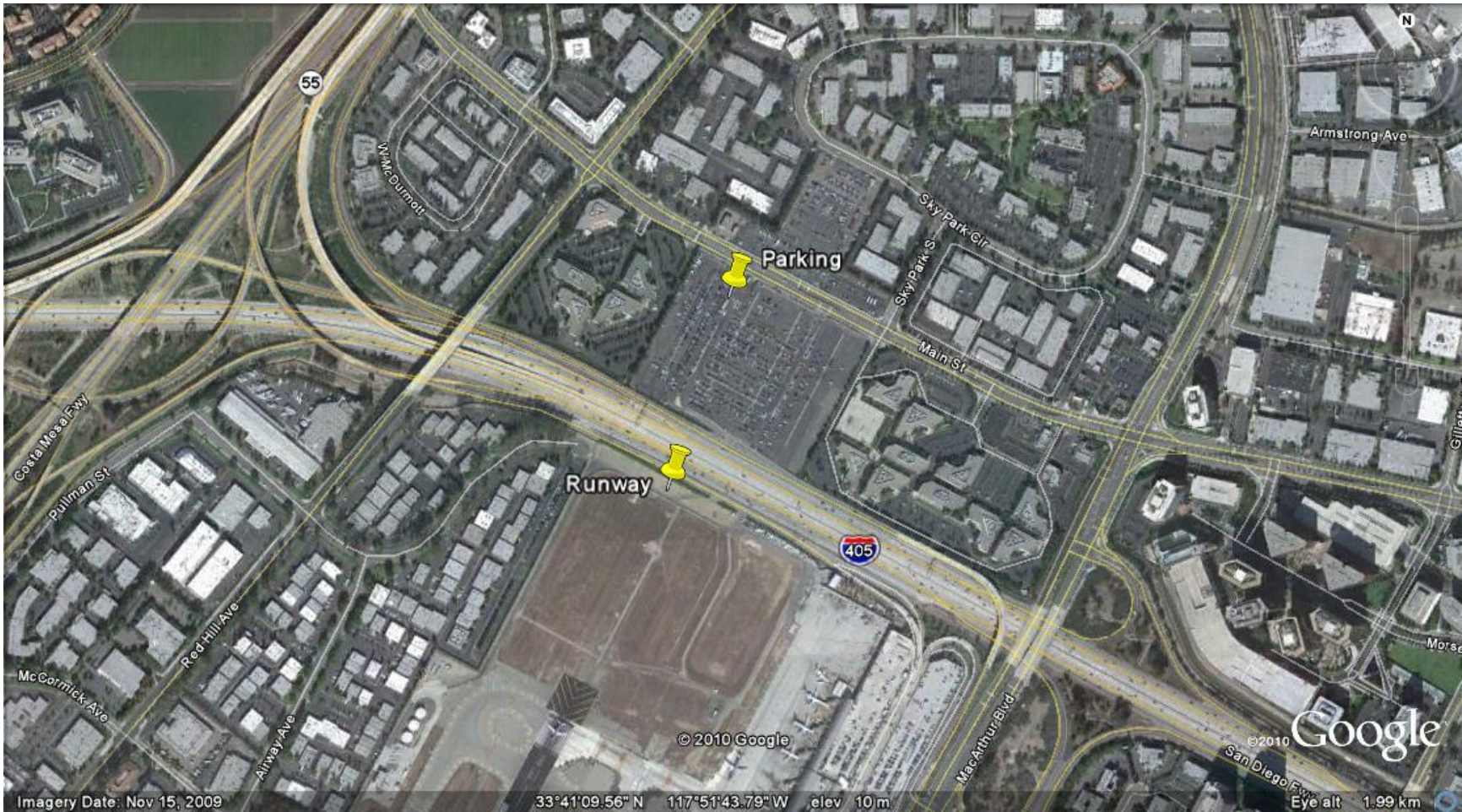
Map 2. Zoom view of sampling stations from Lifeguard Headquarters to Main Street Parking Lot. Source: Google Earth.



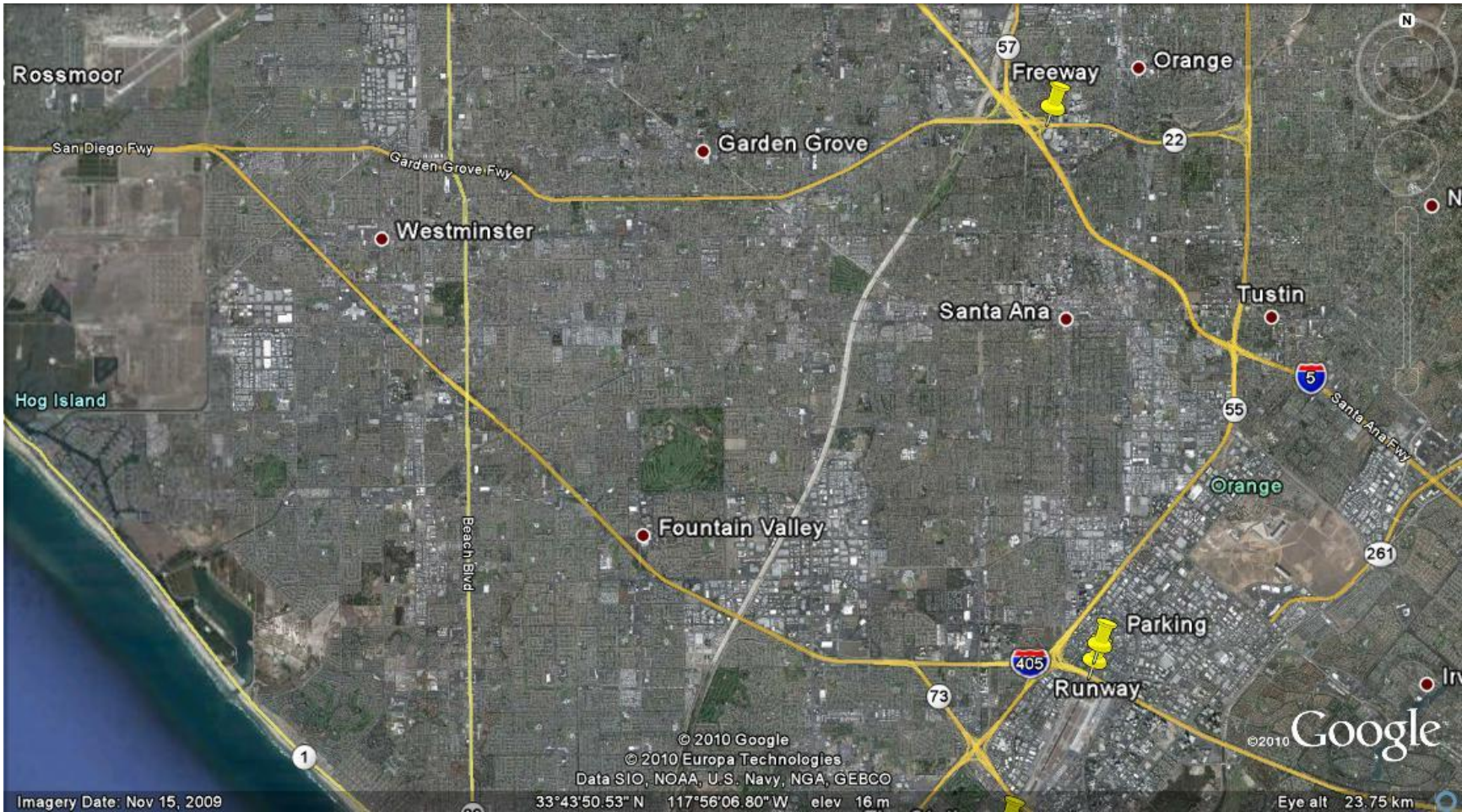
Map 3. Field sampling stations upwind of John Wayne Airport (JWA): Lifeguard Headquarters, Boys' Club and Fire Station sites.
Source: Google Earth.



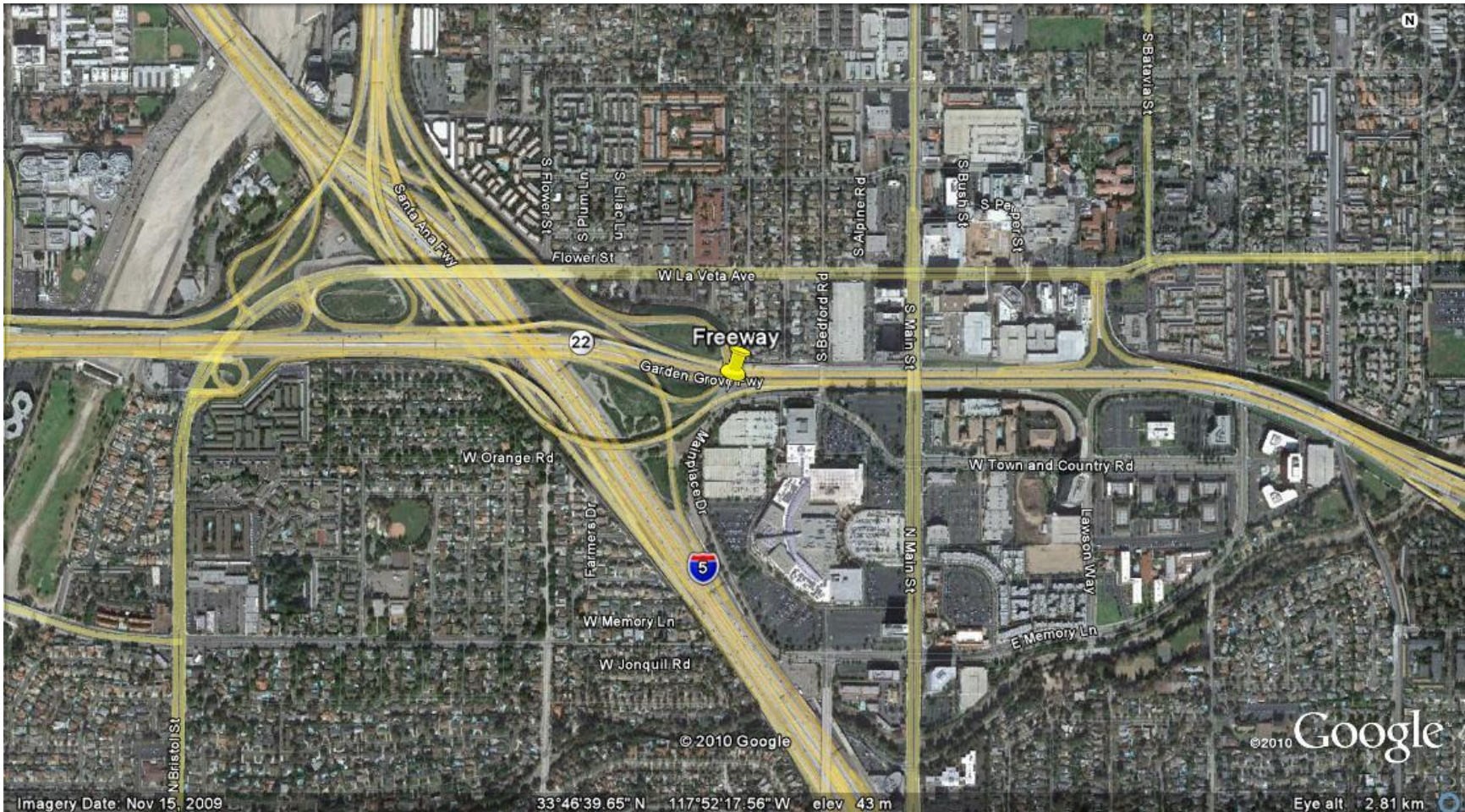
Map 4. Runway sampling station and runway-adjacent sites. The Fire Station site is upwind of the JWA runway. The Parking location is downwind of the runway. Source: Google Earth.



Map 5. Detail view of Runway and Parking sampling stations. Source: Google Earth.



Map 6. Freeway sampling location in relation to the Runway and Parking sites. Source: Google Earth.



Map 7. Detail view of Freeway sampling location. Source: Google Earth.